UNIVERSITY OF CALIFORNIA, SAN DIEGO

Power and Spectrum Efficient Communications in Wireless Ad Hoc Networks

A Dissertation submitted in partial satisfaction of the
Requirement for the Degree Doctor of Philosophy

in

Electrical Engineering (Communication Theory and Systems)

by

Qi Qu

Committee in charge:

Professor Laurence B. Milstein, Chair
Professor William S. Hodgkiss
Professor Tara Javidi
Professor William A. Kuperman
Dr. James R. Zeilder

2008

The dissertation of Qi Qu is approved, and it is acceptable in quality and form for publication on microfilm:

_____

_____

_____

_____

_____

Chair

University of California, San Diego

2008

TABLE OF CONTENTS

LIST OF FIGURES

ACKNOWLWDGEMENTS

I would like to express my immense gratitude and deep appreciation toward my adviser, Professor L. B. Milstein, for all the kindness, patience and understanding he has shown toward me, and all the helpful and insightful suggestions he has given to me, during the past several years. He is always there to listen, to advise, and to help. During my Ph.D studies, I have had a high degree of freedom to choose my research topics, had the chances to attend international conferences, and had the opportunity to be a research intern during the summer, all of these could not have been possible without his support.

I would also like to thank Professor Vaman and Professor Qian at Prairie View A&M University, for their instructive suggestions and enjoyable cooperation during the past several years. Thanks to Professor Zeilder, Professor Javidi, Professor Hodgkiss and Professor Kuperman for taking their valuable time to be my committee members.

I also want to give my deep thanks to my fellow graduate students and friends in the Electrical and Computer Engineering Department for the friendly and stimulating environment. The friendship and encouragement from all my friends in San Diego are also gratefully acknowledged.

Finally, I would like to thank my wife, Lili, for her continuing understanding and help during the past several years. I am also deeply grateful to my parents for their unselfishness, support and encouragement throughout my life. This thesis is dedicated to all of you.

Chapter 2 of this thesis, in full, is a reprint of the material as it appears in Qi Qu, Laurence B. Milstein and Dhadesugoor R. Vaman, "Cross-Layer Distributed Joint Power Control and Scheduling for Delay-Constrained Applications over CDMA-based Wireless Ad-hoc Networks", which is submitted to the *IEEE Transactions on Communications* and is currently under review. The dissertation author was the

primary investigator and author of this publication. This work is supported in part by the US Army Research Office with Research Cooperative Agreement grant No. W911NF-04-2-0054 to the ARO Center for Battlefield Communications (CeBCom) at Prairie View A&M University, U.S. Army Research Office under the Multi-University Research Initiative (MURI) grant No. W911NF-04-1-0224, the Ericsson Corp., and the UC Discovery Program.

Chapter 3 of this thesis, in full, is a reprint of the material as it appears in Qi Qu, Laurence B. Milstein and Dhadesugoor R. Vaman, "Cognitive Radio Based Multi-User Resource Allocation in Mobile Ad Hoc Networks using Multicarrier CDMA Modulation", in *IEEE Journal on Selected Areas in Communications*, Jan. 2008. The dissertation author was the primary investigator and author of this publication. This work is supported by the US Army Research Office with Research Cooperative Agreement grant No. W911NF-04-2-0054 to the ARO Center for Battlefield Communications (CeBCom) at Prairie View A&M University, U.S. Army Research Office under the Multi-University Research Initiative (MURI) grant No. W911NF-04-1-0224, the National Science Foundation under grant No. CCF-0635165, the Ericsson Corp., and the UC Discovery Program.

Chapter 4 of this thesis, in full, is a reprint of the material as it appears in Qi Qu, Laurence B. Milstein and Dhadesugoor R. Vaman, "Cooperative and Constrained MIMO Communications in Wireless Ad Hoc/Sensor Networks", which is being prepared for publication. The dissertation author was the primary investigator and author of this publication. This work is supported by the US Army Research Office with Research Cooperative Agreement grant No. W911NF-04-2-0054 to the ARO Center for Battlefield Communications (CeBCom) at Prairie View A&M University, U.S. Army Research Office under the Multi-University Research Initiative (MURI) grant No. W911NF-04-1-0224, and the UC Discovery Program.

VITA

1980	Born Chengdu, China
2002	B.S.E. University of Electronics Science and Technology of China Chengdu, China
2004	M.S. in Electrical and Computer Engineering University of Miami Coral Gables, Florida, USA
2006	Summer Intern Army Research Office (ARO) Center for Battlefield Communications, Prairie View A&M Univ. (a subsystem of Texas A&M Univ.) Prairie View, Texas, USA
2007	Summer Intern NTT-DoCoMo Communications Lab USA, Inc. Palo Alto, California, USA
2008	Ph.D in Electrical and Computer Engineering (Communication Theory and Systems) University of California, San Diego La Jolla, California, USA

FIELD OF STUDY

Major Field: Electrical and Computer Engineering
Studies in Communication Theory and Systems
Professor Laurence B. Milstein

ABSTRACT OF THE DISSERTATION

Power and Spectrum Efficient Communications in Wireless Ad Hoc Networks

by

Qi Qu

Doctor of Philosophy in Electrical Engineering

(Communication Theory and Systems)

University of California, San Diego, 2008

Professor Laurence B. Milstein, Chair

In wireless ad-hoc networks, power and spectrum are two limited and precious system resources, and how to use them efficiently is the key to provide high performance communications. This dissertation presents a distributed system design framework and algorithms to achieve power-and-spectrum-efficient wireless communications in ad hoc networks.

In the first part, we propose a cross-layer distributed power control and scheduling protocol for delay-constrained applications over mobile CDMA-based ad hoc wireless networks, where power control is employed to combat both the delay occurring on multi-hop wireless ad hoc networks and multiuser interference among mobile users. We also investigate the impact of Doppler spread upon the system

performance, and provide a robust system which employs a combination of power control, and coding/interleaving to combat the effects of Doppler spread by exploiting the time diversity when the Doppler spread gets large.

In the second part, a cognitive radio based multi-user resource allocation framework for mobile ad hoc networks is proposed. In particular, given pre-existing communications in the spectrum where the system is operating, a channel sensing and estimation mechanism is provided to obtain information such as subcarrier availability, noise power and channel gain. Given this information, both frequency spectrum and power are allocated to emerging new users (i.e., cognitive radio users), based on a distributed multi-user resource allocation framework, in order to achieve spectrum-efficient and power-efficient communications.

In the third part, we investigate the issue of cooperative MIMO communications in ad hoc networks, and the issue of cooperative node selection is described, where a source node is surrounded by multiple neighbors and all of them are equipped with a single antenna. Given energy, delay and data rate constraints, a source node dynamically chooses its cooperating nodes from its neighbors to form a virtual MIMO system with the destination node (which is assumed to have multiple antennas), and adaptively allocates the power level and adjusts the constellation size for each of the selected cooperative nodes.

1

Introduction

1.1 Wireless Ad Hoc Networks

A wireless ad hoc network is formed by multiple nodes without the aid of any infrastructure. The lack of infrastructure of ad hoc networks distinguishes them from the infrastructure-based networks, such as cellular networks and wireless local-area networks (WLAN). For example, in a cellular network, a base station (BS) is located in the center of a cell and any communications between mobile nodes should go through the BS. The BS performs all the necessary control and networking functions to any given mobile node within the cell, including handoff and resource management. On the other hand, a WLAN is controlled by an access point which acts like a BS to control all the nodes in the WLAN, including multiple access control.

However, unlike cellular and WLAN, an ad hoc network does not have central control due to the lack of infrastructure. All the networking function should be performed by the wireless nodes themselves in a distributed manner. In essence, ad hoc networks are self-configured, adaptive and distributed, as shown in Fig.1.1.

Wireless ad hoc networks are widely used in the real world due to their flexibility. They can be deployed in areas or situations where infrastructure is not possible or feasible, such as disaster relief and battlefields. Especially in battlefields, central controllers are very vulnerable and, if destroyed by the enemy, the whole network may be rendered useless. One application of this is a sensor network. On the other hand, ad hoc networks can also be applied in home networks to facilitate, for

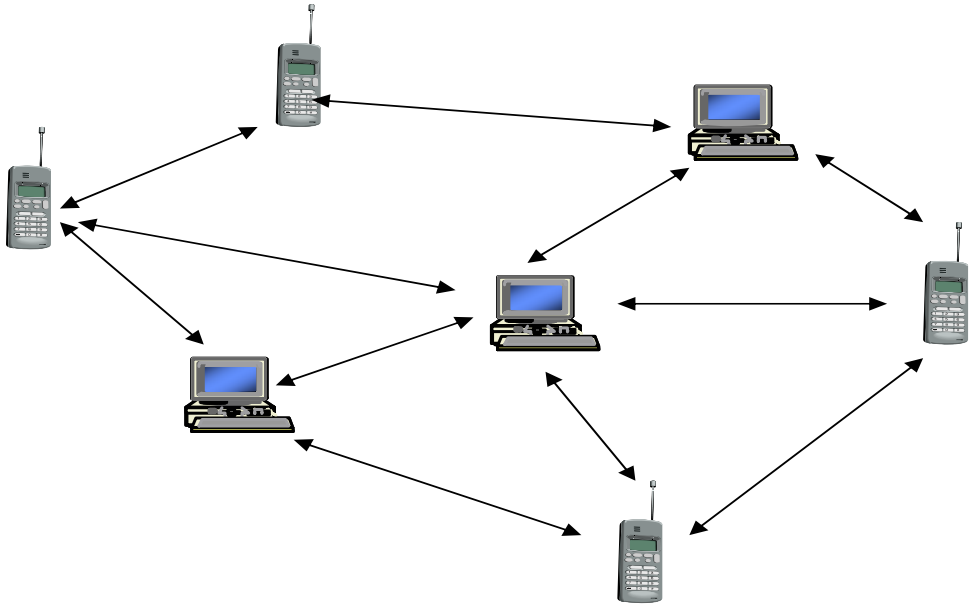

Fig.1.1. An example of wireless ad hoc network.

example, data transfer between a PDA and a laptop, where a central control is not necessary. Also, most of the current wireless network standards include ad hoc capability, such as 802.11 (WiFi) and 802.16 (WiMax).

The wide applications of ad hoc networks fuel the fast development in the design of such networks with the aim to provide reliable and efficient communications. However, the unique features of ad hoc networks compared to its infrastructure-based peers, such as cellular and WLAN networks, make this goal a difficult task.

1.2 Challenges in Wireless Ad Hoc Networks

The flexibility of ad hoc networks comes at the price of no central control. That means all the networking and control functions should be done by each node independently, in a distributed manner, and as a result, a performance penalty is

typically be paid for this flexibility.

On the other hand, system resources are limited, such as the bandwidth of a communication system and the power of each node. Usually, a wireless system is allocated a certain spectrum to operate, and multiple nodes share this spectrum. Also, each node in the network is typically powered by batteries which have limited energy. Hence. a maximization of the spectrum utilization and a minimization of power consumption are desired in ad hoc networks. Therefore, the resource allocation in wireless ad hoc networks is of paramount importance since it enables efficient use of limited system resources. One design challenge is to provide a reliable and robust distributed control for each individual node in a wireless ad hoc network, such that a distributed resource allocation becomes possible.

1.3 Techniques in Ad Hoc Networks

In order to provide robust and reliable communications in wireless ad hoc networks, numerous techniques are employed. Here we provide a brief description on those techniques.

1.3.1 Transmission Power Control and Scheduling

Power control is widely used in cellular networks to combat the well-known near-far problem, and is crucial to maintain good system performance in a cellular network. Distributed iterative power control algorithms have also been proposed for ad hoc networks, and they play an important role in improving the system performance [1, 2]. First of all, they provide a mechanism to guarantee the required wireless-link quality by using the minimum required power such that the battery life of a node can be prolonged and the link between two nodes can be maintained. On the other hand,

when multiple nodes are operating over the same spectral band, power control can be employed to combat the interference among the users [6]. Furthermore, the selection of transmission power of a node also determines the network topology, and thus influences the performance of the employed routing protocol at the network layer.

In a word, as shown in [1], transmission power control in an ad hoc network can potentially improve the throughput of a network greatly, while minimizing the power consumption of each node. Therefore, power control is one of the techniques that are used to achieve power efficient communications in an ad hoc network.

On the other hand, scheduling algorithms are often employed together with power control to schedule conflicting transmissions which cannot be combated by power control alone. For example, in an ad hoc network, a mobile node may want to transmit and receive at the same time, and this kind of conflict cannot be solved by power control. Hence, a scheduling algorithm is necessary to solve this conflict. Recently, joint power control and scheduling algorithms have been studied in the context of ad hoc networks [6, 8].

1.3.2 Multiple Input Multiple Output (MIMO)

MIMO communications have proved to be a promising technique to improve the spectral efficiency and channel capacity of a communication system by utilizing multiple transmit and/or receive antennas and advanced space-time coding algorithms [3]. Numerous works have been proposed and have shown the performance gain of MIMO in infrastructure-based wireless networks, such as cellular networks and WLAN. Recently, there has been increasing interest to extend MIMO techniques to wireless ad hoc networks [4, 67, 68], so that the bandwidth of a network can be exploited efficiently and data rate over the network can be increased.

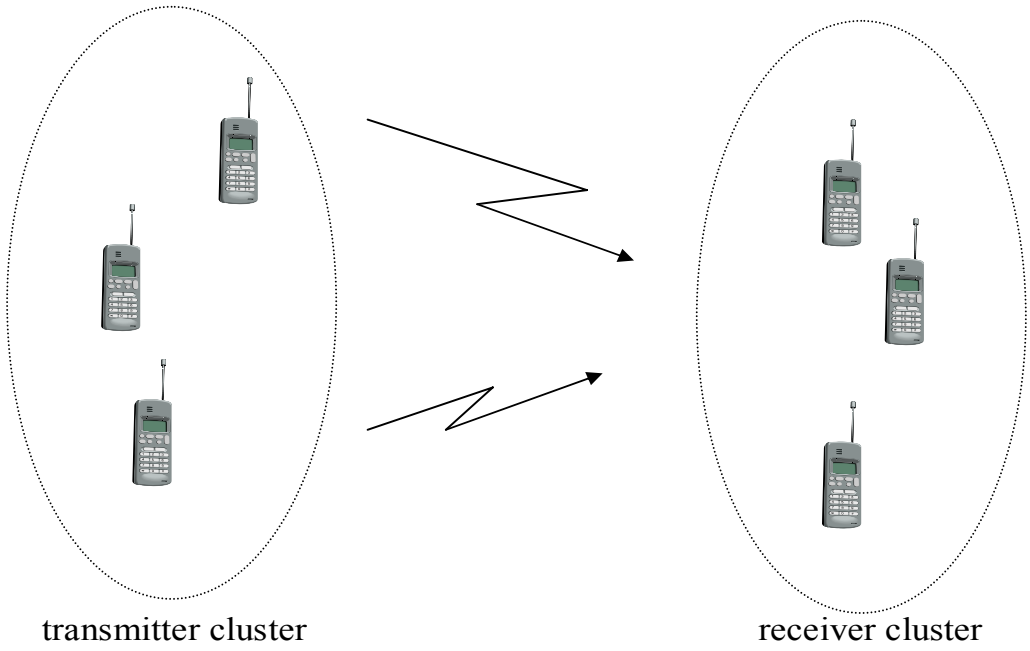

Fig.1.2. An example of cooperative MIMO communication system.

Although the application of MIMO to ad hoc networks is promising, in wireless ad hoc/sensor networks, direct employment of MIMO to each node might not be feasible, since MIMO might require complex transceiver and signal processing modules, which result in high power consumption and high cost for each node. Furthermore, nodes in wireless ad hoc networks/sensor networks are often powered by batteries with limited energy. This makes direct application of MIMO to each node inefficient from a power-efficiency point of view. Also, nodes in an ad hoc/sensor network might be of small physical size, which precludes the implementation of multiple antennas at each node.

As alternatives, cooperative MIMO techniques [69, 70] have been proposed. By the cooperation of multiple nodes, each of which has a single antenna, a virtual MIMO structure can be constructed which supports space-time processing, and thus

the merits of MIMO can still be exploited. As shown in Fig.1.2, three nodes cooperate together to form the transmitter antenna array and three nodes at the receiver side form the receiver antenna array, so that a virtual MIMO structure is formed by the cooperation among nodes.

1.3.3 Cognitive Radio

Cognitive radio is an emerging technique that can greatly improve the spectrum utilization of a communication system. The motivation behind cognitive radio is that most of the spectrum is allocated to specific applications, such as broadcasting TV, but on the other hand, most of the spectrum is under-utilized. In order to improve the spectrum utilization and exploit the spectrum more efficiently, cognitive radio has been proposed [41, 47]. As defined in [41], cognitive radio is an intelligent and adaptive wireless communication system that is made aware of its surrounding environment by sensing or sniffing the spectrum, and is able to adapt its operating parameters, such as transmit power, carrier frequency and modulation format, in real-time to be responsive to the environment dynamics.

The deployment of cognitive radio into wireless ad hoc networks is necessary and beneficial, since in challenging scenarios, such as a battlefield ad hoc network, a communication unit may not be able to operate in a fixed assigned band due to environmental constraints and/or application constraints, but rather have to search for an appropriate band in which to operate. On the other hand, the spectrum utilization information is usually not directly available for users in an ad hoc network. This can impose major difficulties for system design. However, cognitive radio, the technique that allows users to dynamically sense the frequency spectrum, find the available spectrum bands in a target spectral range, and then transmit without introducing excessive interference to the existing users in this spectral range, provides a technique

to solve this problem [41]. Thus, cognitive radio can enhance the performance in terms of spectrum utilization in ad hoc networks, since it allows mobile users within an ad hoc network to share the spectrum more efficiently, and also may allow these users to "borrow" bandwidth from other wireless systems if that bandwidth is not in use.

1.3.4 Cooperation

Generally, mobile nodes within an ad hoc network are independent and each node performs its own task separately. However, in order to improve the network performance, certain degrees of cooperation among multiple mobile nodes are necessary. More specifically, cooperation in an ad hoc network can be used to enhance the power efficiency of the network, improve the throughput of the network, or exploit the spatial diversity/multi-user diversity in the network. Many cooperation schemes have been proposed in the literatures [61, 79, 89], including cooperative allocation of resources, cooperative routing, cluster-based cooperative MIMO and etc.

The cooperation in ad hoc networks usually requires the exchange of some side information among multiple nodes. The overhead induced by the exchange of side information will take extra system bandwidth and power consumption, which usually limits the cooperation of a given node to other nodes to fall within a certain range. Within that range, neighboring nodes can exchange information to improve their own performance by taking into account other users' situations.

1.3.5 Cross-Layer Design Approach

In the traditional ISO protocol stack, each layer only takes into account its own information and performs its operation independent of other layers. However, better system performance can be expected if multiple layers can cooperate and share

information. For example, the physical layer can adjust the power level and modulation size based not only on the channel state information, but also on the network conditions and/or application requirements, such as delay. This kind of cooperation is done via the cross-layer design approach, where, based on application requirements and system constraints, multiple layers work together and exchange information, and adjust their operating parameters interdependently. Recently, many works have been proposed to improve system performance, such as power efficiency and spectrum efficiency, via a cross-layer design approach [6, 15].

1.4 Motivation and Thesis Outline

In wireless ad hoc networks, power and spectrum are two limited and precious system resources, and how to use them efficiently is the key to provide high performance communications in wireless ad hoc networks. Based on the previous discussions, in order to achieve high-performance communications in wireless ad hoc networks, multiple protocol layers should be able to work together in a cross-layer manner, and a distributed algorithm is necessary to efficiently exploit the system resources. Therefore, in this thesis, the focus is on how to achieve power-efficient and spectrum-efficient wireless communications in ad hoc networks via cross-layer design approach in a distributed manner. The outline of this thesis is as follows:

In Chapter II, we propose a cross-layer distributed power control and scheduling protocol for delay-constrained applications over mobile CDMA-based ad hoc wireless networks. Herein, we propose a novel scheme where power control is employed to combat delay occurring in multi-hop wireless ad hoc networks via cross-layer information exchange. Based on that, a distributed power control and scheduling protocol is proposed to control the incurred delay as well as the multiple access interference (MAI). Unlike other previous work on power control and

scheduling, we also investigate the impact of Doppler spread upon the system performance, and provide a robust system which employs a combination of power control and coding/interleaving to combat the effects of Doppler spread by exploiting the time diversity when the Doppler spread gets large. Hence, our proposed approach can function appropriately over a wide range of channel conditions.

In Chapter III, we propose a cognitive radio -based multi-user resource allocation framework for mobile ad hoc networks using multi-carrier DS CDMA modulation over a frequency-selective fading channel. In particular, given pre-existing communications in the spectrum where the system is operating, in addition to potential narrow-band interference, a channel sensing and estimation mechanism is provided to obtain information such as subcarrier availability, noise power and channel gain. Given this information, both frequency spectrum and power are allocated to emerging new users (i.e., cognitive radio users), based on a distributed multi-user resource allocation framework, in order to satisfy a target data rate and a power constraint of each cognitive radio user, while attempting to avoid interference to the existing communications as well as to minimize total power consumption of the cognitive radio users.

In Chapter IV, we investigate the issue of cooperative node selection in MIMO communications for wireless ad hoc/sensor networks, where a source node is surrounded by multiple neighbors and all of them are equipped with a single antenna. Given energy, delay and data rate constraints, a source node dynamically chooses its cooperating nodes from its neighbors to form a virtual MIMO system with the destination node (which is assumed to have multiple antennas), as well as adaptively allocates the power level and adjusts the constellation size for each of the selected cooperative nodes. In order to optimize system performance, we jointly consider the optimization of all these parameters, given the aforementioned system constraints. We

consider cases both with and without channel state information. Heuristic algorithms, such as maximal channel gain (MCG) and least channel correlation (LCC) algorithms are proposed in order to exploit available system information and to solve the constrained optimization problem.

In Chapter V, we provide summaries for each chapter individually, and conclude our contributions in this thesis. Finally, we provide some suggestions for possible future work.

2

Joint Power Control and Scheduling over CDMA -based Wireless Ad Hoc Networks with Delay Constraints

2.1 Introduction

Multiple benefits can be provided by judiciously controlling transmission power in wireless ad hoc networks. It can minimize the consumed power of a network while simultaneously alleviating the impacts of interference, thus the QoS requirement can be satisfied and system capacity can be increased. This has been extensively studied in [5-10] for cellular networks as well as for single-hop ad hoc networks. But these references have only focused on the tradeoff between power control and interference. However, in real-time applications, reducing delay could be as equally important as mitigating interference, and how to employ power control to reduce delay, which includes transmission delays over intermediate links as well as queuing delays at intermediate nodes due to queuing policy and/or channel conditions (deep fading/high MAI) over multi-hop wireless ad hoc network is absent from those previous works. On the other hand, in order to achieve efficient spatial/time/frequency reuse, scheduling conflicting transmissions has attracted considerably attention, and efficient scheduling algorithms have been proposed for both unicast transmission [6, 7, 11, 12, 13] and

multicast/broadcast transmission scenarios [8, 14], but typically with the assumption that perfect channel knowledge is available.

It has been shown in [15] that a cross-layer design framework can greatly improve system performance. Recently, this design approach has been extensively studied in [6, 15]. The purpose of this work is to consider the design of a cross-layer distributed power control and scheduling approach under both a delay constraint and an interference constraint. The cross-layer framework consists of distributed power control at the physical layer to combat both delay incurred by multi-hop transmission and channel conditions, a distributed scheduling algorithm at the link layer to eliminate conflicting transmissions in a CDMA-based wireless ad hoc network. Also, the cooperation between the physical layer and the link layer requires the cross-layer information exchange among the physical layer, the link layer, the network layer as well as the application layer. The constrained optimization problem under both the delay and the interference constraints is solved via three consecutive steps: delay control, scheduling and power control. Based on these three consecutive steps, the complexity of the constrained optimization problem is greatly reduced and the power control at the physical layer is substantially simplified. Finally, we investigate the impact of Doppler spread upon the system performance. Furthermore, we provide a robust system which employs a combination of power control, coding and interleaving to combat the effects of Doppler spread by exploiting the time diversity as the Doppler spread increases.

The organization of this chapter is as follows: in Section 2.2, we provide a brief discussion on the background and motivation; Section 2.3 presents the details of the proposed cross-layer distributed protocol; simulation results are provided in Section 2.4; finally, a summary and conclusions are included in Section 2.5.

2.2 Background and Motivation

In this chapter we consider the use of CDMA due to its capability to allow concurrent transmissions [5, 16, 17, 31, 36]. Note that in most of the current literature, the CDMA-based MAC protocols for ad hoc networks are generally based on random channel access [17, 31] where a node with a packet to transmit can start immediately using RTS/CTS exchange [18], without considering the channel conditions and the interference to other nodes. As a result, the well-known near-far problem may occur. To alleviate this problem, a controlled CDMA-based MAC protocol is desired to improve the system performance, as shown in this work as well as in [5].

There are three tradeoffs involved in power control design in a multihop network: *power vs. interference*, *power vs. delay* and *power vs. throughput*. The first tradeoff is widely studied [5, 6, 7, 8, 9, 10], where the power consumption of a network is minimized while the interference over each intended link is kept below a threshold; however, to the best of our knowledge, there is no work in the literature to address the second tradeoff over multi-hop links. The delay in a multi-hop ad-hoc network is mainly due to two sources: transmission delay on each hop and queuing delay induced at each intermediate node due to queuing policy and/or severe channel conditions (deep fading and/or high MAI). That is, the larger the number of intermediate nodes between the source and destination pair, the larger is the potential delay. In the current literature, the queuing delay is reduced by means of priority-based scheduling algorithms at the queues [13]. However, an alternative way to decrease the overall end-to-end delay is to increase the transmission power of a node, so that the transmission range of a node increases and thus fewer hops are needed from the source to the destination. However, increasing transmission power causes more interference to other active nodes in the system. Therefore, reducing delay and minimizing interference are two conflicting goals, and it is necessary to jointly consider the above

two tradeoffs. Finally, reducing delay means fewer hops between the source and the destination. The smaller hop count implies longer distance for a single hop, and results in a lower available data rate. As a consequence, the throughput will decrease. On the other hand, in order to keep a high data rate, more intermediate nodes are needed, and unavoidably, larger delay. Therefore, in a wireless multihop networks, reducing delay and achieving high throughput are also two conflicting goals. Therefore, in this work, we consider the design of power control which takes into account all the three tradeoffs.

As we know, the power control algorithm in DS-CDMA networks generally needs channel state information. A potential drawback of the existing cross-layer designs for power control and/or scheduling is that a small Doppler spread assumption is typically made, which often results in a perfect channel estimate assumption [5-8, 12-14]. Unfortunately, in practice, this assumption does not hold. In a mobile ad hoc network, Doppler spread might not be small. Since an increase of Doppler spread means the coherence time decreases, the estimates are thus noisier than they would be for a static channel. Therefore, in order to provide a possible solution to solve this problem, we first make use of a MMSE estimator in order to explicitly incorporate the impact of Doppler spread into the estimation procedure, and then we provide a scheme to combat the negative effects of Doppler spread, where coding/interleaving is employed together with power control in order to exploit the potential time diversity when Doppler spread gets large. Thus, a simple but relatively robust system is achieved in face of a wide range of channel conditions in wireless ad hoc networks.

2.3 Proposed Cross-Layer Distributed Protocol

We consider an asynchronous slotted CDMA-based ad hoc network with n users uniformly distributed in a certain geographic area, each using coherent M-ary

QAM modulation. Every node has an omni-directional antenna. For node i, the number of bits that can be supported, b_i, can be computed as [27]

$$b_i = \left\lfloor \log_2 \left(1 + \frac{3 \cdot \zeta_i}{\left[Q^{-1}\left(P_e / 4 \right) \right]^2} \right) \right\rfloor, \tag{2.1}$$

where ζ_i is the signal-to-interference-plus-noise-ratio (SINR), P_e is the required BER and $Q(\cdot)$ is the Gaussian tail function.

For each time slot, a node generates a packet to transmit (its own packet) with probability p, randomly destined to one of other nodes, or has a relay packet to transmit. In the design, we use two non-overlapping frequency channels, one for data transmission and the other for control messages. A unique spreading code is assigned to each node using some code assignment protocol [20] for data transmission, and a common spreading code is used over the control channel. Thus, we can achieve simultaneously transmission and reception from both the data channel and the control channel [5]. Also, we assume that the data channel and the control channel have the same channel conditions in both directions. The slot duration, T_s, is assumed to be larger than the fixed packet size to allow a guard interval which allows a preamble for both code and carrier synchronization. Also, the packet size in terms of number of chips and the chip rate are fixed. We further assume that the geographic location of other nodes can be obtained and provided to a node by location discovery schemes [21, 22]. In this chapter, we have put our focus on the performance improvement achieved by the cooperation between physical layer and MAC layer and the routing is not explicitly considered. Instead, routing is assumed to be known *a priori* for each source and destination pair as discussed in a later section. Thus, this work does not give the routing protocol the opportunity to determine the real optimal next hop. We may expect further performance improvement by incorporating power efficient routing into the proposed framework, though, with increased system complexity. However, it is out of

the scope of this work.

We let $\underline{Tx}$ and $\underline{Rx}$ be the transmitting node set and the associated receiving node set, each of which has m nodes, $m \le n$. $Tx(i)$ is the index of the i-th node in the transmitting node set and $Rx(i)$ is the index of its corresponding desired receiving node, $i = 1, 2, \ldots, m$, and $Tx(i)$ will cause MAI to $Rx(j)$ if $i \neq j$. Also, we let $D\{Tx(i)\}$ represent the delay for the packet to be transmitted at node $Tx(i)$ and we assume we can ignore both the processing delay and the propagation delay. $\zeta_{Tx(i)Rx(i)}$ is the SINR threshold to enable a successful reception. T_{max} is the maximum allowable delay for each packet. Finally, $P_{Tx(i)Rx(i)}$ is the power employed. Then, the constrained power optimization can be described as

$$\min\left\{\sum_{i=1}^{m} P_{Tx(i)Rx(i)}\right\} \tag{2.2}$$

s.t. ***C*1**: $D\{Tx(i)\} \le T_{\max}, \quad i = 1,2,...,m;$

***C*2**: *No node can receive and transmit at the same time and* $Rx(i) \neq Rx(j)$ *if* $i \neq j, i, j = 1,2,...,m;$

***C*3**: $SINR_{Tx(i)Rx(i)} \ge \zeta_{Tx(i)Rx(i)}$ *and* $0 \le P_{Tx(i)Rx(i)} \le P_{\max,}\ i = 1,2,...,m;$

***C*1** and ***C*3** represent the delay constraint and the interference constraint, respectively; ***C*2** indicates the validity constraint that a node cannot receive and transmit at the same time and a node is not allowed to receive from multiple desired nodes simultaneously. Unfortunately, the minimization of the total power under all the three constraints is very complex to solve analytically. Therefore, in this chapter, to make the optimization problem tractable, we divide the problem into three consecutive steps instead of solving it directly. As illustrated in Fig. 2. 1, the proposed approach is carried out at the start of each time slot and we first check the delay requirement for each transmission and schedule the current transmission to satisfy the delay requirement using power control; then, we check the validity of the scenario to avoid conflicting transmissions

which can not be eliminated by power control; lastly, we execute the distributed power control algorithm to minimize the power consumption while satisfying the QoS (SINR) of each receiver.

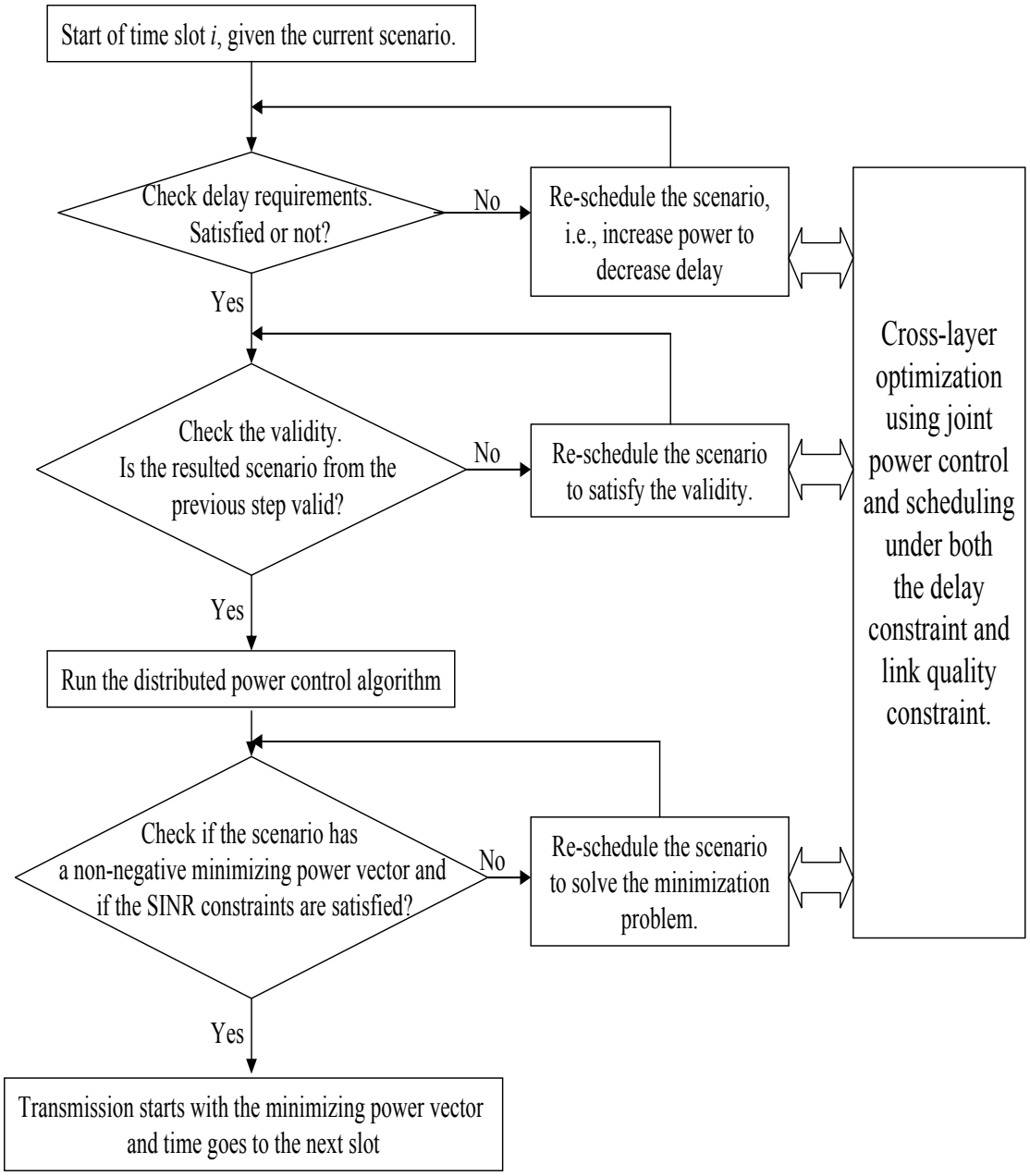

Fig. 2. 1. Illustration of the proposed joint power control and scheduling approach.

The reason we need to split the optimization problem into three consecutive steps is due to the lack of fixed infrastructure of an ad hoc network, and so any centralized control that depends upon infrastructure is not possible. The advantage of our approach is that we do not put the constraints on delay and validity into the power control optimization, and that results in a very simple power control optimization algorithm at physical layer. Furthermore, all the three steps can be implemented in distributed manners, as we will discuss in what follows. However, the consequence of this division is that the performance is suboptimal. The mismatch mainly comes from the delay control and validity check, since they are designed to guarantee the delay and validity constraints separately and might not be able to always find the global optimal transmission scenario. However, the global optimal depends on the optimization of the underlying routing, which is out of the scope of this chapter.

2.3.1 Delay Control

Since in this work we take into account the delay requirement, the delay modeling and delay calculation at the start of each time slot become important. Suppose for a packet, there are initially H hops from the source to the destination. Since we have assumed that the packet size and the chip rate are constant, the transmission delay $T_t^{(h)}$ on the h-th intermediate link is a constant for any h. We then have $T_t^{(h)} = T_t$, h=1, 2, …, H. Let $T_q^{(h)}$ be the queuing delay at the h-th node. Then the total delay T_{tot} is given by

$$T_{tot} = H \cdot T_t + \sum_{h=2}^{H} T_q^{(h)} . \tag{2.3}$$

If T_{tot} is larger than the threshold T_{max}, then the delay requirement cannot be satisfied. However, we can increase the transmission power at the source node to decrease the hop count, H. The criteria used here is that first we decrease the hop count

by 1. Then, we check the delay again, and if the delay is satisfied, the delay checking phase ends; otherwise, we decrease the hop count by 2 and we repeat the algorithm until the delay requirement is satisfied. If the source node and the destination node are connected directly and the delay is still not satisfied, this transmission is denied to save network resources.

We employ the average queuing delay $\bar{A}_q^{(h)}$ at node h as an estimate of $T_q^{(h)}$ in (2.3). It is worth noting that, due to this fact, our system fits those systems with average delay penalties instead of a hard delay constraint. Since our system is a slotted-CDMA system with slot duration T_s, the average queuing delay $\bar{A}_q^{(h)}$ is linearly proportional to the average number of packets queued in node h, $\bar{I}_q^{(h)}$, thus,

$$E\left[T_q^{(h)}\right] \equiv \overline{A}_q^{(h)} = T_s \times \bar{I}_q^{(h)} . \tag{2.4}$$

We now derive the average number of packets in the queue of a node in the system. In an ad hoc network, at any time slot, a node may generate its own packet to transmit and/or receive a relay packet to transmit, and the two events are independent Bernoulli processes. Let p and p_r be the two probabilities, respectively. Although a node attempts to transmit a packet at each time slot, its transmission may be deferred with probability p_d due to the embedded power control and scheduling considerations. Therefore, the queue of a node can be modeled as a $G/G/1$ queuing system [23]. We can easily see that the service time T is a geometric distribution with *pmf*

$$P\left(T = kT_s\right) = p_d^k \times \left(1 - p_d\right), \qquad k = 0, 1, 2, ... \tag{2.5}$$

Then, the average service time (inverse of the average service rate, μ) and the variance σ_s^2 of the service time can be computed, respectively, as

$$E[T] = \sum_{k=0}^{\infty} kT_s \times P\left(T = kT_s\right) = \sum_{k=0}^{\infty} kT_s \times p_d^k \times \left(1 - p_d\right) = T_s p_d / (1 - p_d) , \tag{2.6}$$

and

$$\sigma_s^2 = T_s^2 p_d / \left(1 - p_d\right)^2 . \tag{2.7}$$

Let Y be the r.v. representing the interarrival time. From the arrival aspect, we have two independent arrival processes as discussed above. Therefore, as shown in Appendix A, letting $(1 - p_r)(1 - p) = t$, the first two moments of the interarrival time Y are

$$E[Y] = \frac{T_s(1 - t - pp_r)}{1 - t}. \tag{2.8}$$

and

$$E[Y^2] = \frac{T_s^2(1 + t)(1 - t - pp_r)}{(1 - t)^2}. \tag{2.9}$$

Also, we let σ_Y^2 denote the variance of Y.

According to [24], with $\rho = \lambda/\mu$ and $\lambda = E[Y]$, the average number of packets of node h, $\bar{I}_q^{(h)}$, in a $G/G/1$ queuing system, can be bounded by

$$\frac{\lambda^2(\sigma_s^2 + \sigma_Y^2)}{2(1 - \rho)} - \frac{1 + \rho}{2} \le \bar{I}_q^{(h)} \le \frac{\lambda^2(\sigma_s^2 + \sigma_Y^2)}{2(1 - \rho)}, \tag{2.10}$$

which means that the difference between the upper and the lower bounds is $(1 + \rho)/2$, and since $0 < \rho < 1$, this difference is always between 1/2 and 1. Thus, we are able to determine the average queue length to within an accuracy of between 0.5 and 1 packet (depending on the value of ρ), which is typically satisfactory for any practical application [24]. Clearly, the average queuing delay $\bar{A}_q^{(h)}$ is a function of three parameters: p, p_r and p_d, Herein, p is a pre-specified probability for each node. However, p_r is dependent on the network topology, as well as the underlying routing protocol, and p_d is dependent on the embedded joint power control and scheduling approach. These two parameters are difficult to determine analytically, but can be estimated at each node on-the-fly, and the information can be provided to the source node via the routing discovery procedure to facilitate the delay checking and scheduling phase. This is easy to implement by inserting a particular field into the

routing control packet during the routing discovery procedure and will not induce any additional complexities and computational burden.

2.3.2 Validity Check and Distributed Scheduling

As shown in Fig. 2. 1, after the delay control, the algorithm goes into its second step, where the validity of the scenario is checked. The objectives consist of 1). Not allowing a node to transmit and receive simultaneously; 2). Not allowing a node to receive from more than one desired node. As a result, some nodes' transmissions might be deferred, and the criteria used to defer transmissions should take into account the throughput of the network, that is, trying to keep as many nodes as possible active in order to maintain a high throughput. The above scheduling algorithm can be implemented in a distributed manner, since we use two non-overlapping frequency channels, one for data transmission and the other for control message exchange. Hence, a node in the network can check if its transmission is valid via the information exchange over the control channel with the use of RTS/CTS control packets in IEEE 802.11 compliant protocols [25]. In case the validity of a node is violated, the node will schedule the conflicting transmissions using a multihop latency aware (MLA) algorithm [26] to determine which transmission is allowed to proceed, based on their relative priorities. We assume in the control channel some side information, such as the remaining hop count of a packet H_r and the remaining lifetime T_r, can be exchanged within the RTS/CTS control packets [25]. For each node, the information of H_r and T_r can be available to the scheduling via cross-layer information exchange. Clearly, the less the remaining lifetime a packet has, and the more remaining hops it has to traverse, the more urgent the packet is. Therefore, the ranking function of a packet is defined as [26]

$$\gamma(H_r, T_r) = T_r^b / H_r \,, \tag{2.11}$$

where b is non-negative and represents the relative weight of H_r and T_r. As a result, for a node whose validity is not satisfied, the node computes the corresponding γ for each packet, and the packet with the smallest $\gamma(H_r, T_r)$ is transmitted during the current slot, while all other conflicting transmissions are deferred. Thus, unlike [6], where a central controller is employed for scheduling, in our proposed approach a distributed scheduling algorithm is implemented with the use of a side channel which is orthogonal to the data channel. We further assume that the side information, i.e., H_r and T_r, is protected by enough FEC codes and no errors would occur on that.

2.3.3 Distributed Power Control

We model the wireless links as fading channels plus path loss factor η. Therefore, the channel can be described as

$$h(t) = u(t) \times \frac{1}{d^{\eta/2}} \,, \tag{2.12}$$

where $u(t)$ represents Rayleigh fading process, d is the distance between transmitter and receiver and η is the path loss exponent which is taken to be 4. If we express $u(t)$ as $u(t) = \alpha(t)e^{j\varphi(t)}$, then $u(t)$ is flat fading and can be viewed as a complex Gaussian r.v. with zero mean and variance $2\sigma^2$, where $\alpha(t)$ is Rayleigh distributed and $\varphi(t)$ is uniformly distributed in $[0, 2\pi]$.

As discussed previously, the objective of the power control is to minimize the power consumption, while satisfying both the delay constraint and the SINR constraint. Given the transmission scenario after the delay control and validity check, we only have to minimize the total power subject to a constraint on the SINR at each receiver. Let $\underline{N}$ represent the set of the active nodes and P_{ij} be the transmitted power from node i

to node j. The SINR threshold for node i to enable a successful reception at node j is ζ_{ij}. The processing gain of the CDMA system is M, and the maximum power of a node is P_{max}. Thus, the power control problem can be formulated as a constrained optimization problem:

$$\min_{P_{ij}} \sum_{i,j\in\underline{N}} P_{ij} \tag{2.13}$$

subject to

$$\begin{cases} SINR_{ij} \geq \zeta_{ij} \\ 0 < P_{ij} \leq P_{\max} \end{cases}, \forall i, j \in \underline{N} . \tag{2.14}$$

The SINR of node j can be expressed as

$$SINR_{ij} = \frac{P_{ij} \cdot \alpha_{ij}^2 / d_{ij}^{\eta}}{\sigma_N^2 + P_{MAI}^j}, \tag{2.15}$$

where σ^2_N is the thermal noise power at the receiver and P^j_{MAI} is the multiple access interference power at node j due to other interferers in the network, and can be shown to be [27]

$$P_{MAI}^j = \frac{2\sum_{x\neq i} P_{xj} \cdot \alpha_{xj}^2 / d_{xj}^{\eta}}{3M}, \tag{2.16}$$

where x represents a transmitter other than the intended transmitter i, P_{xj} is its transmission power, α_{xj} is its fading coefficient and d_{xj} is the distance between node x and node j.

Since it is desirable for the mobile nodes to transmit at the minimum power to maintain the required SINRs, the inequality representing the SINR constraint in (2.14) can be re-written as an equality $SINR_{ij} = \zeta_{ij}$. Hence, according to [9], the constrained power minimization problem can be solved using the following iterative algorithm at each transmitting node in a distributed manner:

$$P_{ij}(k+1) = \min\left\{ P_{\max}, \frac{\zeta_{ij}}{SINR_{ij}(k)} \cdot P_{ij}(k) \right\}, \tag{2.17}$$

where $SINR_{ij}(k)$ is the SINR at node j at iteration k. If all the nodes converge within a pre-set maximum number of iterations, and the SINR constraints of all the nodes are satisfied, then the minimizing power vector is found and the power control succeeds. Thus, a distributed power control can be achieved at each transmitting node and the convergence of such an iterative algorithm given by (2.17) is investigated in [9]. It was demonstrated in [9] that this algorithm converges exponentially fast to the optimal power vector, if such an optimal exists. Along the same lines, similar power control algorithms can be designed to have faster convergence rates, but may have higher complexity. In this work, (2.17) is employed to solve the distributed power control optimization.

However, if the optimal power vector does not exist, the transmissions must be re-scheduled such that an optimal power vector can be found. Therefore, we defer the transmission of the node with minimum SINR if power control fails. It has been shown in [10] that deferring the transmission of a node with minimum SINR is an efficient way to facilitate the solution of the constrained optimization problem. Furthermore, this scheduling algorithm can be implemented in a distributed manner, since the SINR values can be known by all other nodes, for example, by broadcasting the SINR values to all the transmitting nodes via a control channel.

Finally, from the above discussion, we see that in order to solve the problem of power control, we need to know the values of fading vector $\underline{\boldsymbol{\alpha}}$ for the current time slot. However, in previous works investigating power control algorithms, it has been assumed that channel information is perfectly available, and the fading is slow, i.e., small Doppler spread. In what follows, we discuss the estimation of the fading vector $\underline{\boldsymbol{\alpha}}$ and the impact of channel estimation error and Doppler spread upon the system performance.

2.3.4 Channel Estimation

From (2.12), we see that we only need to estimate $u(t)$, which is a complex Gaussian r.v.. Since generally, for power control algorithms, it is assumed that $u(t)$ is constant between two power control commands, for the i-th slot we need to estimate $u(i)$. As shown in [28], the autocorrelation function of a Rayleigh fading is

$$E\left[u(i)u^*(i-p)\right] = 2\sigma^2 J_0\left(2\pi f_d p T_s\right), \tag{2.18}$$

where $2\sigma^2$ is the variance of the fading process $u(t)$; $J_0(.)$ is the zero-th order Bessel function; T_s is the slot duration in our system; finally, $f_d = vf_c/C$ is the maximum Doppler spread, v is the velocity of a mobile node, f_c is the carrier frequency and C is the speed of light. We use the following notations:

$u(i)$: the actual fading value for time slot i;

$\hat{u}(i)$: the estimated fading value for time slot i, where the estimate at the transmitter is based on noisy past fading values measured at the receiver;

$\tilde{u}(k)$, $k = i\text{-}1,\ldots, i\text{-}V$: the measured fading value. We assume that the measured value at the receiver is corrupted by an additional complex Gaussian process $\underline{e}$, where $\tilde{u}(k) = u(k) + e(k)$ and $\underline{e}$ is also zero-mean with variance σ_e^2. Furthermore, we assume $\underline{e}$ is uncorrelated with $\underline{u}$ and $e(i)$ is uncorrelated with $e(j)$ if $i \neq j$.

If the estimate of $u(i)$ is based on V previous noisy channel samples [$\tilde{u}(i\text{-}1)$, $\tilde{u}(i\text{-}2),\ldots, \tilde{u}(i\text{-}V)$], then, using the following linear predictor of order V, we have

$$\hat{u}(i) = \sum_{j=1}^{V} b_j(i) \cdot \tilde{u}(i-j), \tag{2.19}$$

where $b_j(i)$, j = 1, 2, …, V, are the linear prediction coefficients. Under the Linear Minimum Mean Square Error criteria (LMMSE) [19], the coefficient vector $\underline{\boldsymbol{b}}(i) = [b_1(i), b_2(i),\ldots, b_V(i)]^T$ is

$$\underline{b}(i) = \underline{\underline{R}}^{-1}(i) \cdot \underline{r}(i), \tag{2.20}$$

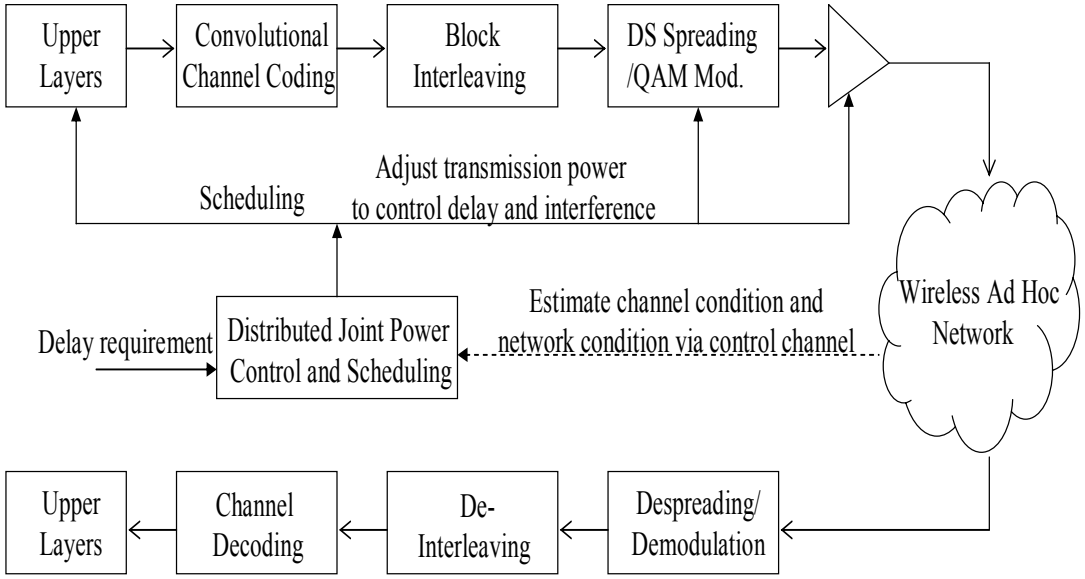

Fig. 2. 2. Illustration of the proposed joint power control and scheduling based on the combined use of power control, coding and interleaving.

where $\underline{R}$(i) is the V-by-V autocorrelation matrix of the V previous noisy channel samples, whose (p, q)-th element for p, q = 1, 2, …, V,

$$R(i)_{p,q} = E\left[\tilde{u}(i-p)\tilde{u}^*(i-q)\right] = 2\sigma^2 J_0\left(2\pi f_d |p-q| T_s\right) + \sigma_e^2 \delta_{p.q} \qquad (2.21)$$

where $\delta_{p,q}$ is the Kronecker delta function. Also, $\underline{r}(i)$ is the V-by-1 cross-correlation between the V previous noisy channel samples and the desired actual fading coefficient, whose p-th element, p = 1, 2, …, V, is given by

$$r(i)_p = E\left[u(i)\tilde{u}^*(i-p)\right] = E\left[u(i)u^*(i-p)\right] = 2\sigma^2 J_0\left(2\pi f_d p T_s\right) \qquad (2.22)$$

Therefore, given the past samples measured at the receiver, we can easily estimate the fading value for the current time slot at the transmitter. Those past samples measured at the receiver can be fed back to the transmitter via the control channel.

2.3.5 Coding and Interleaving

It is well known that as the Doppler spread increases, the coherence time decreases and the accuracy of the channel estimates degrades, since the channel samples are less correlated and the observation time available to both make and use the channel estimates is decreased. In other words, power control is less effective in handling the effects of fast fading and, as a result, the performance of DS-CDMA suffers. Fortunately, there is a counter balancing effect in DS-CDMA that leads to improved performance as the coherence time becomes smaller. When the coherence time gets small, the channel samples will be less correlated. This provides the potential for time diversity if coding and interleaving are used [29].

As shown in Fig. 2. 2, power control is used together with coding and interleaving in order to provide robust performance in a DS-CDMA wireless ad hoc network. In the proposed approach, we use a convolutional code and a block interleaving. Since the channel estimation accuracy cannot be guaranteed, we do not employ adaptive channel coding schemes. Instead, regardless of the channel conditions, a fixed rate r convolutional code and a fixed block interleaver (N, B) with interleaving length B -1 are used.

We have assumed that the MAI can be modeled as an additive Gaussian noise process that is independent of the thermal noise, which is modeled as an additive white Gaussian noise process. Thus, an upper bound on the bit error probability of the decoder of a rate r convolutional code is as follows [27]:

$$P_e \le \sum_{d=d_f}^{\infty} \beta(d) P_2(d). \tag{2.23}$$

In (2.23), d_f is the free distance of the convolutional code and the coefficients $\{\beta_d\}$ represent the number of symbol errors in two paths separated by distance d. The function $P_2(d)$ is the first event error probability and is related to the channel

conditions. For a network with n nodes, if we consider the transmission from node i to node j, in the scenario we are analyzing, the conditional $P_2(d)$, conditioned on the channel, can be approximated as in (2.24). The details are provided in Appendix B:

$$P_2\left(d \mid \boldsymbol{\alpha}\right) \le Q\left(\frac{1}{2} \cdot \frac{D_{\min}^{(M)} \sum_{l=1}^{d} \alpha_{m(l)}^2}{\left[\left(\sigma_N^2 + P_{MAI}\right) \cdot \sum_{l=1}^{d} \alpha_{m(l)}^2 + \sum_{i=1}^{d-1} \sum_{j=i+1}^{d} \alpha_{m(i)} \alpha_{m(j)} R_I\left(m(i) - m(j)\right) \right]^{\frac{1}{2}}} \right) \tag{2.24}$$

where $D^{(M)}_{min}$ is the smallest distance between two points in the M-QAM constellation, σ^2_N is the thermal noise power at the receiver, P_{MAI} is the multiple access interference power due to other interferers in the network, as in (2.15), and R_I is the correlation function of the multiple access interference (MAI) term, which is modeled as additive Gaussian noise. Since we want to investigate the impact of Doppler spread, MAI is not assumed to be white as in previous work [5, 6, 29]. Also, $\{m(l), l=1,\ldots,d\}$, with $m(1)< m(2)<\ldots< m(d)$, is the index of the set of d symbols in which the two paths differ, i.e., $m(l)$ is the position of the l-th non-zero symbol in the trellis of the convolutional code. Plugging (2.24) into (2.23), we obtain an approximation for the conditional residual bit error rate with convolutional coding out of the decoder of the desired user in the system.

As will be seen in the next section, the combined use of power control, coding and interleaving are, to some degree, complementary, resulting in robust overall system performance to the Doppler spread, and thus providing improved performance for a large range of channel conditions. In addition, it is worth noting that when channel coding is used, the spreading gain should be reduced due to the chip rate constraint as: $r_s \times M / r_c \le C$, where r_s, r_c, C and M are the information data rate, the channel coding rate, the chip rate and the processing gain, respectively.

Finally, consider the effect of overall delay due to the use of coding and interleaving. At a source node, as long as the queue is not empty, we can do the interleaving for a packet in the queue while it is waiting in the queue, thus there is no interleaving delay occurred. At the destination, since we need to receive a whole packet before it can be sent to the upper layers, and de-interleaving takes place after a packet is received. Therefore, the de-interleaving delay is only the processing delay associated with the de-interleaving procedure and it can be so small that the de-interleaving delay can be ignored. On the other hand, for the channel coding, since we still are able to encode when a packet is waiting in the queue of a node as long as the queue is not empty, there is no encoding delay. As for the decoding delay, since in this work a fixed-length packet size is employed regardless whether or not coding is used, the decoding delay introduced by convolutional code only occurs with the use of the maximum-likelihood decoding at the receiver, which is typically small [30].

2.4 Simulation Results and Discussion

In this section, we evaluate the performance of the algorithm, and compare it with the IEEE 802.11 scheme. Then we illustrate the impact of Doppler spread on the system performance. Finally, we show the complementary effects of using coding and interleaving to power control in a CDMA-based wireless ad hoc network. We start with the description of simulation setup.

We examine the performance of an ad hoc network with n = 15 nodes uniformly distributed in an area of size 200×200 m^2. Each node generates data packets to one of the other nodes with probability p for each time slot (p is the same for all nodes). The queue size of each node is unlimited, and the packets in a queue are served on a FIFO basis. In order to compare our approach with other schemes, we set the maximum allowable delay requirement T_{max} = 200 ms and the thermal noise power =

-55 dBm for all the schemes. Also, a common DS spreading code is used for all 802.11 receivers. At the final destination of a packet, the packet cannot be considered as "*correctly received*" if the delay requirement and/or SINR constraint are not satisfied. The convolutional code used is a rate 1/2 code with generator polynomials $(133, 171)_{oct}$ and the block interleaver size is $(N_I, B_I) = (11, 745)$. The modulation sizes used are BPSK, QPSK and 16-QAM, and the SINR threshold, ζ, in the power control step is determined as in (2.1) for different modulation sizes/rates.

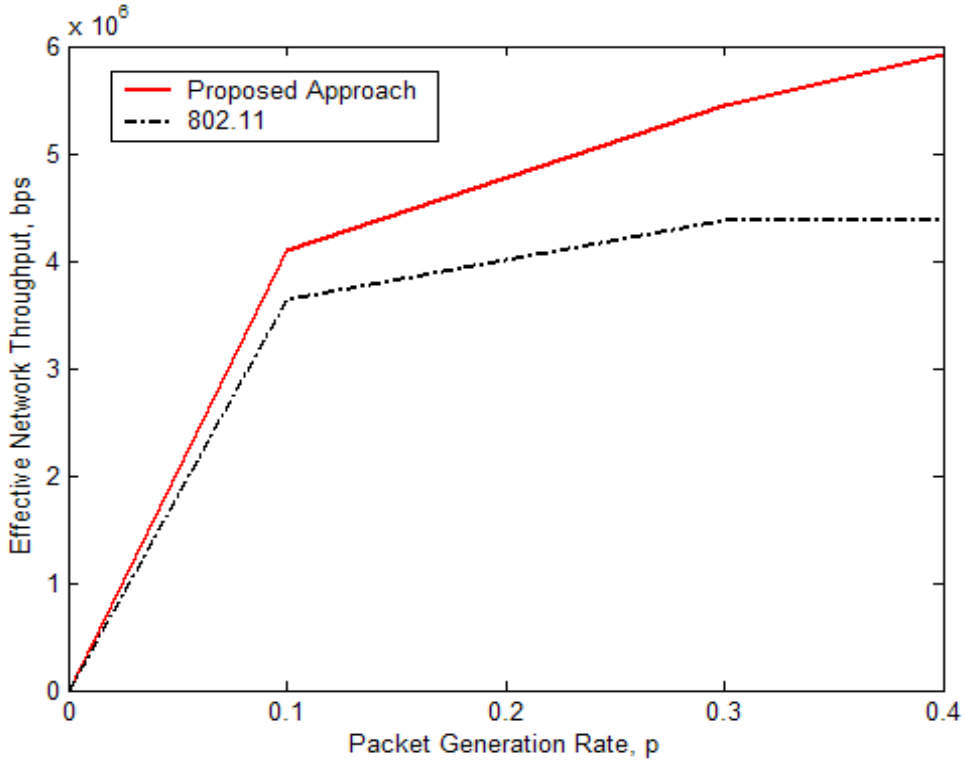

Fig. 2. 3. Performance comparison (effective throughput) between the proposed approach and IEEE 802.11 scheme; no coding/interleaving is used.

The routing protocol is the same for the two comparison schemes, and in order to reduce the impact of a specific routing algorithm, we employ the concept of the position-based protocol [33, 34] which assumes that the position information of each node is known by all other nodes, and the routing decision is only based on the

positions of the source, the destination and the neighboring nodes. Since the goal of this chapter is to evaluate the performance enhancement by the cooperation between the MAC layer and the physical layer, and as discussed previously, although the design of an advanced routing scheme can further improve the performance in a delay-constrained ad hoc network for both schemes, this is out of the scope of this chapter. In order to take into account the *delay vs. throughput* tradeoff associated with the delay control process, a simple scheme is employed: when delay control takes place, if the hop count is decreased by one, the modulation size is also decreased to the adjacent lower level in the employed modulation size set, and this results in a lower transmission rate. This simple scheme is only used to reflect the *delay vs. throughput* tradeoff and show the impact of this tradeoff. More advanced design procedures can be found in [34].

In Fig. 2. 3 to Fig. 2. 6, we initially evaluate the performance of the proposed approach where the channel estimate is perfect. In Fig. 2. 3, we illustrate the effective throughput of the proposed approach and the 802.11 comparison system. It is seen that throughput gain can be achieved by our approach relative to 802.11. The performance gain is due, first of all, to our approach that allows concurrent transmissions within the neighborhood of a receiving node through the distributed scheduling algorithm, while 802.11 does not; secondly, under both the delay and SINR constraints, our approach can adaptively adjust each transmitting node's power to avoid packet losses due to excessive delay at intermediate nodes and/or packet losses due to fading/MAI. Furthermore, when packet generation rate is low, say ≤ 0.1, the 802.11 comparison system can achieve a close performance to our approach, but when p increases, our approach outperforms it. This is due to the fact that when traffic is low, delay requirement can be easily satisfied since the queuing delay may be small, however, when traffic is high, delay requirement is hard to achieve without delay control since at

this time we may have large queuing delay at each intermediate node and thus delay control is necessary.

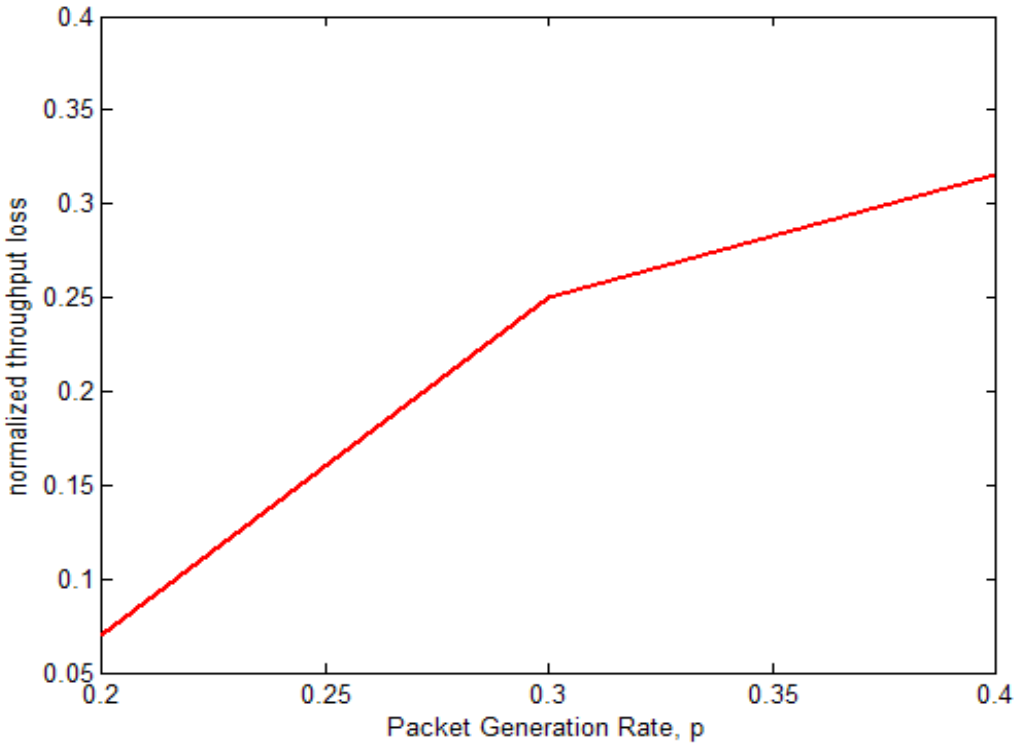

Fig. 2. 4. Normalized throughput loss for the proposed approach; normalized to the throughput of the case without considering the delay-throughput tradeoff; no coding/interleaving is used.

In Fig. 2. 4, we illustrate the normalized throughput loss of the network when the simple rate adaptation is used for the proposed approach. As we can see, when p is small, the loss is marginal since the delay is not stringent and the delay constraint can be satisfied for most of the transmissions. However, when p increases, the loss also gets large. This shows the effect of the delay-throughput tradeoff: when we reduce the delay, the throughput is also decreased. But, the proposed approach can still achieve performance gain compared to the 802.11 comparison system, as shown in Fig. 2. 3.

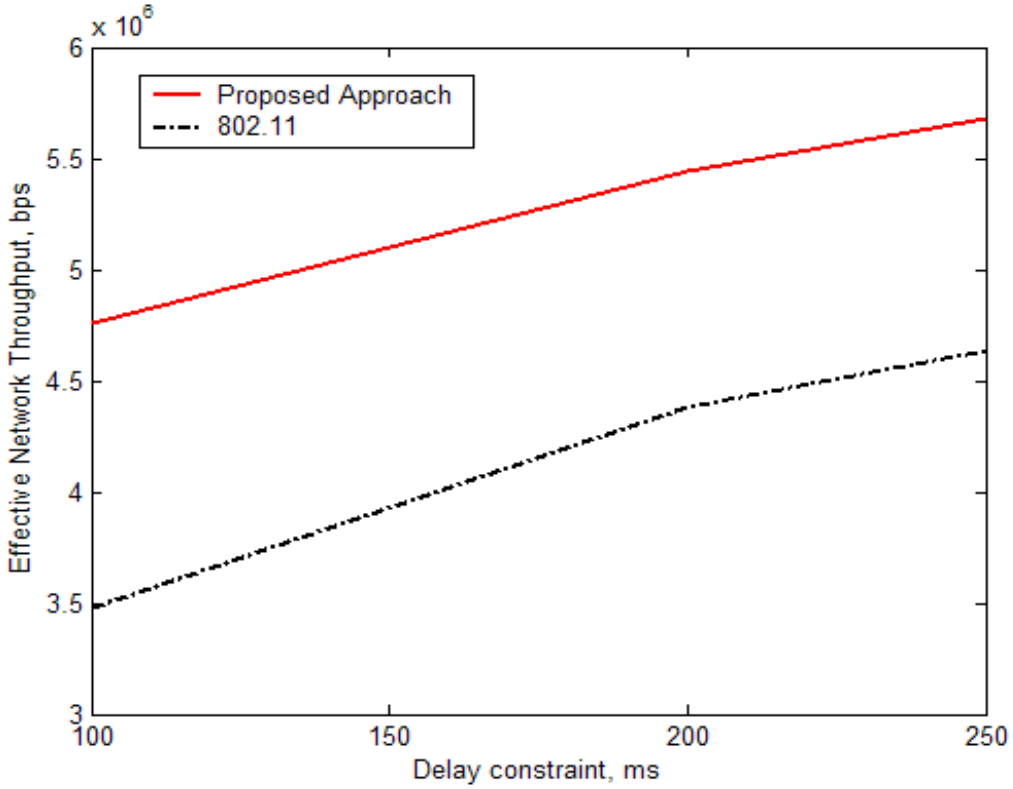

Fig. 2. 5. Performance comparison as a function of maximum allowable delay, between the proposed approach and the IEEE 802.11 scheme; $p = 0.3$; no coding/interleaving is used.

In Fig. 2. 5, we demonstrate the performance in terms of throughput as a function of maximum allowable delay requirement. First of all, we can observe that our approach can significantly outperform the 802.11 scheme when T_{max} varies; secondly, it is clear that when T_{max} becomes smaller, our approach suffers from some performance loss, this is caused by the throughput-delay tradeoff as discussed previously; finally, both 802.11 and the proposed approach can achieve improved performance when T_{max} increases since as T_{max} relaxes, more information can be correctly received at destinations.

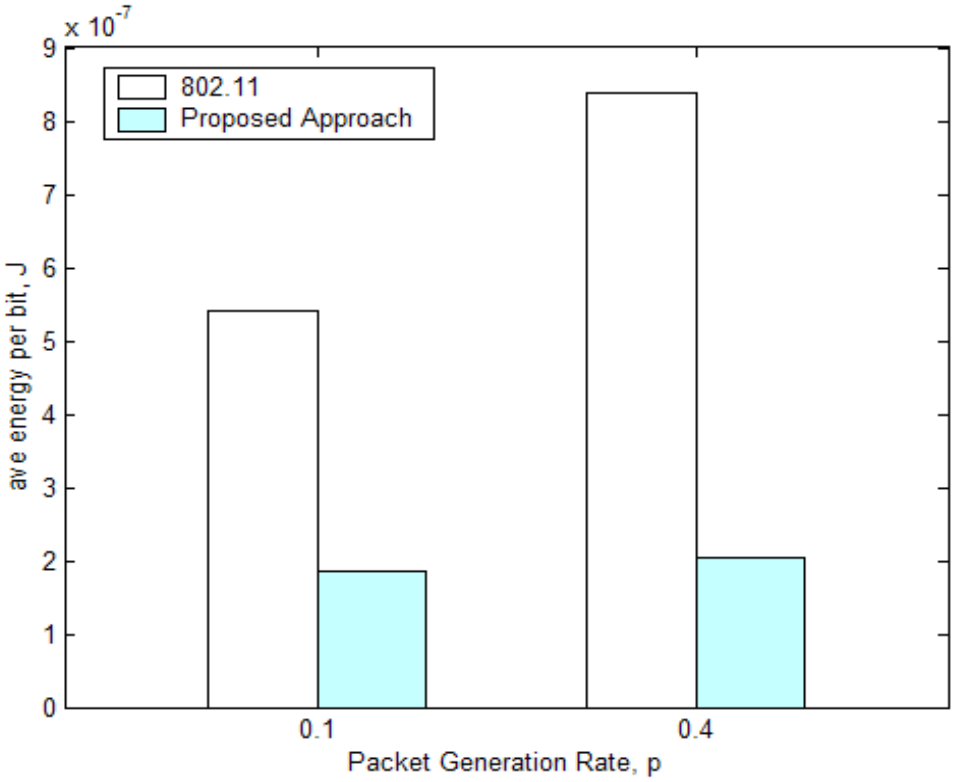

Fig. 2. 6. Performance comparison (average-energy-per-bit) between the proposed approach and the IEEE 802.11 scheme; no coding/interleaving is used.

In Fig. 2. 6, we illustrate the average-energy-per-bit at different packet generation rates, p. This metric can be used to evaluate the efficiency of a network, since it is actually the average energy employed for each correctly received bit. As can be seen in Fig. 2. 6, as p gets large, the energy consumption also increases since we generally need more power to combat the increased interference as traffic increases. On the other hand, energy savings can be achieved with the use of the proposed approach compared to the 802.11 scheme.

Up to this point, we have evaluated the system performance for perfect channel estimates. In Fig. 2. 7, we first demonstrate the performance degradation induced by the increase of Doppler spread; then we present the performance of a robust system which employs a combination of power control together with coding and interleaving

to combat the impact of Doppler spread and channel estimation errors. In Fig. 2. 7, we can clearly see that, for the cases of no coding and interleaving is employed, as Doppler spread gets large, the system throughput degrades substantially. The reason is, as Doppler spread gets large, the underlying channel becomes less correlated. Hence, accurate channel estimation is hard to obtain and as a result, power control works poorly.

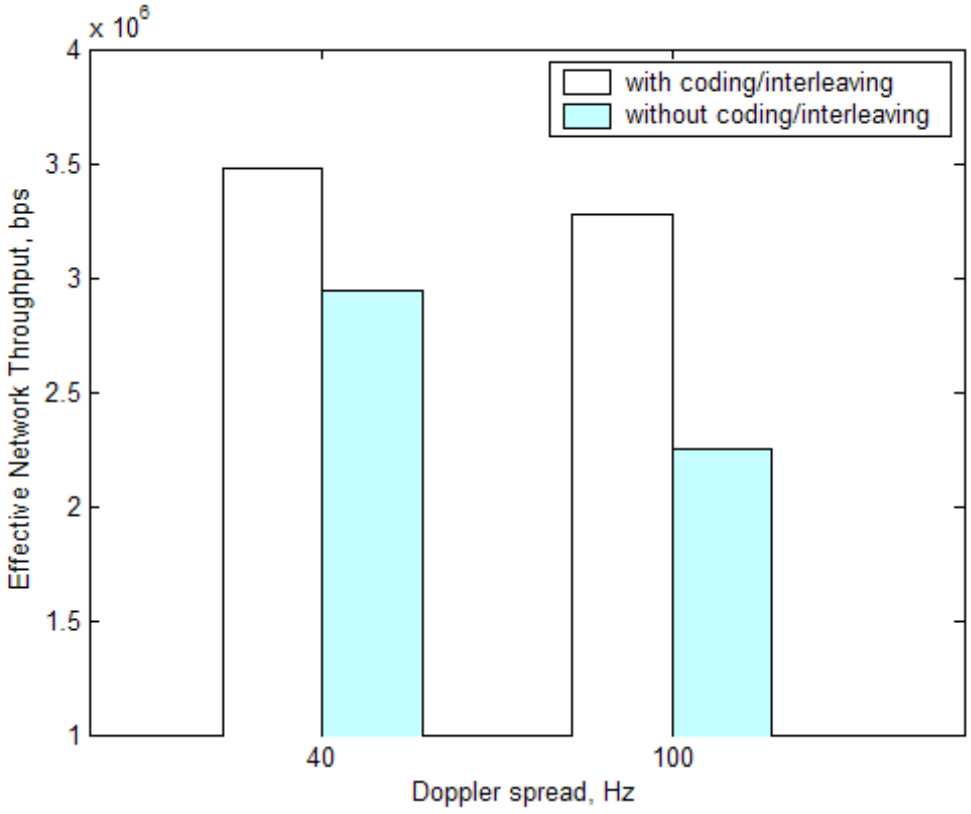

Fig. 2. 7. Performance as a function of Doppler spread; $p = 0.3$; σ_e^2 = -9dB; coding and interleaving are used.

Consider now the use of power control together with coding/interleaving. Fig. 2. 7 plots the performance when the combination of power control, coding and interleaving are used, as a function of Doppler spread. As can be seen, the performance of the combined use of power control, coding and interleaving is considerably better

than using power control alone since by using coding/interleaving, we can exploit the increased time diversity as Doppler spread increases, thus we can provide a complementary effect to power control and results in a relatively robust system. We, in particular, observe a significant improvement in performance at large Doppler spread.

2.5 Summary and Conclusions

In this chapter, we proposed a cross-layer distributed joint power control and scheduling approach for delay-sensitive applications, such as multimedia, over CDMA-based wireless ad hoc networks. The cross-layer framework consisted of distributed power control at physical layer, and distributed scheduling algorithm at MAC layer. Herein, we have taken into account a delay constraint as well as an SINR constraint for system performance optimization, and proposed a novel delay control mechanism where power control is used to combat delay. The constrained optimization problem under both the delay and SINR constraints was solved via three simple but effective steps: delay control, validity scheduling and power control. Based on these three consecutive steps, the complexity of the optimization problem was greatly reduced and the power control at the physical layer was substantially simplified. Finally, we investigated the impact of Doppler spread and channel estimation errors upon the system performance, and provided a robust system which employed the combination of power control, coding and interleaving to combat the effects of Doppler spread by exploiting the time diversity when the Doppler spread got large. Simulation results have demonstrated the effectiveness of the proposed approach.

It is worth noting that for any distributed system, where it is unavoidable to exchange information among users or neighbors, overhead issues should be carefully considered. In our work, we need to exchange information among users for the validity check and the power control, but since our system is designed for small/moderate-sized

networks, the overhead issue might not be a serious problem. However, as the network size increases, the problem of scalability becomes an important issue. A realistic approach to network scalability is to use a logical structure, e.g., a clustered-structure, to a physically unstructured ad hoc wireless network [32]. The concept of a sub-network, i.e., a cluster, where a set of mobile users is assigned to the sub-network manager (cluster head) is often desirable to ensure end-to-end communications, and can facilitate the implementation of the proposed framework to a network of very large size to avoid excessive overhead.

2.6 Appendix

2.6.1 Derivation of the Statistics of the Inter-Arrival Time, Y

We let "own" represent the event that a node's own packet is the first occurring packets and "relay" represent the event that a relay packet occurs first. Thus, we have the following general expression for the conditional PMF of Y, given an own packet occurs first:

$$P\left(Y = nT_s,\, n = 1,2... \middle| own\right) = \left(1 - p_r\right)\left[\left(1 - p\right)\left(1 - p_r\right)\right]^{n-1}\left(p + p_r - pp_r\right). \tag{2.25}$$

If we let $(1 - p_r)(1 - p) = t$, the conditional first moment of the inter-arrival time Y is

$$E\left[Y \middle| own\right] = \sum_{n=1}^{\infty} nT_s \times P\left(Y = nT_s \middle| own\right) = T_s\left(1 - p_r\right) \times \frac{1}{1-t}. \tag{2.26}$$

Following the same line, we can find the conditional first moment given that a relay packet occurs first, $E[Y|\text{relay}]$, as

$$E\left[Y \middle| relay\right] = \sum_{n=1}^{\infty} nT_s \times P\left(Y = nT_s \middle| relay\right) = T_s\left(1 - p\right) \times \frac{1}{1-t}. \tag{2.27}$$

Therefore, $E[Y]$ can be calculated as

$$\begin{aligned} E[Y] &= P(own)\cdot E[Y \mid own] + P(relay)\cdot E[Y \mid relay] \\ &= p\cdot E[Y \mid own] + p_r \cdot E[Y \mid relay] \end{aligned}. \tag{2.28}$$

So,

$$E[Y] = \frac{T_s(1-t-pp_r)}{1-t}. \tag{2.29}$$

Similarly, $E[Y^2]$ can be shown to be as

$$E[Y^2] = \frac{T_s^2(1+t)(1-t-pp_r)}{(1-t)^2}. \tag{2.30}$$

2.6.2 Derivation for the First Event Error Probability $P_2(d)$

If we consider the transmission of sequence $\boldsymbol{s}$ from a transmitter to its corresponding receiver, and the channel vector between them is $\boldsymbol{\alpha}$ and α_i is the corresponding channel gain for the i-th symbol. Then we have

$$\underline{y}_i = \alpha_i \cdot \underline{s}_i + \underline{v}_i, \tag{2.31}$$

where $\underline{y}_i$ is the output from the demodulator for the i-th received symbol and can be expressed in a vector form in both the I/Q branches as $\underline{y}_i = [y_i^{(I)}\ y_i^{(Q)}]$. Similarly, $\underline{s}_i$ is vector form of the i-th transmitted symbol, and $\underline{v}_i$ is the vector form of the sum of MAI, I, and thermal noise, N. Both the MAI and the noise are assumed to be zero-mean additive Gaussian random variables. We assume that the decoder chooses a wrong path $\hat{\boldsymbol{s}}$ instead of $\boldsymbol{s}$. This implies that the Euclidean distance between the received sequence and the transmitted sequence $\boldsymbol{s}$ is larger than that between the received sequence and the decoded sequence $\hat{\boldsymbol{s}}$. Thus, the conditional $P_2(d|\boldsymbol{\alpha})$, conditioned on $\boldsymbol{\alpha}$, can be shown to be

$$P_2\left(d \mid \boldsymbol{\alpha}\right) = \Pr\left\{\sum_{i=1}^{\infty}\left(\left\|\underline{y}_i - \alpha_i \cdot \hat{\underline{s}}_i\right\|^2 - \left\|\underline{y}_i - \alpha_i \cdot \underline{s}_i\right\|^2\right) < 0\right\}. \tag{2.32}$$

Since the decoded sequence differs from the transmitted sequence only in d positions, by plugging (2.31) into (2.32), from [35], we have

$$P_2\left(d \mid \boldsymbol{\alpha}\right) = \Pr\left\{\sum_{l=1}^{d}\left(\alpha_{m(l)}^2 \left\|\hat{\underline{s}}_{m(l)} - \underline{s}_{m(l)}\right\|^2 - 2\alpha_{m(l)}(\hat{\underline{s}}_{m(l)} - \underline{s}_{m(l)}) \cdot \underline{v}_{m(l)}\right) < 0\right\}, \quad (2.33)$$

where $m(l)$ is the position of the l-th non-zero symbol in the trellis of the convolutional code. Recalling that $\underline{v}_{m(l)} = \underline{N}_{m(l)} + \underline{I}_{m(l)}$, we can expand the above equation into both the I-branch and Q-branch, as shown in [35], yielding

$$\begin{aligned} P_2\left(d \mid \boldsymbol{\alpha}\right) = \Pr\{\sum_{l=1}^{d}\Big(\alpha_{m(l)}^2 \left\|\hat{\underline{s}}_{m(l)} - \underline{s}_{m(l)}\right\|^2 &- 2\alpha_{m(l)}(\hat{s}_{m(l)}^{(I)} - s_{m(l)}^{(I)}) \cdot N_{m(l)}^{(I)} - 2\alpha_{m(l)}(\hat{s}_{m(l)}^{(I)} - s_{m(l)}^{(I)}) \cdot I_{m(l)}^{(I)} \\ &- 2\alpha_{m(l)}(\hat{s}_{m(l)}^{(Q)} - s_{m(l)}^{(Q)}) \cdot N_{m(l)}^{(Q)} - 2\alpha_{m(l)}(\hat{s}_{m(l)}^{(Q)} - s_{m(l)}^{(Q)}) \cdot I_{m(l)}^{(Q)}\Big) < 0\} \\ \triangleq \Pr\left[\sum_{l=1}^{d} X(l) < 0\right] &\triangleq \Pr\left[X < 0\right] \end{aligned} \quad (2.34)$$

In (2.34), since N and I are assumed to be zero-mean Gaussian random variables, $X(l)$ and X can then be modeled as conditional Gaussian random variables, conditioned on $\boldsymbol{\alpha}$. The conditional mean and conditional variance of $X(l)$ can be shown to be

$$E\left(X(l) \mid \boldsymbol{\alpha}\right) = \alpha_{m(l)}^2 \left\|\hat{\underline{s}}_{m(l)} - \underline{s}_{m(l)}\right\|^2 \quad (2.35)$$

$$\begin{aligned} Var\left(X(l) \mid \boldsymbol{\alpha}\right) &= E\left(\left[X(l) - E\left[X(l)\right]\right]^2\right) \\ &= E([-2\alpha_{m(l)}(\hat{s}_{m(l)}^{(I)} - s_{m(l)}^{(I)}) \cdot N_{m(l)}^{(I)} - 2\alpha_{m(l)}(\hat{s}_{m(l)}^{(I)} - s_{m(l)}^{(I)}) \cdot I_{m(l)}^{(I)} \\ &\quad - 2\alpha_{m(l)}(\hat{s}_{m(l)}^{(Q)} - s_{m(l)}^{(Q)}) \cdot N_{m(l)}^{(Q)} - 2\alpha_{m(l)}(\hat{s}_{m(l)}^{(Q)} - s_{m(l)}^{(Q)}) \cdot I_{m(l)}^{(Q)}]^2) \\ &= 4\alpha_{m(l)}^2 \left\|\hat{\underline{s}}_{m(l)} - \underline{s}_{m(l)}\right\|^2 \left(\sigma_N^2 + P_{MAI}\right) \end{aligned} \quad (2.36)$$

In (2.35) and (2.36), we let $\|\hat{\underline{s}}_{m(l)} - \underline{s}_{m(l)}\| = D_{m(l)}$, and an upper bound of the error probability $P_2(d)$ can be achieved by assuming that, for all $m(l)$, $D_{m(l)}$ is equal to the worst-case value [35], which is defined to be D_o. Then, based on (2.35) and (2.36), we have the following:

$$E\left(X(l)\middle|\boldsymbol{\alpha}\right)=\alpha_{m(l)}^2 D_o^2 \quad \text{and} \quad Var\left(X(l)\middle|\boldsymbol{\alpha}\right)=4\alpha_{m(l)}^2 D_o^2\left(\sigma_N^2+P_{MAI}\right) \tag{2.37}$$

Now, since $X=\sum_{l=1}^{d} X(l)$, we can obtain the conditional mean and variance for the variable X as

$$E\left(X\middle|\boldsymbol{\alpha}\right)=D_o^2\sum_{l=1}^{d}\alpha_{m(l)}^2\,, \tag{2.38}$$

$$\begin{aligned} &Var\left(X\middle|\boldsymbol{\alpha}\right)=E\left(\left[X-E(X)\right]^2\right)\\ &=E([\sum_{l=1}^{d}-2\alpha_{m(l)}(\hat{s}_{m(l)}^{(I)}-s_{m(l)}^{(I)})\cdot N_{m(l)}^{(I)}-2\alpha_{m(l)}(\hat{s}_{m(l)}^{(I)}-s_{m(l)}^{(I)})\cdot I_{m(l)}^{(I)}\,.\\ &\quad -2\alpha_{m(l)}(\hat{s}_{m(l)}^{(Q)}-s_{m(l)}^{(Q)})\cdot N_{m(l)}^{(Q)}-2\alpha_{m(l)}(\hat{s}_{m(l)}^{(Q)}-s_{m(l)}^{(Q)})\cdot I_{m(l)}^{(Q)}]^2) \end{aligned} \tag{2.39}$$

Since the thermal noise samples are independent, but the MAI samples are, in general, correlated, then, according to [35], the above equation becomes

$$\begin{aligned} &Var\left(X\middle|\boldsymbol{\alpha}\right)\\ &=4D_o^2\left(\sigma_N^2+P_{MAI}\right)\sum_{l=1}^{d}\alpha_{m(l)}^2+\\ &\sum_{i=1}^{d-1}\sum_{j=i+1}^{d}4\alpha_{m(i)}\alpha_{m(j)}\left(\hat{s}_{m(i)}^{(I)}-s_{m(i)}^{(I)}\right)\left(\hat{s}_{m(j)}^{(I)}-s_{m(j)}^{(I)}\right)\cdot E\left[I_{m(i)}^{(I)}I_{m(j)}^{(I)}\right]\\ &+\sum_{i=1}^{d-1}\sum_{j=i+1}^{d}4\alpha_{m(i)}\alpha_{m(j)}\left(\hat{s}_{m(i)}^{(Q)}-s_{m(i)}^{(Q)}\right)\left(\hat{s}_{m(j)}^{(Q)}-s_{m(j)}^{(Q)}\right)\cdot E\left[I_{m(i)}^{(Q)}I_{m(j)}^{(Q)}\right]\\ &=4D_o^2\left(\sigma_N^2+P_{MAI}\right)\sum_{l=1}^{d}\alpha_{m(l)}^2+4D_o^2\sum_{i=1}^{d-1}\sum_{j=i+1}^{d}\alpha_{m(i)}\alpha_{m(j)}R_I\left(m(i)-m(j)\right) \end{aligned} \tag{2.40}$$

where

$$R_I\left(m(i)-m(j)\right)=E\left[I_{m(i)}^{(Q)}I_{m(j)}^{(Q)}\right]=E\left[I_{m(i)}^{(I)}I_{m(j)}^{(I)}\right]. \tag{2.41}$$

Thus, the conditional $P_2(d|\boldsymbol{\alpha})$, conditioned on $\boldsymbol{\alpha}$, can be shown to be

$$P_2\left(d\,|\,\boldsymbol{\alpha}\right) \le Q\left(\frac{1}{2}\cdot\frac{D_o\sum_{l=1}^{d}\alpha_{m(l)}^2}{\left[\left(\sigma_N^2+P_{MAI}\right)\cdot\sum_{l=1}^{d}\alpha_{m(l)}^2+\sum_{i=1}^{d-1}\sum_{j=i+1}^{d}\alpha_{m(i)}\alpha_{m(j)}R_I\left(m(i)-m(j)\right)\right]^{\frac{1}{2}}}\right). \tag{2.42}$$

As can be seen, in order to have an upper bound of $P_2(d|\boldsymbol{\alpha})$, D_o should be as small as possible. Thus, D_o may be selected as the minimum distance between two points in the employed M-QAM constellation, $D^{(M)}_{\min}$. Finally, by replacing D_o in (2.42) with $D^{(M)}_{\min}$, we have

$$P_2\left(d\,|\,\boldsymbol{\alpha}\right) \le Q\left(\frac{1}{2}\cdot\frac{D^{(M)}_{\min}\sum_{l=1}^{d}\alpha_{m(l)}^2}{\left[\left(\sigma_N^2+P_{MAI}\right)\cdot\sum_{l=1}^{d}\alpha_{m(l)}^2+\sum_{i=1}^{d-1}\sum_{j=i+1}^{d}\alpha_{m(i)}\alpha_{m(j)}R_I\left(m(i)-m(j)\right)\right]^{\frac{1}{2}}}\right). \tag{2.43}$$

Acknowledgement

This chapter, in full, is a reprint of the material as it appears in Qi Qu, Laurence B. Milstein and Dhadesugoor R. Vaman, "Cross-Layer Distributed Joint Power Control and Scheduling for Delay-Constrained Applications over CDMA-based Wireless Ad-hoc Networks", which is submitted to the *IEEE Transactions on Communications* and is currently under review. The dissertation author was the primary investigator and author of this publication.

3

Cognitive Radio Based Multi-User Resource Allocation in Mobile Ad Hoc Networks

3.1 Introduction

In wireless multi-user communications, how to efficiently utilize the system resources, such as frequency spectrum and power, and to provide high quality transmission, are the main challenges for the deployment of next generation systems. To address these challenges, multi-user resource allocation based on multi-carrier modulation, such as orthogonal frequency division multiplexing (OFDM), has attracted extensive attention [37, 38, 39, 40], where subcarrier band, data rate and power are adaptively allocated to each user. However, the results of these research efforts are limited, since they are typically intended for the downlink of a cellular system where, given the available frequency spectrum, a base station (BS) is used to coordinate the cooperation between the users within a cell and optimally distribute the system resources. Furthermore, the resource allocations as in [37-40] are performed by assuming that the spectral utilization information is known *a priori* with the aid of a BS, which is not realistic in scenarios where infrastructure is not available, such as in ad hoc networks.

In challenging scenarios, such as a battlefield ad hoc network, a communication unit may not be able to operate in a fixed assigned band due to environmental constraints and/or application constraints, but rather have to search for an appropriate

band in which to operate from time to time. On the other hand, the spectrum utilization information is not directly available for users. These can impose major difficulties for system design. However, cognitive radio, a technique that allows users to dynamically sense the frequency spectrum, find the available spectrum bands in a target spectral range, and then transmit without introducing excessive interference to the existing users in this spectral range, provides a technique to solve this problem [41]. In order to facilitate the dynamic spectrum access in such a cognitive radio based network, various schemes have been proposed. In [42], by using a partially observable Markov decision process, cognitive MAC protocols are proposed to optimize the system performance, while limiting the interference to primary users via optimal channel allocation strategies; in [43], a spectrum-sharing problem in an unlicensed band is studied under game-theoretic approaches; in [44], the authors investigate the cooperative spectrum sensing in cognitive radio networks, and show that cooperation among users can significantly increase the agility of cognitive radio users, and hence improve the system performance; also [45] presents a sensing-throughput tradeoff in cognitive radio networks, and shows how to maximize the achievable throughput for the CR users under the constraint that the primary users are sufficiently protected.

In this chapter, we design a multi-user resource allocation framework using a cognitive radio perspective. In particular, we consider a multi-carrier system where the entire spectral range is first sensed, and then the un-used subcarrier bands are employed by cognitive radio (CR) users, thus increasing the spectral utilization. Because we must avoid noticeable interference to existing users, we propose a mechanism to detect the availability of a subcarrier by sensing the RF spectrum, as well as to estimate the noise power and the channel gain for each free subcarrier. Then, given all the obtained information, as well as a power constraint and a target data rate for each CR user, a distributed spectrum and power allocation approach is proposed. In

order to protect the primary users and facilitate the dynamic access process, i.e., combat possible transmission conflicts due to detection errors and the lack of a central control, we also provide an adaptive power control algorithm with user protection and adaptive rate control. In general, this chapter presents a system design framework for cognitive radio networks, which includes the main components of a cognitive radio system, and shows how the system performance is affected by underlying system parameters.

It is worth pointing out that the focus of this chapter is to design a military cognitive radio system where given the existing communications (primary users) over a spectral range, how to accommodate new users (cognitive radio users) into the system without interfering with the existing communications. Once a new user successfully accesses the system and starts transmission, it then becomes a primary user. The definitions of primary user and cognitive radio user in this chapter are slightly different from those in commercial cognitive radio systems.

The organization of the rest of the chapter is as follows: in Section 3.2, we provide the system description and the problem formulation; in Section 3.3, we describe the detection and estimation mechanism necessary for the system to function properly, as well as the detailed algorithms for spectrum management and power control; in Section 3.4, we present simulation results and corresponding discussions; finally, a summary and conclusions are provided in Section 3.5.

3.2 System Description and Problem Formulation

We consider a multicarrier DS CDMA system [42] in conjunction with a wireless ad hoc network. The wireless channel is modeled as a frequency-selective, Rayleigh fading channel. We let the available frequency spectrum be divided into M equi-width frequency bands, each with bandwidth B, where M is the total number of

subcarriers. We assume, as in [46], by an appropriate choice of subcarrier width, that each subcarrier experiences flat fading. In addition, we use bandlimited multicarrier waveforms to eliminate the interference between different subcarriers. In this chapter, for simplicity, we assume that the entire spectrum is divided into a fixed number of subcarriers. At a given time instant, we assume N CR transmitter-receiver pairs want to access the channel, and the i-th pair, $i = 1,\ldots,N$, has a specified data rate requirement, R_i and a bit-error-rate requirement, BER_i. However, some primary users may already be using the same frequency spectrum, and so some subcarrier bands may already be in use. In order to avoid interference to the pre-existing communications (primary users), those occupied subcarriers should be detected and should avoid being used by the CR users. Thus, a detection/estimation mechanism is proposed in this chapter to first detect the availabilities of subcarriers for each CR user, and then to estimate the corresponding noise power and channel gain for each available subcarrier. We define the set of free subcarriers available to user i as F_i, and assume there are A_i free subcarriers in that set[1]. F_i is obtained by the detection mechanism, but due to detection errors, not all decisions will be correct.

We let $P_i^{(k)}$ be the transmit power allocated to transmitter i on the k-th available subcarrier, where $k = 1,\ldots,A_i$, and $P_i^{(k)} = 0$ if transmitter i does not use subcarrier k. We also let $\alpha_{ij}^{(k)}$ indicate the channel gain between the i-th transmitter and the j-th receiver on subcarrier k, and assume it contains both path loss and fading effects. At the k-th available subcarrier of the i-th CR receiver, the corresponding noise floor power spectral density is defined to be $S_i^{(k)}(f)$, and is estimated via a detection/estimation mechanism to be discussed in a later section. It is worth noting that $S_i^{(k)}(f)$ may represent three sources of noise/interference: thermal noise, interference caused by

[1] The available subcarrier set F_i for user i indicates the number of free subcarriers and their positions in the spectrum. The number of available subcarriers A_i and the positions of these subcarriers in F_i may be different for different i due to detection errors.

primary users if a subcarrier availability detection error occurs, and possible narrowband interference (NBI) generated by jammers. In this chapter, the NBI generated by enemy jammers is assumed to be bandlimited white Gaussian noise with power spectral density $S_J(f)$ as in [46]:

$$S_J(f) = \begin{cases} \frac{n_J}{2}, & f_J - \frac{W_J}{2} \le |f| \le f_J + \frac{W_J}{2} \\ 0, & otherwise \end{cases}, \tag{3.1}$$

where f_J and W_J are the center frequency and the bandwidth of the interference, respectively. Each user is assumed to be hit by NBI with probability P_{NBI}, and both f_J and W_J can be random. Furthermore, the effect of the noise, the NBI and the possible interference from primary users (referred to below as just "noise") at the i-th cognitive radio receiver is modeled as a random process with noise power $N_i^{(k)}=\int_B S_i^{(k)}(f)df$.

We further let $b_i^{(k)}$ be the number of bits-per-symbol transmitted by cognitive radio user i on its k-th subcarrier, and we employ M-ary quadrature amplitude modulation (MQAM). By assuming the use of coherent demodulation, the number of bits that can be transmitted over user i's k-th subcarrier can be shown to be [27, *Eq*. 5.2-80]

$$b_i^{(k)} = \min\left\{ b_{\max}, \left\lfloor \log_2\left(1 + \frac{3 \cdot \zeta_i^{(k)}}{\Omega}\right) \right\rfloor \right\}, \tag{3.2}$$

where b_{max} is determined by the maximum allowable signal constellation; $\zeta_i^{(k)}$ is the instantaneous signal-to-interference-plus-noise-ratio on the k-th subcarrier of user i, and Ω is related to the corresponding BER requirement on that link, and can be expressed as

$$\zeta_i^{(k)} = \frac{P_i^{(k)} \cdot \alpha_{ii}^{(k)}}{I_i^{(k)} + N_i^{(k)}}. \tag{3.3}$$

In (3.3), $I_i^{(k)}$ is the interference on the k-th subcarrier of user i caused by other cognitive radio users which employ the same subcarrier k and is modeled as additional Gaussian

noise and $N_i^{(k)}$ is the noise power on the k-th subcarrier of user i as described previously. Given the N CR users who want to access the spectrum and the pre-existing primary users over the spectrum, $I_i^{(k)}$ represents the interference induced by other cognitive radio users who are allocated to use the k-th subcarrier of user i by the resource allocation algorithm; on the other hand, $N_i^{(k)}$ is partially due to some pre-existing primary users when a detection error occurs, i.e., the k-th subcarrier of user i is incorrectly declared to be available to user i and is actually shared by some other primary user. It is worth noting that if the number of primary users and cognitive radio users sharing a subcarrier is large enough, $I_i^{(k)}$ and $N_i^{(k)}$ can be approximated as Gaussian noise due to the central limit theorem. Unfortunately, it is hard to guarantee that condition to be satisfied. However, as in Appendix A, it was shown that even if the number of users is not large, we still can approximate the interference as Gaussian noise as long as the spreading gain is sufficiently large. Similar results can also be found in [48, 49]. Finally,

$$\Omega = \left[Q^{-1}\left(\frac{BER_i^{(k)}}{4} \right) \right]^2, \tag{3.4}$$

where $Q(\cdot)$ is the Gaussian tail function.

Our problem now is as follows: at a given instant, N CR users have data to transmit over the spectrum, but there are already some pre-existing users that occupy the spectrum. In order to avoid interference to existing primary users, each CR user has to detect the availability of each subcarrier, and it can only select subcarriers from its corresponding available subcarrier set F_i, $i = 1,\ldots,N$. By appropriately selecting the subcarriers, the objective is to minimize the required power consumption of all the CR users while satisfying the BER and data rate requirements of each of them. The goal is to find the optimal subcarrier assignment for each CR user, as well as the corresponding optimal power and bit allocations. Mathematically, we formulate the

problem as follows:

$$\min\left(\sum_{i=1}^{N}\sum_{k=1}^{A_i} P_i^{(k)}\right), \quad \textit{subject to} \tag{3.5}$$

$$\textbf{C1}: \ \sum_{k=1}^{A_i} P_i^{(k)} \le P_{\max}, \ i=1,\ldots,N. \qquad \textbf{C2}: \ \sum_{k=1}^{A_i} b_i^{(k)} \ge R_i, \ i=1,\ldots,N.$$

C3: The detected available subcarrier set F_i has A_i subcarriers, $i=1,\ldots,N$.

Note that constraint **C1** represents the power constraint of each user; **C2** involves the data rate requirement of each user; **C3** attempts to ensure that the existing communications would not be interfered by emerging new transmissions. The system attempts to satisfy the data rate requirement of each CR user, while avoiding interference to existing primary users. If user i does not use the k-th subcarrier, then $P_i^{(k)} = 0$ and $b_i^{(k)} = 0$. As discussed above, it is obvious that in order to solve this constrained optimization problem, we must know the following information: available subcarrier set F_i, noise floor power spectral density $S_i^{(k)}(f)$ and channel gain $\alpha_{ij}^{(k)}$. However, this information is typically not available to users in a mobile ad hoc network. Therefore, in the following section, we provide a cognitive radio approach to detect/estimate the necessary information such that the multi-user resource allocation on frequency spectrum, transmission power and transmitted data rates can be solved jointly.

3.3 Proposed Cognitive Radio Based Resource Allocation

The system is designed from a cognitive radio perspective, where a cognitive process is exploited whenever a mobile user plans to send data over the network. In particular, each cognitive process starts with a passive channel sensing at the transmitter of the RF stimuli at each subcarrier band and determines if a subcarrier has been occupied by pre-existing users. Also, the noise power and the corresponding

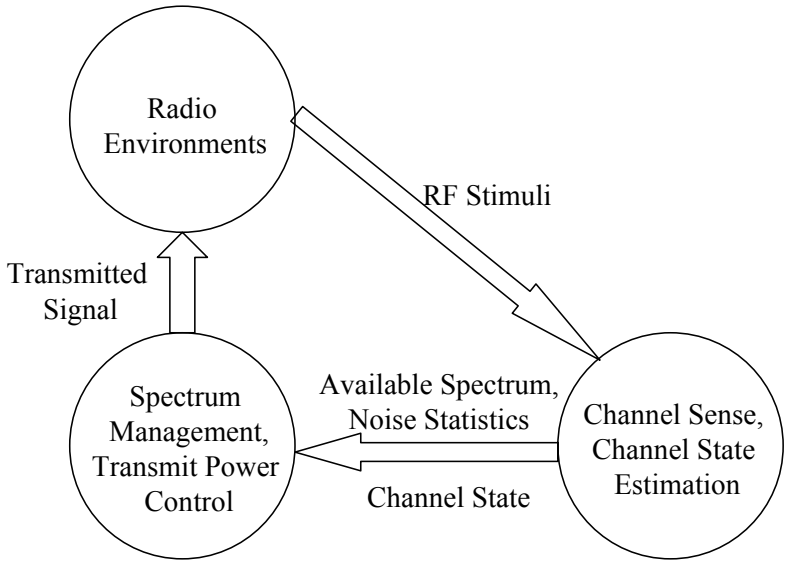

Fig. 3. 1. Cognitive cycle at each user.

channel gain at each available subcarrier are measured by the receiver. When the transmitter collects all the necessary information via a reliable feedback channel, spectrum management and power control are executed in order to allocate appropriate spectral bands and associated power levels to each user. The previous description forms a cognitive cycle as shown in Fig. 3. 1. In this section, we first describe a cognitive radio based mechanism for channel sensing and estimation; then we present an efficient framework for the spectrum and power management.

3.3.1 Detection and Estimation of Necessary Parameters

3.3.1.1 Distributed and Cooperative Subcarrier Availability Detection

Subcarrier availability detection is of paramount importance to avoid interference to existing primary communications. In general, not all the parameters of the existing primary signals are known, which means a waveform-based correlation method for signal detection at a given subcarrier is not feasible. As a consequence, one may consider power-based sensing. However, at high SNR, an energy detector is

nearly optimal [50], but it functions poorly at relatively low SNR, which is generally the case for signal detection in cognitive radio networks. For more details on other detection schemes, please refer to [44, 55, 64, 65, 66].

In this chapter, we employ the multitaper spectrum estimation method (MTM) due to its accuracy and near-optimality [41, 51], combined with singular value decomposition (SVD), to detect the availability of a subcarrier. We assume that each CR node in the network can sense the subcarrier channels in order to determine which channels are currently occupied by primary users. In particular, this method consists of two steps: at the first step, a node employs MTM to obtain the best possible expansion coefficients as defined in (3.6) below. Since the coefficients of the expansion contain both the contributions from the background noise and possible interference caused by existing users, at the second step, singular value decomposition is performed over the obtained expansion coefficients in order to isolate the effects of noise and interference. The computational complexity of this method is relatively high, but it is feasible and manageable as shown in Appendix B.

For a given subcarrier of a particular CR user, the user senses the RF stimuli from the given subcarrier and obtains a time sample series with V samples. Then it computes the expansion coefficients for that subcarrier based on the time series. The expansion coefficients are obtained by windowing the data with a Slepian sequence and then performing a Fourier transform [52]. As in [52, 53], we can compute those expansion coefficients whose energy are concentrated inside a resolution bandwidth, $2w$, which is a parameter used to control the estimation variance (see [52]) as

$$y_n(f) = \sum_{i=0}^{V-1} x(i) v_i^{(n)} e^{-j2\pi fi} \quad n = 0,1,...,K-1, \tag{3.6}$$

where $x(i)$ is the i-th sample of the time series and $v_i^{(n)}$ is the i-th sample of the n-th Slepian sequence with parameters V and w. Finally, K is the number of Slepian

sequences and equals $2wV$ [53]. The fast Fourier transform (FFT) can be employed to achieve an efficient computation of (3.6), thus the computation delay for the above process can be negligible.

In order to account for variations of the spectrum at different spatial locations, and thus to improve the detection reliability, after we obtain the expansion coefficients $y_n(f)$, where $n = 0, 1,\ldots, K\text{-}1$, for a given subcarrier, each node may send this information to its neighbors via a control channel for cooperation. Use of cooperation in wireless networks has been investigated extensively, especially to achieve diversity gains [54], and in a cognitive radio scenario, it is realistic to assume that users can exchange calculated information to achieve some kind of cooperation [55]. We assume node i receives H-1 sets of the $\underline{y}_n^{(h)}(f)$, $h = 1,\ldots, H\text{-}1$, from its H-1 neighbors, and, as a special case, if $H = 1$, there is no such cooperation and node i makes use of only its own information. At node i, we can form a spatial-temporal $H\times K$ matrix as [51]

$$\underline{\underline{A}}(f)=\begin{bmatrix} y_0^{(1)}(f) & y_1^{(1)}(f) & \cdots & y_{K-1}^{(1)}(f) \\ y_0^{(2)}(f) & y_1^{(2)}(f) & \cdots & y_{K-1}^{(2)}(f) \\ \vdots & \vdots & & \vdots \\ y_0^{(H)}(f) & y_1^{(H)}(f) & \cdots & y_{K-1}^{(H)}(f) \end{bmatrix}, \tag{3.7}$$

where each row is obtained at different spatial points, and each column is obtained by using different Slepian sequences [51]. Each entry of $\underline{\underline{A}}(f)$ has a contribution from the background noise process and has a contribution due to interference, if any. Since we are only interested in the possible interference caused by existing users, in order to isolate the possible interference from the background noise, a complex singular value decomposition is performed upon the above matrix [51, 56], resulting in

$$\underline{\underline{A}}(f)=\sum_{k=0}^{K-1}\eta_k(f)\underline{u}_k(f)^{+}\underline{v}_k(f), \tag{3.8}$$

where $\underline{u}_k(f)$ and $\underline{v}_k(f)$ represent a left singular vector and a right singular vector, respectively, "+" represents Hermitian transposition, and $\eta_k(f)$ is the k-th singular value,

with $\eta_0(f) \geq \eta_1(f) \geq \ldots \geq \eta_{K-1}(f) \geq 0$. Note that $\eta_k^2(f)$ is the associated k-th 'eigenvalue', and it provides an effective frequency domain signal detection parameter which is caused by unknown interference as a function of frequency [51, 56]. As shown in [56], by performing SVD on $\underline{\underline{A}}(f)$ and keeping only the first few largest terms of $\eta_k^2(f)$, we can significantly reduce the background noise while retaining most of the interference signal. Typically, only the largest eigenvalue $\eta_0^2(f)$ is used as a signal detection parameter [56].

Now at time t, we obtain the values for $\eta_k^2(f, t)$, $k = 0, 1, \ldots, K-1$, and $\eta_k^2(f, t)$ represents the eigenvalue at time t. If we choose the largest eigenvalue $\eta_0^2(f, t)$ as the desired detection parameter, we would like to form the detection statistic $D(t)$ at time t for the j-th subcarrier at node i as[2]

$$D(t) = \int_B \left|\eta_0(f,t)\right|^2 df \ . \tag{3.9}$$

However, because we only have estimates of a discrete set of frequencies, we replace (3.9) with

$$D(t) \approx \sum_{l=1}^{L} \left|\eta_0\left(f_c - \frac{B}{2} + l \cdot \Delta f, t\right)\right|^2 \cdot \Delta f \ , \tag{3.10}$$

where we divide the subcarrier bandwidth B into L bins of width Δf, and where f_c is the subcarrier frequency.

Since, if a subcarrier is occupied by existing users there is interference superimposed on the background noise at the sensing node, $D(t)$ in this case would be larger than that in a case where such a subcarrier is not occupied by existing users. Therefore, we can declare a particular subcarrier to be available or not based on a threshold comparison. At time t, the decision regarding the status of a particular subcarrier is made according to the following rules:

(1). Current status is available (3.11)

---

[2] As in [41], $D(t)$ can be interpreted as an estimate of the interference temperature.

- Declared to be unavailable *iff* $D(t) - D_0 > \Delta$ and $D(t + iT_s) - D_0 > \Delta$, $i = 0, 1, \ldots, J$.
- Declared to be available, otherwise.

(2). Current status is unavailable (3.12)

- Declared to be available *iff* $D(t) - D_0 \leq \Delta$.
- Declared to be unavailable, otherwise.

In (3.11) and (3.12), D_0 is the typical value of $D(t)$ when only the random background noise is present; Δ is a guard interval for detection and J is a pre-specified number of time slots with duration T_s. The decision rule (1) can be explained as follows: given the current status that a subcarrier is available at time t, if the detection statistic $D(t)$ exceeds the pre-set threshold and $D(t)$ remains higher than the threshold for a pre-specified number of time slots, then the status is declared to be unavailable. However, if at time t, the detection statistic $D(t)$ exceeds the pre-set threshold, but then drops below the threshold, the status would not change and the subcarrier remains available. Decision rule (2) has a similar interpretation. By sensing all the subcarriers, the i-th user can determine its available subcarrier set F_i, having A_i free subcarriers. However, since false alarms and missed detections both can occur, the system must be designed to accommodate these errors. Note that the selection of Δ affects the system performance in the following way. If Δ is small, a detection error would most likely be a false alarm, and if Δ is large, a detection error would most likely be a missed detection.

In order to lower the probability of detection error, we allow cooperation among mobile users. More specifically, if there is no central controller available, a *partially* cooperative scheme can be implemented whereby each CR user will broadcast its available subcarrier set F_i to its neighbors via control packets. Each cognitive radio transmitter can then collect such information and use a simple majority logic to determine the status of each subcarrier. Hence, enhanced system performance can be expected due to the diversity gain associated with this local cooperation.

For illustration purposes, we assume, for the k-th subcarrier of the i-th user, that

the detection error probability is $Pe_i^{(k)}=Pe$, for all i, and that a node receives H-1 decision sets from its neighbors. Then, the residual detection error probability for the k-th subcarrier becomes

$$Pe^{(k)} = \sum_{i=\lceil H/2 \rceil+1}^{H} \binom{H}{i} [Pe]^i [1-Pe]^{(H-i)} . \tag{3.13}$$

In an ad hoc network with satisfactory overall network throughput, the number of neighbors of a node might be approximately 6 – 8 [57]. In Fig. 3. 2, we show the performance of this cooperation scheme when the initial detection error probability $Pe_i^{(k)} = Pe$ = 0.05 or 0.1, for all i, and for $H \leq 11$. As we can see, when H increases, $Pe^{(k)}$ decreases significantly, even when H is not large, say $H \leq 5$. Therefore, we can greatly reduce the detection error probability by using cooperation, and thus improve system performance. The entire detection procedure is simplified in Fig. 3. 3.

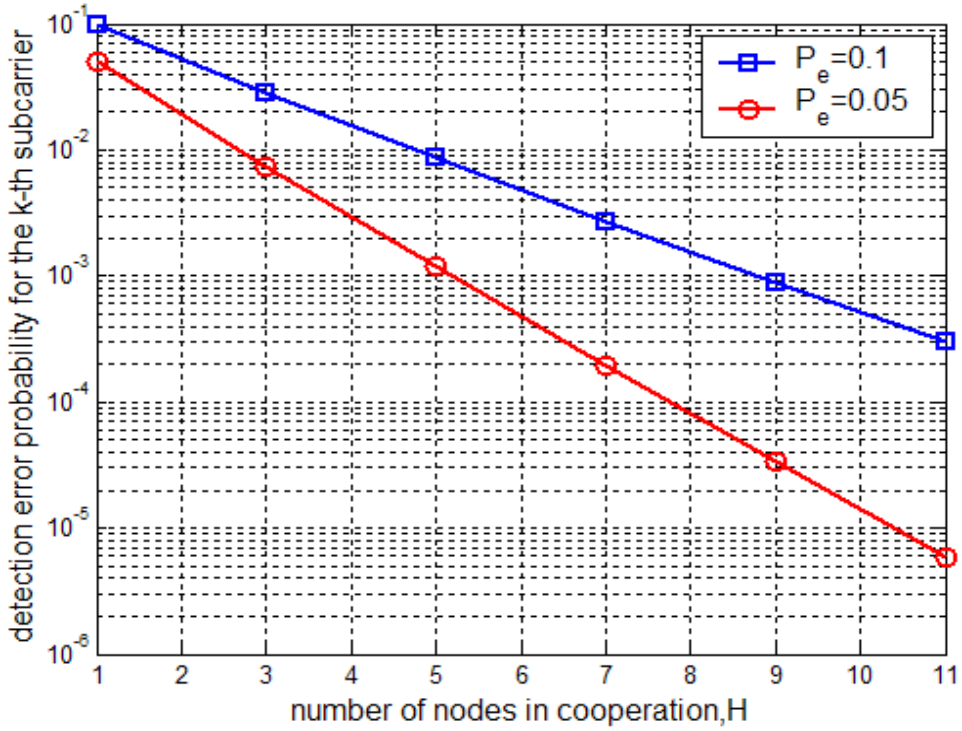

Fig. 3. 2. Distributed cooperation to reduce the detection error probability.

3.3.1.2 Noise Floor Power Spectrum Density (PSD) Estimation

After detection of the available subcarrier set for the *i*-th cognitive transmitter, at the corresponding receiver the noise power spectral density of the *k*-th free subcarrier, $S_i^{(k)}(f)$, is estimated. The sources of the noise power are a combination of thermal noise, possible NBI, and primary users when detection error occurs. As discussed previously, the statistics of the noise are assumed to be Gaussian with noise power $N_i^{(k)}=\int_B S_i^{(k)}(f)df$. From (6) and [53, *Eq*. 2.4], the noise PSD, $S_i^{(k)}(f)$, at the *k*-th available subcarrier of the *i*-th receiver can be estimated as

$$S_i^{(k)}(f) = \frac{1}{K}\sum_{n=0}^{K-1}\left|y_n(f)\right|^2 . \tag{3.14}$$

It has been shown in [58] that the multitaper spectral estimate in (3.6) and (3.14) can be viewed as an "approximation" of a *maximum-likelihood* power spectrum estimate. Finally, we can compute the noise power as

$$\begin{aligned} N_i^{(k)} &= \int_B S_i^{(k)}(f)\,df \\ &\approx \sum_{l=1}^{L} S_i^{(k)}\left(f_c - \frac{B}{2} + l\cdot\Delta f\right)\cdot\Delta f \end{aligned}, \tag{3.15}$$

where the subcarrier bandwidth B is divided into L segments of width Δf.

At user *i*, for its *j*-th subcarrier

1. Compute $y_n(f)$, $n = 0,\ldots,K\text{-}1$;
2. Partial cooperation may be performed by exchanging the information on $\mathbf{y}_n(f)$ among its neighbors;
3. Form $A(f)$ and perform singular value decomposition (SVD);
4. Form the detection statistic $D(t)$;
5. Perform the threshold comparison and obtain the available subcarrier set;
6. Partial cooperation is performed by exchanging the available subcarrier set among its neighbors;
7. And majority logic applies to obtain the final available subcarrier set.

Fig. 3. 3. Distributed cooperative subcarrier detection procedure.

3.3.1.3 Channel Gain Estimation

Since power control requires channel state information for each available subcarrier, channel estimation is needed in any power control system. However, it is well known that as the Doppler spread increases, the coherence time decreases and the accuracy of the channel estimates degrades, since the channel samples are less correlated and the observation time available to both make and use the channel estimates is decreased. We now focus our attention on the impact of Doppler spread on the estimation performance. In the literature, there have been many papers that discuss the estimation error due to noise and Doppler spread, but rarely do they result in a closed-form expression. However, in [59], a simple approximation for the estimation error σ_e^2, obtained with the use of a Linear Minimum-Mean-Square-Error (LMMSE) estimator, is

$$\sigma_e^2 = r(0)\left[1 - \frac{1}{r(0)}\int_{-T_eB_d}^{T_eB_d} \frac{S^2(f)}{S(f)+\sigma_p^2} df\right], \tag{3.16}$$

where $r(0)$ is the power of the fading process that we will normalize to unity, T_e is the interval between two adjacent channel samples, B_d is the maximum Doppler spread, σ_p^2 is the noise power and $S(f)$ is the Doppler power spectrum over the normalized Doppler frequency $[-T_eB_d,\ T_eB_d]$. In order to further simplify this expression, we assume a uniform Doppler spectrum within $[-T_eB_d,\ T_eB_d]$; that is, $S(f)=S_0$, for f in $[-T_eB_d,\ T_eB_d]$. It has been shown in [59] that this assumption can appropriately mimic the true performance in (3.16), even if the Doppler power spectrum is not uniform. Then, according to [59], we have

$$\sigma_e^2 = r(0)\left[1 - \frac{1}{r(0)} \cdot \frac{S_0^2}{S_0+\sigma_p^2} \times 2T_eB_d\right] = \frac{r(0)\left(S_0+\sigma_p^2\right) - S_0^2 \cdot 2T_eB_d}{S_0+\sigma_p^2}. \tag{3.17}$$

By using the fact that $r(0)= S_0 \cdot 2T_eB_d$, (3.17) can be reduced to

$$\sigma_e^2 = \frac{r(0)}{1 + SNR^{eff}}, \tag{3.18}$$

where SNR^{eff} is the effective SNR defined as

$$SNR^{eff} = \frac{r(0)}{\sigma_p^2 2T_e B_d} \approx SNR \cdot \frac{T_c}{T_e}, \tag{3.19}$$

and the coherence time $T_c \approx 1/2B_d$ which leads to the last step in (3.19).

It is evident that σ_e^2 is a monotonically decreasing function of SNR^{eff}, and as the coherence time T_c increases, σ_e^2 decreases. This is consistent with the fact that a smaller Doppler spread, i.e., a larger coherence time, can improve the estimation performance since it allows averaging over more symbols which are highly correlated to each other. In this chapter, we assume the distribution of channel estimation error to be a Gaussian random variable with zero mean and variance σ_e^2, as in [60]. Therefore, the estimated channel gain can be expressed as the sum of the actual channel gain and a Gaussian random variable with zero mean and variance σ_e^2, as in (3.18).

3.3.2 Spectrum Management and Power Control

In essence, the aims of the spectrum management and power control for this cognitive radio based multi-user ad hoc network are to optimally select the available subcarriers and the associated power levels for each CR user, so as to satisfy the constraints on power and data rate for each user, as stated in (3.5). Ideally, a global optimum solution is desired. However, finding such a global optimum solution requires an exhaustive search. In our case, with N potential new CR users, each of which has A_i available subcarriers, $i = 1,\ldots, N$, and a data rate requirement of R_i bits, $i = 1,\ldots, N$, the total number of possible allocations is $\prod_{i=1}^{N} A_i^{R_i}$, and the exhaustive search turns out to be infeasible due to the computational burden. In order to alleviate the computational complexity, we propose a distributed multi-user resource allocation

approach which attempts to search for a suboptimal solution.

In order to jointly allocate subcarriers and power levels, we first define an indicator to represent the quality of the *k*-th free subcarrier of the *i*-th user as the ratio of the corresponding channel gain to the noise-plus-interference power:

$$Q_i^{(k)} = \frac{\alpha_{ii}^{(k)}}{N_i^{(k)}}, \tag{3.20}$$

where $\alpha_{ii}^{(k)}$ is the associated channel gain and $N_i^{(k)}$ is the noise power on the *k*-th subcarrier of user *i*. Since, in our applications, a central controller is not available due to the lack of infrastructure of ad hoc networks, a distributed algorithm is needed. In this subsection, we provide a distributed multi-user resource allocation approach where only the 'local' information is needed at each cognitive radio user. In order to lower the detection error, a partially cooperative scheme is used, as discussed previously.

We assume that time is divided into equi-length slots. At the time-of-interest, there are multiple CR users who want to transmit. After the detection and estimation procedures, each user has its 'local' information available at the transmitter side, i.e., available subcarrier set, channel state information, and noise power. With only this local information, a CR user has to perform the resource allocation individually: any given CR user assumes that no other users will share the resources with it; then, the user sorts its available subcarriers from the best to the worst, based on the *Q* values (3.20); finally, it selects the ordered subcarriers from the best to the worst sequentially until it satisfies the data rate requirement, and employs the minimum required power on each selected subcarrier. After that, it starts transmissions. However, since there are actually multiple CR users sharing the resources, some subcarriers may have been chosen by multiple CR users. Then, a conflict may occur and the received *SINR* of a user would be below the desired one. To quantify how likely such a conflict is, assume that *N* CR users are present, and each of them will select *k* free subcarriers for their

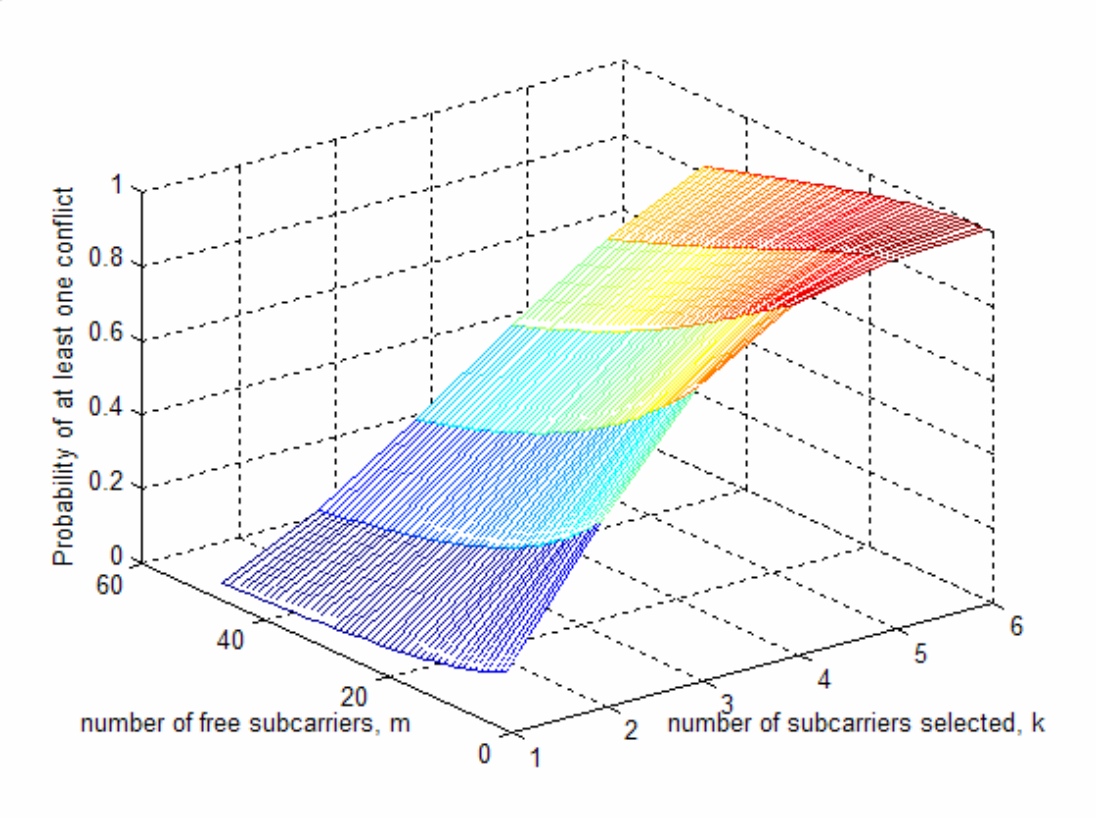

Fig. 3. 4. Illustration of the probability of at least one conflict is found for $N = 3$.

transmissions from a common available subcarrier set F of size m. Then, a lower bound on the probability of at least one conflict can be shown to be (See Appendix C for details)

$$\Pr\{at\ least\ one\ conflict\ is\ found\} \geq 1 - e^{-\frac{\binom{N}{2}k^2}{m}}. \qquad (3.21)$$

As we can see in Fig. 3. 4 with $N = 3$, the probability is relatively high, especially when $k \geq 4$ and $m \leq 32$. Note also that, when P_{NBI} is large, the system is likely to produce a large number of detection errors, and thus make m very small.

Hence, now the problem is as follows: for a given conflicting subcarrier, where Q users are overlaid on it, we want to minimize the total power consumption for all the Q users while satisfying the data rate requirement of each user. Assume $\underline{P} = [P_1, P_{2,\ldots},$

$P_Q]$, $\underline{B} = [B_1, B_2, ..., B_Q]$, and $\underline{\zeta} = [\zeta_1, \zeta_2, ..., \zeta_Q]$ are the transmit power vector, the data rate vector and the corresponding *SINR* threshold vector, respectively, for the Q users on the conflicting subcarrier. For user i, $i = 1,..,Q$, the corresponding received *SINR* is

$$SINR_i = \frac{\alpha_{ii} \cdot P_i}{\sum_{j \neq i} \alpha_{ji} \cdot P_j + N_i}, \tag{3.22}$$

where α_{ij} is the channel gain between the i-th transmitter and the j-th receiver, and it contains the effects of path loss, fading, as well as processing gain, and N_i is the noise power at the i-th receiver. In order to satisfy the data rate requirement of user i, the received *SINR* should satisfy $SINR_i \geq \zeta_i$. Now, the *SINR* expressed in (3.22) can be defined for all the Q users as follows:

$$\left(\underline{\underline{I}} - \underline{\underline{\Lambda}}\right) \cdot \underline{P}^T \geq \underline{\mu}, \tag{3.23}$$

where $\underline{\underline{I}}$ and $\underline{\underline{\Lambda}}$ are Q-by-Q matrixes and $\underline{\underline{\Lambda}}$ is defined as $\underline{\underline{\Lambda}} = [h_{ij}]_{Q \times Q}$ such that $h_{ij} = \zeta_i \cdot \alpha_{ji}/\alpha_{ii}$ for $i \neq j$ and $h_{ij} = 0$ for $i = j$; finally, $\underline{\mu} = [\zeta_i \cdot N_i/\alpha_{ii}]_{Q \times 1}$. The transmit power P_i is upper-bounded by P_{i_max}, which denotes the maximum power of each user on the subcarrier. The matrix $\underline{\underline{\Lambda}}$ has nonnegative entries. If we let λ_{max} be the maximum eigenvalue of $\underline{\underline{\Lambda}}$, we then have the following well-known lemma:

Lemma 1: An optimal power vector $\underline{P}^* > 0$ exists, which satisfies (3.23) with equality if $0 < \lambda_{max} < 1$.

Proof: Based on Perron-Frobenius theorem. See [9] for details. □

In [9], Foschini and Miljanic proposed a simple iterative distributed power control (DPC) algorithm to solve (3.23) such that the optimal power vector $\underline{P}^*$ can be found:

$$P_i(k+1) = \frac{\zeta_i}{SINR_i(k)} \cdot P_i(k), \tag{3.24}$$

where $P_i(k)$ and $SINR_i(k)$ are the power level and the associated *SINR* for the k-th subsequent time slot on that particular subcarrier of user i, $i = 1,..,Q$, respectively. Each user can then independently adjust its power based on (3.24), attempting to exactly

meet the required *SINR* threshold. Now, some natural questions are: 1) how to protect the primary users on a subcarrier when detection errors occur; 2) how to protect a CR user once it is admitted to the system; 3) how to find $\underline{P}^*$ if $\lambda_{max} > 1$, i.e., when it is not feasible to find an optimal power vector for all the Q users; 4) what the effect is of a maximum power constraint. In what follows, we propose an adaptive power control algorithm with user protection and adaptive rate control (APC/UP/ARC) to address the four questions, based on the prior work in [63].

We first introduce the following definitions: user i, $i = 1,..,Q$, is in the active user set X(k) during the k-th step *iff* user i is originally a primary user or user i is a cognitive radio user such that its $SINR_i(k) \geq \zeta_i$. That is, once a CR user's *SINR* is satisfied, it then becomes an active user. Similarly, user i, $i = 1,..,Q$, is in the transition user set Y(k) during the k-th step *iff* user i is originally a CR user and $SINR_i(k) < \zeta_i$. We also define a protection margin, δ, for users in X(k) where δ is slightly larger than 1. Now, the APC/UP algorithm is described as follows [63]:

$$P_i(k+1) = \begin{cases} \dfrac{\delta \cdot \zeta_i}{SINR_i(k)} P_i(k), & if\ i \in \mathrm{X}(k) \\ \delta \cdot P_i(k), & if\ i \in \mathrm{Y}(k) \end{cases}. \tag{3.25}$$

It is worth noting that in APC/UP, users in X(k) adjust their power levels based on (3.24), but with a target $\delta \cdot \zeta_i$. On the other hand, users in Y(k) increase their power levels at the geometric rate δ. The protection margin δ is used to compensate for the interference induced by CR users, and users in Y(k) update their power levels gradually so that limited interference is imposed upon active users in each step. This APC/UP power control algorithm has the following important properties [63]:

***Proposition* 1** (*Protection for Active Users*): for any $\delta > 1$, for an arbitrary k and every $i \in$ X(k), we have $SINR_i(k) \geq \zeta_i \Rightarrow SINR_i(k+1) \geq \zeta_i$ during the evolution of the APC/UP power control process.

***Proposition* 2** (*Limited Power Increase*): for any $\delta > 1$ and an arbitrary k, if $i \in$ X(k) and $SINR_i(k) \geq \zeta_i$, we have $P_i(k+1) \leq \delta \cdot P_i(k)$.

Proposition 3 (*Transition User SINR Increase*): for any $\delta > 1$, for an arbitrary k and every $i \in Y(k)$, we have $SINR_i(k) \leq SINR_i(k+1)$.

Proof: See [63] for details. □

The first proposition shows that when a user enters X(k) with its *SINR* requirement satisfied at time k, it can guarantee that condition from then on. This proposition provides inherent protection to active users, which is significant in a cognitive radio network. Proposition 2 demonstrates that active users in X(k) with their *SINR* requirements satisfied only increase their power levels gradually in order to induce limited interference and thus admit other CR users more easily. Proposition 3 shows that a CR user's *SINR* is non-decreasing, and thus eventually it can reach its target *SINR*. Thus, the first two questions raised previously have been addressed by this APC/UP power control algorithm. However, as the APC/UP algorithm evolves, if there is no optimal power vector which can satisfy the *SINR* requirements of all the Q users with the current data rate vector $\underline{B} = [B_1, B_{2, \ldots,} B_Q]$, some of CR users cannot gain access, since their *SINR* requirements cannot be satisfied. Therefore, it is beneficial that those users who cannot gain access decrease their data rate, and thus, decrease the corresponding *SINR* requirements. To accomplish this, consider the following adaptive rate control (ARC) algorithm, to be used together with the APC/UP algorithm. Each CR user pre-sets a time duration T_i within which it tries to access the system; if it does not gain access after T_i steps, it will compute a time control interval ΔT_i (See (3.26) below) which is a decreasing function of the difference between its current *SINR* and its target one; if, after $T_i + \Delta T_i$ steps, it still cannot gain access, it will decrease its data rate by ΔB and repeat the above process. It continues in this mode until it gains access successfully or stops transmission because B_i is less than or equal to zero. The APC/UP/ARC algorithm can be briefly described as follows:

Step 1: After CR user i starts transmission, it measures its current $SINR(k)$. If $SINR(k) \geq \zeta_i$, CR user i becomes an active user and then adjusts its power according to (3.25); if not, it goes to Step 2.

Step 2: If $k \in \{K_0, K_0+1,\ldots, K_0+T_i+\Delta T_i-1\}$, CR user i adjusts its power using (25) and goes back to Step 1 with $k = k+1$. K_0 is time slot index when user i starts using its current data rate B_i. ΔT_i is computed as a function of the distance between the current *SINR* and its threshold [63]

$$\Delta T_i = f\left(\zeta_i - SINR_i(T_i)\right) = \left\lfloor A\exp\left(-\beta(\zeta_i - SINR_i(T_i))\right)\right\rfloor, \qquad (3.26)$$

where $A \geq 0$ and $\beta \geq 0$; $\lfloor\ \rfloor$ is the integer part of the argument. Then, ΔT_i is a decreasing function of the

distance between its *SINR* at step T_i and the threshold.

Step 3: If $k = K_0 + T_i + \Delta T_i$, user i decreases its data rate by ΔB. If $B_i > 0$, it updates its *SINR* threshold ζ_i and goes back to Step 1 with $k = k+1$; if $B_i \leq 0$, user i stops its transmission.

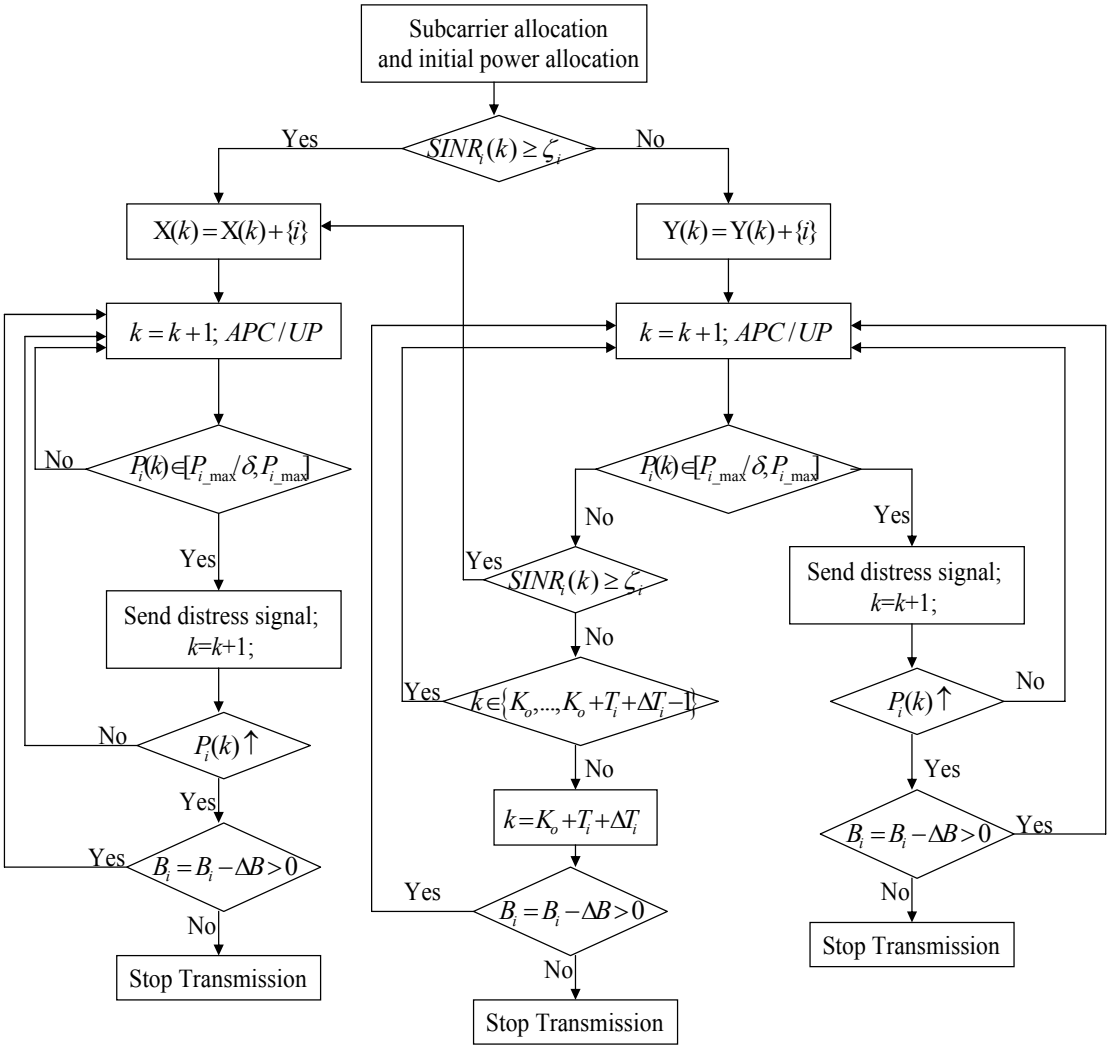

Fig. 3. 5. Illustration of the distributed spectrum and power allocation with APC/UP/ARC.

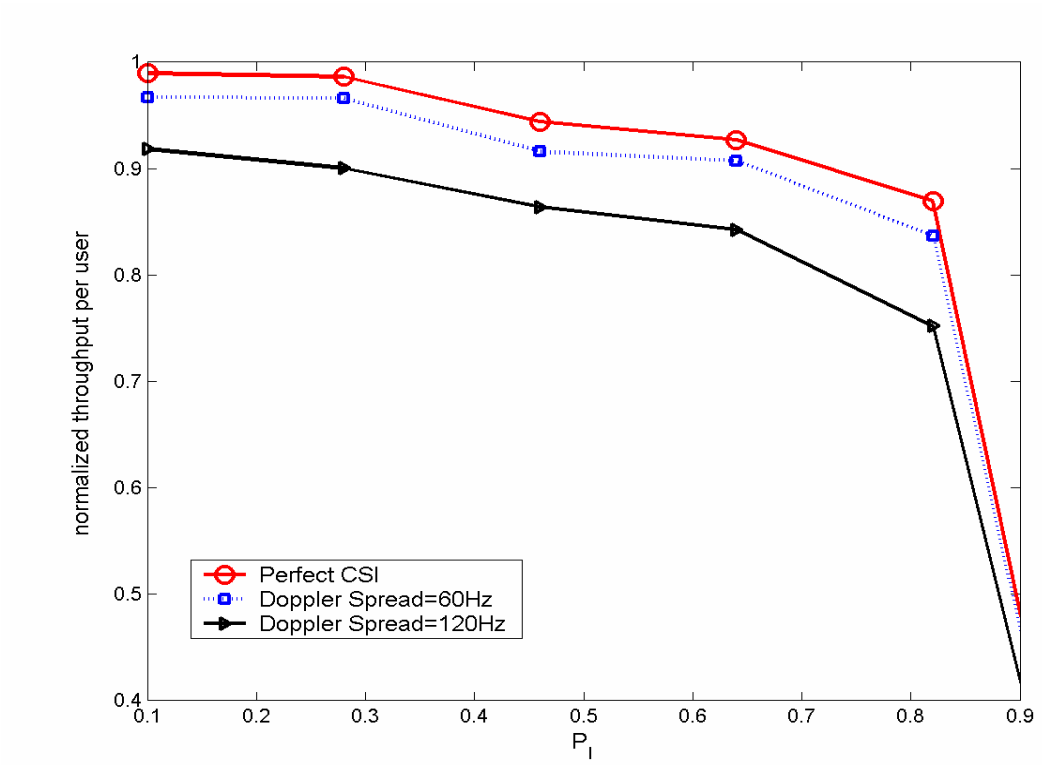

Fig. 3. 6. Normalized throughput per user vs. P_I; $P_N = 0.4$; control channel BW = 128 KHz; with cooperation.

Now we have addressed the third question raised previously by using the APC/UP/ARC algorithm. More specifically, when the current scenario of Q users is not feasible, a CR user will adjust its data rate independently, until it gains access or it stops transmission. Finally, we have the fourth question to be solved where a maximum power constraint, P_{i_max}, is imposed for each user in X(k) and Y(k). When CR users attempt to access the system, they keep powering up their power levels, thus more interference will be induced to users in X(k). As a result, users in X(k) also have to increase their power levels, as in (3.25), otherwise their *SINR* requirements cannot be satisfied. However, if a power constraint is present, it is possible that, at some point, the power level of an active user cannot increase further, and its *SINR* will fall below the threshold. It is also possible that a CR user has to exceed its power constraint in

order to satisfy its *SINR* threshold. Motivated by the distress signaling concept in [63], our mechanism can be described as follows: when user i is approaching its power constraint P_{i_max}, and its current power $P_i(k)$ ϵ $[P_{i\_max}/\delta, P_{i\_max}]$, a distress signal is broadcast, and each CR user in the vicinity of the distressed user i will decrease its data rate by ΔB, and thus decrease its power level. Then, user i will experience less interference and lower its power level. However, if after user i broadcasts the distress signal, its power is still increasing, user i then has to decrease its data rate by ΔB in order not to exceed its power constraint.

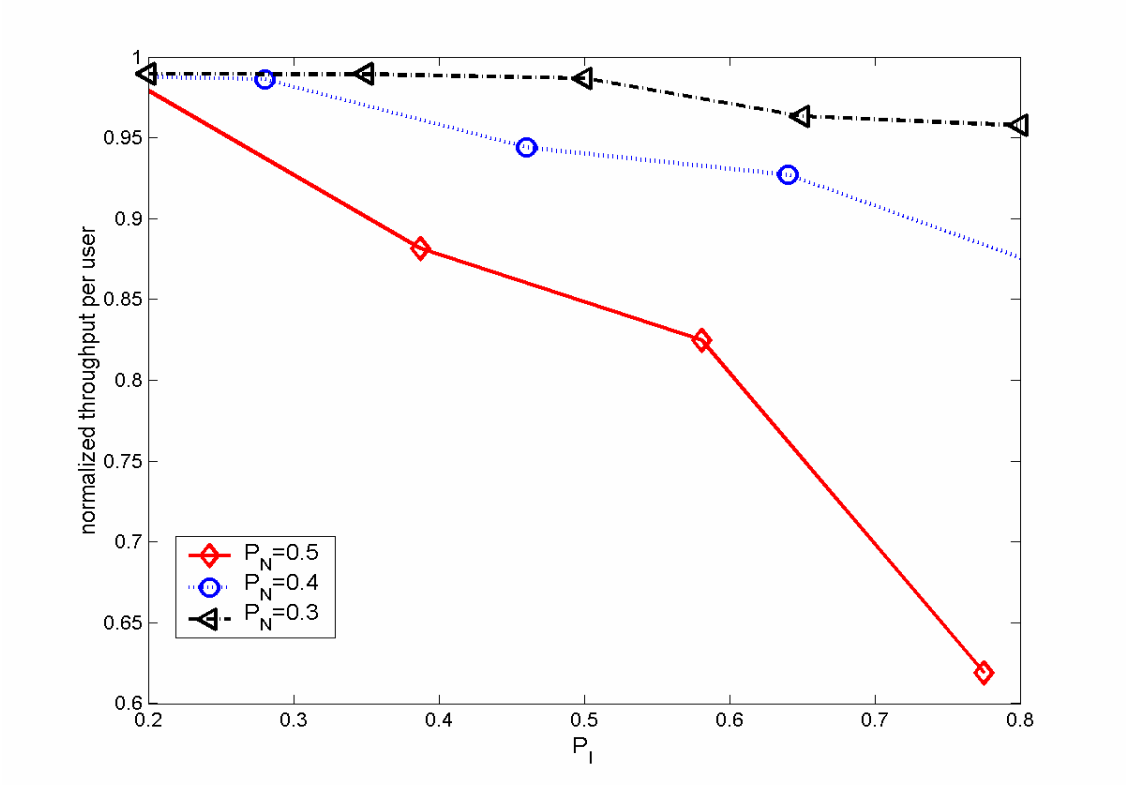

Fig. 3. 7. Normalized throughput per user vs. P_I and P_N; Perfect channel estimate; control channel BW = 128 KHz; with cooperation.

The complete procedure of the proposed APC/UP/ARC algorithm is illustrated in Fig. 3. 5. Therefore, by using the proposed APC/UP/ARC algorithm, each user can

independently adjust its power level and perform distributed rate control with only its local *SINR* measurements, and thus a conflict can be solved in a distributed manner when it occurs.

3.4 Simulation Results and Discussion

In this section, we present the simulation results and evaluate the impact of key parameters upon system performance. We examine the performance of an ad hoc network with 30 nodes randomly distributed in an area of size 200×200 m^2. There are 64 subcarriers in the multicarrier system, and each subcarrier experiences flat Rayleigh fading. The path loss exponent is 4, and the thermal noise power density of each subcarrier is -145 dBm/Hz [62]. We assume that the data rate requirement of each cognitive radio transmitter can be modeled as a Gaussian random variable. The mean and variance of this random variable are taken to be 35 bits-per-symbol duration and 20% of the mean, respectively. Since the maximum number of bits that a subcarrier can support is set to be 7-bits-per-*M*-ary QAM symbol, a user typically employs multiple subcarriers for its transmission. The BER requirement of the system is 10^{-4}, and the maximum power of each user is set to be 100 mw. P_I is the probability of a subcarrier being occupied by a primary user, and P_N is the probability of NBI overlaying a subcarrier of a given user. Each CR user seeks access into the system for T_i = 30 time slots and the protection margin is taken to be 1.125 [63].

In Fig. 3. 6, we show the normalized throughput-per-user as a function of P_I and the Doppler spread. Note that there are two reasons why the performance degrades when P_I increases. As P_I increases, more primary users are present and less system resources are left for CR users, thus more conflicts occur; also, as P_I increases, the number of detection errors also increases. However, due to the proposed node cooperation and the proposed power control algorithm, the performance degradation

due to the increase of P_I is marginal, especially when P_I is small, say $P_I \leq 0.5$. Furthermore, we note that when Doppler spread is present, performance degrades further due to the channel estimation error. This is consistent with our previous discussion: as Doppler spread increases, the coherence time decreases and the accuracy of the channel estimates degrades. As a result, system performance degrades.

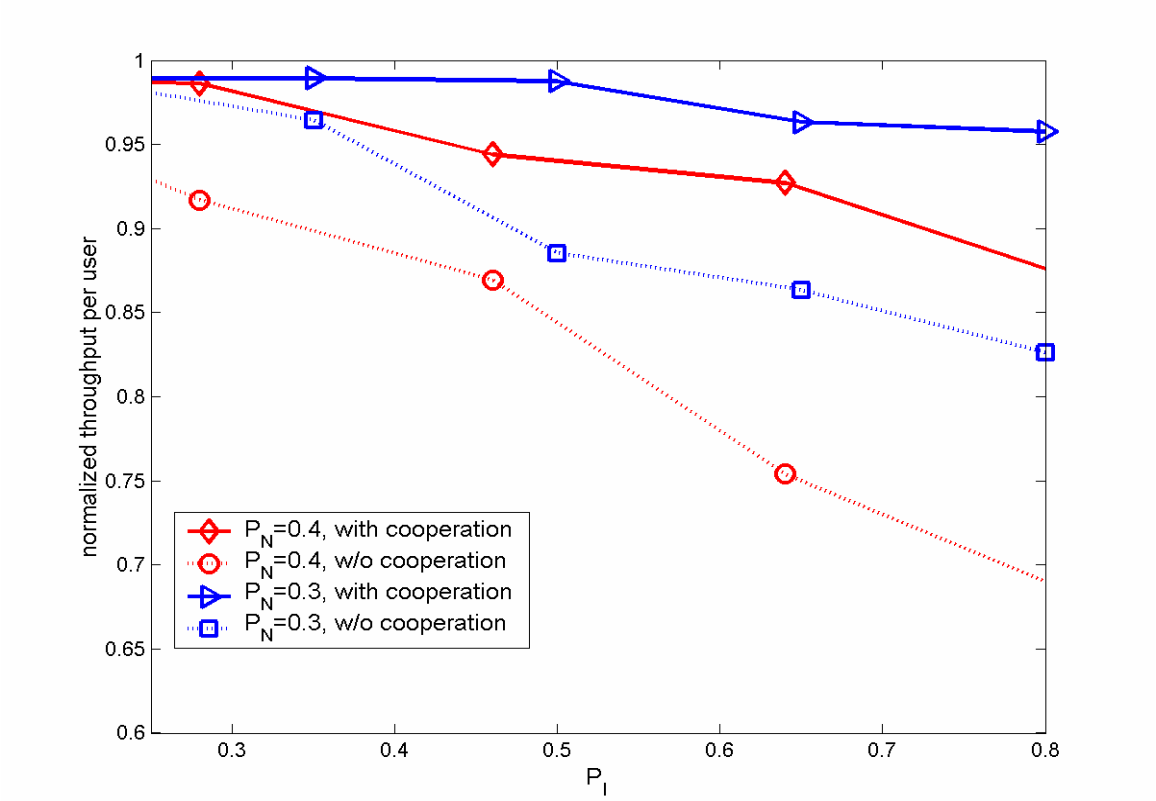

Fig. 3. 8. Normalized throughput per user vs. P_I; Perfect channel estimate; control channel BW = 128 KHz.

In Fig. 3. 7, we show the normalized throughput-per-user as a function of both P_I and the probability of NBI being present, P_N. As we can see, when P_I increases, the system performance degrades, which is consistent with Fig. 3. 6. However, when P_N is relatively small, the system performance is good even when P_I is large. Alternatively, as P_N increases, the NBI causes more performance degradation for a given P_I, and

when P_N is relatively large, system performance degrades significantly when P_I is also large, since more detection errors occur and less system resources are available to CR users.

We demonstrate the impact of the local node cooperation upon the system performance in Fig. 3. 8. Note that the performance degradation with local cooperation is much more graceful compared to the case where no cooperation is used. In particular, the performance without cooperation degrades very rapidly as the P_I and P_N become large. Therefore, local node cooperation, as discussed previously, is highly desirable for the distributed approach to achieve satisfactory performance.

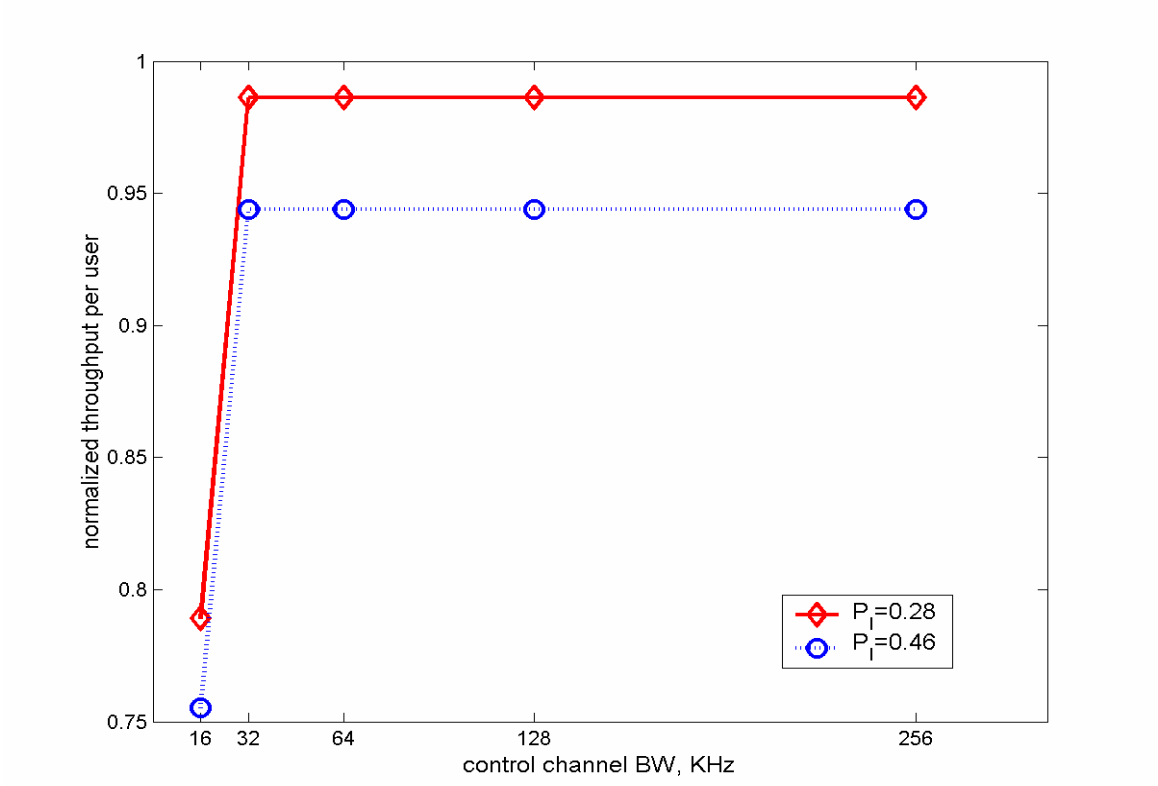

Fig. 3. 9. Normalized throughput per user vs. control channel BW; P_N = 0.4; Perfect channel estimate; with cooperation.

Finally, in Fig. 3. 9, we show the impact of control channel bandwidth upon the

system performance. When a high-bandwidth control channel of 256 KHz is available, the information (the available subcarrier set, and the channel estimate and the noise power estimate of each available subcarrier) of all the 64 subcarriers can be exchanged between a receiver and its corresponding transmitter, thus yielding good performance. Note that when the control channel bandwidth reduces from 256 KHz to 32 KHz, there is almost no performance degradation. This is due to the fact that, on the one hand, each user orders the subcarriers from the best to the worst, and always picks the best subcarriers for its transmission. On the other hand, when the control channel bandwidth is reduced from 256 KHz to, say, 32 KHz, although it is not possible to feed back the information of all the 64 subcarriers, each user always orders the subcarriers and feeds back the information of the best subcarriers. As a result, when the control channel bandwidth reduces from 256 KHz to 32 KHz, a user would pick the same set of subcarriers for its transmission, and so the system performance is the same. Therefore, as we can see, generally, in order to provide satisfactory system performance, a high-bandwidth control channel which can exchange all the information of all the 64 subcarriers between a transmitter and its corresponding receiver is not necessary for our system, say, 256 KHz. Instead, a low-bandwidth control channel which is able to feed back information of part of the subcarriers, say 32 - 128 KHz, is sufficient. However, when control channel bandwidth reduces further, i.e., to 16 KHz, system performance degrades significantly, since now the system cannot provide sufficient feedback information to perform the resource allocation.

3.5 Summary and Conclusions

In this chapter, we proposed a cognitive radio based multi-user resource allocation framework for mobile ad hoc networks using multi-carrier DS CDMA modulation over a frequency-selective fading channel. More specifically, given the

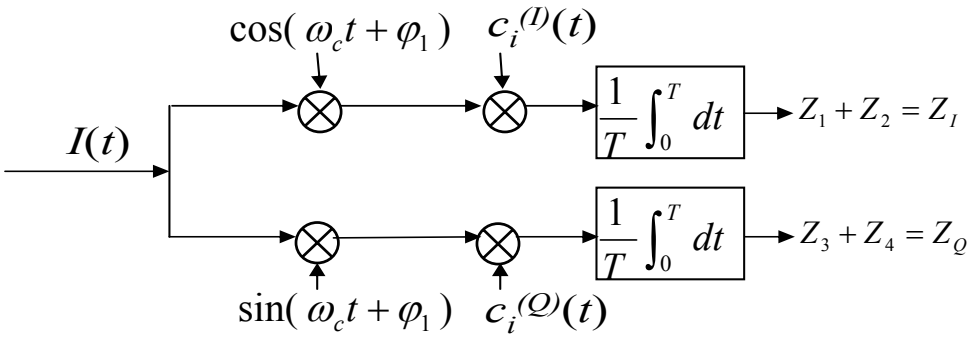

Fig. 3. 10. Receiver structure.

existing spectral conditions and existing primary users, we first proposed a detection and estimation mechanism to detect the availability of each subcarrier, as well as to estimate the channel state information and the noise power; based on that, a distributed resource allocation approach was provided to jointly allocate spectral bands, power and data rate among multiple cognitive radio users. Finally, we investigated the performance of the system under different scenarios and examined the impact of multiple key parameters.

3.6 Appendix

3.6.1 Justification on Gaussian Approximation

As shown in Fig. 3. 10, let node *i* be transmitting a QAM symbol with duration *T* to node *j* while there is an interferer, node *k*, on the same subcarrier with central carrier frequency ω_c. $c_k^{(I)}(t)$ and $c_k^{(Q)}(t)$ are two random spreading sequences of interferer *k* in the in-phase and the quadrature branch. We assume that the random spreading sequences are long enough so that each chip of $c_k^{(I)}(t)$ and $c_k^{(Q)}(t)$ can be approximated as an *i.i.d.* random variable taking 1 or -1 equally probable with chip

duration T_c. We further assume that the spreading sequences used at the desired receiver j are deterministic. Then, the received interference term at node j from interferer k before de-spreading and demodulation is

$$I(t) = A_k^{(I)} c_k^{(I)}(t-\tau)\cos(\omega_c t + \theta) + A_k^{(Q)} c_k^{(Q)}(t-\tau)\sin(\omega_c t + \theta), \qquad (3.27)$$

where $A_k^{(I)}$ and $A_k^{(Q)}$ are the received amplitudes; τ is the delay induced in transmission and θ is the phase parameter including both the original phase and the phase shift.

At node j, after demodulation and de-spreading at both the I and Q branches, the final outputs at the I and Q branches are as follows:

$$\begin{aligned} Z_I &= \frac{1}{T}\int_0^T \frac{A_k^{(I)}\cos(\theta_1)}{2} c_k^{(I)}(t-\tau)c_i^{(I)}(t)dt + \frac{1}{T}\int_0^T \frac{A_k^{(Q)}\sin(\theta_1)}{2} c_k^{(Q)}(t-\tau)c_i^{(I)}(t)dt \\ &= Z_1 + Z_2 \\ Z_Q &= \frac{1}{T}\int_0^T \frac{A_k^{(I)}\sin(\theta_1)}{2} c_k^{(I)}(t-\tau)c_i^{(Q)}(t)dt + \frac{1}{T}\int_0^T \frac{A_k^{(Q)}\cos(\theta_1)}{2} c_k^{(Q)}(t-\tau)c_i^{(Q)}(t)dt \\ &= Z_3 + Z_4 \end{aligned}, \qquad (3.28)$$

where Z_I and Z_Q are the outputs at the I and Q branches of the desired receiver j, respectively; θ_1 is the relative phase between the interferer node k and the receiver j. $c_i^{(I)}(t)$ and $c_i^{(Q)}(t)$ are deterministic spreading sequences at the desired receiver j. Therefore, the first term of Z_I is as follows:

$$\begin{aligned} Z_1 &= \frac{1}{T}\int_0^T \frac{A_k^{(I)}\cos(\theta_1)}{2} c_k^{(I)}(t-\tau)c_i^{(I)}(t)dt \\ &= \frac{A_k^{(I)}\cos(\theta_1)}{2T}\left(\tau\cdot\sum_{n=0}^{L-1} c_k^{(I)}(n-1)\cdot c_i^{(I)}(n) + (T_c-\tau)\cdot\sum_{n=0}^{L-1} c_k^{(I)}(n)\cdot c_i^{(I)}(n)\right) \end{aligned}. \qquad (3.29)$$

In (3.29), the term in the first summation, $c_k^{(I)}(n\text{-}1)c_i^{(I)}(n)$, can be replaced by an *i.i.d* random variable $C_1(n)$ taking 1 or -1 equally likely, since $c_i^{(I)}(n)$ is deterministic and $c_k^{(I)}(n\text{-}1)$ is an *i.i.d* random variable taking 1 or -1 equally likely. So, the summation is over a sequence of L *i.i.d* random variables. Similarly, $c_k^{(I)}(n)c_i^{(I)}(n)$ can be replaced by

an *i.i.d* random variable $C_2(n)$ taking 1 or -1 equally likely. Thus, Z_1 can be expressed as

$$Z_1 = \frac{A_k^{(I)} \cos(\theta_1)}{2T}\left(\tau \cdot \sum_{n=0}^{L-1} C_1(n) + (T_c - \tau) \cdot \sum_{n=0}^{L-1} C_2(n) \right). \tag{3.30}$$

As long as the spreading gain L is sufficiently large, the two summations in (3.30) can be approximated as conditionally Gaussian due to the central limit theorem, conditioned on the channel. The same process applies to Z_2, Z_3, and Z_4, and, as a result, the interference term Z_I and Z_Q at node j due to interferer node k can be approximated as conditional Gaussian noise.

Therefore, even when the number of interferers is not large, as long as the processing gain is sufficiently large, the interference from other users can still be approximated as additional Gaussian noise.

3.6.2 Computational Complexity Analysis for Subcarrier Availability Detection

We assume the spectrum has M subcarriers, and that each of these subcarriers has been divided into L bins of width Δf. We use K Slepian sequences of duration V in the estimation. At each frequency of interest, in order to choose the largest eigenvalue $\eta_0^2(f)$ as the desired detection parameter, we need:

a. $K \cdot \log_2(K)$ additions (use quick sort algorithm to search for the largest singular value $\eta_0(f)$ from $\eta_k(f)$, $k = 0, 1, \ldots, K\text{-}1$).
b. 2 multiplications (using $\eta_0(f)$ to compute $\eta_0^2(f)$ and $\eta_0^2(f) \cdot \Delta f$).
c. K Fast Fourier transforms (FFT) of length V, and 1 singular value decomposition (SVD) on a matrix of dimension $H \times K$.

Therefore, in order to form $D(t)$ at time t to update the subcarrier status for all the subcarriers, a node should perform:

a. $M \cdot L \cdot (1 + K \cdot \log_2(K))$ additions.

b. $M \cdot L \cdot 2$ multiplications.

c. $M \cdot L$ SVD and $M \cdot L \cdot K$ FFT.

The computational complexity increases linearly with M, L, and K. Generally, M is fixed in a real system and we can vary L and K to tradeoff detection performance and system complexity according to the given performance constraints and the hardware complexity limitations. Therefore, although the complexity is relatively high, it is feasible and manageable in a real system and can provide higher performance than other detection mechanisms as shown in [41].

3.6.3 Probability of Conflict for the *N*-User Case

We first assume user i picks a set of subcarriers, $S_i = [x_1^{(i)}, x_2^{(i)}, \ldots, x_k^{(i)}]$. Assuming each user selects a subcarrier from F with equal probability, for any two-user pair, user i and user j, given $x_1^{(i)}$, the probability of Pr $\{x_1^{(j)} \neq x_1^{(i)}\} = 1 - 1/m$. Then, the probability of no conflict in S_j to $x_1^{(i)}$ is

$$\Pr\left\{no\ conflict\ in\ S_j\ to\ x_1^{(i)}\right\} = \left(1-\frac{1}{m}\right)\left(1-\frac{1}{m-1}\right)\cdots\left(1-\frac{1}{m-k+1}\right) \le \left(1-\frac{1}{m}\right)^k . \tag{3.31}$$

Therefore, the probability of no conflict in S_j to S_i is

$$\Pr\left\{no\ conflict\ in\ S_j\ to\ S_i\right\} \le \left(\left(1-\frac{1}{m}\right)^k\right)^k = \left(1-\frac{1}{m}\right)^{k^2} . \tag{3.32}$$

So, the probability of no conflict in all two-user pairs is

$$\Pr\left\{no\ conflict\ in\ all\ two\ user\ pairs\right\} \le \left[\left(1-\frac{1}{m}\right)^{k^2}\right]^{\binom{N}{2}} . \tag{3.33}$$

Finally, the probability of at least one conflict is found can be shown to be

$$\Pr\{at\ least\ one\ conflict\ is\ found\} \geq 1-\left[\left(1-\frac{1}{m}\right)^{k^2}\right]^{\binom{N}{2}} \geq 1-e^{-\frac{\binom{N}{2}k^2}{m}}, \qquad (3.34)$$

where the last step comes from the fact that $1 - x \leq e^{-x}$, when x is small.

Acknowledgement

This chapter, in full, is a reprint of the material as it appears in Qi Qu, Laurence B. Milstein and Dhadesugoor R. Vaman,"Cognitive Radio Based Multi-User Resource Allocation in Mobile Ad Hoc Networks using Multicarrier CDMA Modulation", in *IEEE Journal on Selected Areas in Communications*, Jan. 2008. The dissertation author was the primary investigator and author of this publication.

4

Cooperative and Constrained MIMO Communications in Wireless Ad Hoc Networks

4.1 Introduction

In modern wireless communications, enhanced spectral efficiency can be achieved by the use of multiple-input-multiple-output (MIMO) systems. Recently, MIMO has attracted extensive attention and various techniques have been proposed for both cellular systems and ad hoc networks [67, 68] to achieve improved system performance. However, in wireless ad hoc/sensor networks, direct employment of MIMO to each node might not be feasible, since MIMO might require complex transceiver and signal processing modules, which result in high power consumption. Furthermore, nodes in wireless ad hoc networks/sensor networks are often powered by batteries with limited energy. This makes direct application of MIMO to each node inefficient from a power-efficiency point of view. Also, nodes in an ad hoc/sensor network might be of small physical size, which precludes the implementation of multiple antennas at each node.

As alternatives, cooperative MIMO techniques [69, 70] have been proposed. By the cooperation of multiple nodes, each of which has a single antenna, a virtual MIMO structure can be constructed which supports space-time processing, and thus improved system performance can be expected. In [69, 71], it has been shown that by

using this type of cooperation, cooperative MIMO can achieve better energy and delay performance compared to a Single Input Single Output (SISO) system, even considering the required overhead in a MIMO system. In [72], space-time coded cooperative diversity protocols are proposed to combat multipath fading. More specifically, the protocols exploit the spatial diversity available among a collection of nodes that can relay messages for one another such that the destination node can effectively average the fading. In [73], adaptive spatial multiplexing techniques for distributed MIMO systems are proposed, together with link adaptation based on available channel state information. Further performance gain can be achieved by appropriate power allocation among nodes that join the cooperation [74, 75]. In [74], optimal energy distribution is proposed with an attempt to minimize the link outage probability, while in [75], with only mean channel gain information, a source node jointly selects the cooperative nodes from its neighbors and optimally allocates power to each cooperative node in order to minimize outage probability.

However, the focus of the previous work (with a noticeable exception in [69]) is just one part of the entire cooperation procedure. More specifically, in order to achieve cooperative MIMO, a source node should first distribute data information to other cooperative nodes; this is the first stage or the “local distribution” stage. After each cooperative node receives information from the source node, the second stage is carried out by using a particular cooperative protocol, where the source node and the cooperative nodes collaborate together to form a virtual MIMO system and transmit to the destination node. The second stage is sometimes referred to as “long haul” transmission. Most previous work, such as [70-75], only focused on the second stage, without considering the effects in the first stage. In order to have a complete view of cooperative MIMO in wireless networks, both stages should be jointly considered. For example, the number of cooperative nodes should be chosen very carefully by taking

into account the energy consumption and the delay induced at the local distribution stage, and this might limit the number of nodes used for cooperation. Furthermore, in order to improve the system performance against channel impairments, such as deep fades, joint power control and rate adaptation should also be considered such that the power level and rate assigned to each cooperative node can be adaptively adjusted in order to achieve robust system performance.

Therefore, in this chapter, for a cooperative MIMO system with uncoded spatial multiplexing, we jointly consider the selection of cooperative nodes and the power/rate allocation among the selected nodes in order to minimize the bit-error-rate performance of the system. More specifically, we quantify the energy and delay induced during the local distribution stage; then, for the long haul transmission stage, given a subset of cooperating nodes, we express the system performance as a function of that subset of nodes, and the power/data rate allocated to each node; after that, we form a multi-variable optimization problem to maximize the performance at the destination node, taking into account both stages and the energy/delay/rate constraints. Finally, we investigate how to select the cooperative nodes and how to solve the optimization problem where the source node either has perfect instantaneous channel state information (CSI), or the source node only knows the channel correlation information. It is worth noting that the problem of cooperative node selection is similar to the problem of antenna selection in MIMO [84-86], but in this chapter, it is applied with distinct application scenarios and different system constraints.

This chapter is organized as follows: in Section 4.2, we present the system description and problem formulation, including the system channel models, the receiver structure, and the optimization problem when both stages are jointly considered; in Section 4.3, we quantify the energy consumption and delay induced during the local distribution stage; in Section 4.4, we investigate the selection

algorithms which are employed to choose the subset of cooperative nodes under different system conditions; in Section 4.5, we briefly describe the procedure which is used to realize the cooperation; finally, simulation results and discussions are presented in Section 4.6, followed by a conclusion in Section 4.7.

4.2 System Description and Problem Formulation

4.2.1 System and Channel Models

We assume that the source node can form a virtual MIMO system by cooperating with its neighbors, where all such nodes, including the source node, have a single antenna. However, the destination node is assumed to be large enough so that multiple receiver antennas can be implemented. For example, this scenario might correspond to one where multiple soldiers with small carry-on communication units want to transmit to a destination node mounted on a vehicle. Here, we assume that the source node has K-1 neighbors, and we want to select N out of the K nodes to form a virtual MIMO system, including the source node. The destination node is assumed to have R receive antennas, where $R \geq K$. The distance between the source node and the destination node is D_1, and the neighbors of the source node are randomly distributed within a radius of D_0 of the source node. Here, we assume $D_1 >> D_0$, so that the distance between each cooperative node and the destination node can be approximated as D_1 [69].

The wireless channels between the source node and its neighbors are assumed to experience *i.i.d.* frequency-flat Rayleigh fading with parameter σ_0^2 plus path loss with path loss exponent equal to 4. On the other hand, the channel between the cooperative cluster with N nodes (source node plus cooperative neighbors) and the destination node is assumed to experience a combination of frequency-flat Rayleigh

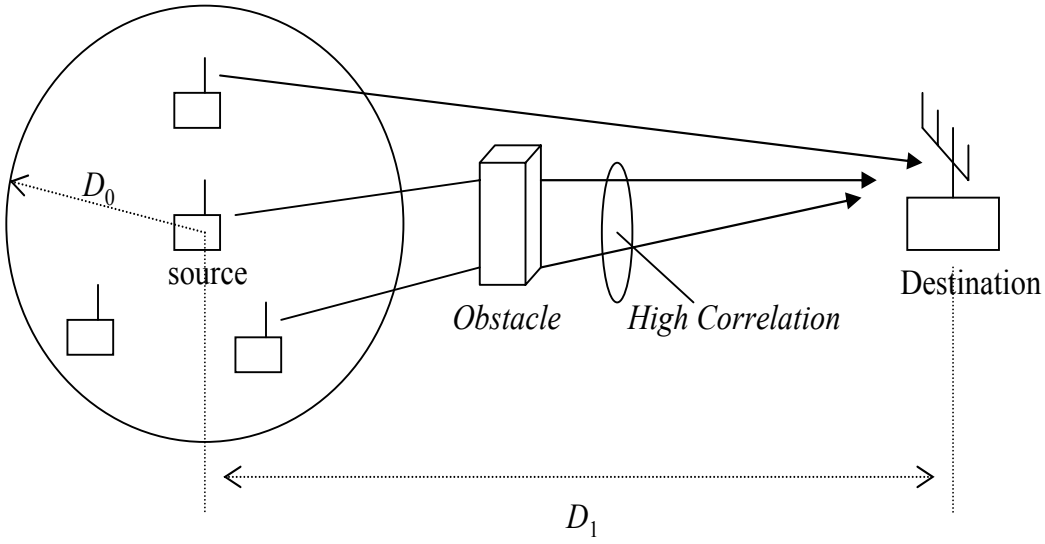

Fig. 4. 1. Illustration of the system model.

fading with parameter σ_1^2, shadowing, and path loss with loss exponent equal to 4. The wireless channel is assumed to be slowly-varying and is taken to be constant within the duration of its coherence time. In wireless transmission, high correlation can be induced between propagation paths by shadowing if they are blocked by the same obstacle, such as a tree or a building [76]. In this chapter, for simplicity, we only consider the correlation effect caused by shadowing. Typically, channel correlation caused by shadowing exhibits distance dependence, and thus we model the channel correlation between any two given cooperative nodes using an exponential model as in [76]:

$$\rho = \beta^{\frac{d}{D}}, \tag{4.1}$$

where ρ is the correlation between the two nodes separated by distance d, and β is the correlation between two nodes separated by distance D. β and D can be measured by field tests and then can be used to calculate the correlation between any two nodes [76]. The system model is illustrated in Fig. 4. 1, where a source node selects 2 out of its 3

neighbors to form the virtual MIMO system with the destination.

We assume that the system is time-slotted, where the time synchronization among the nodes can be achieved through some kind of beaconing (as in IEEE 802.11). At the receiver, the multiple cooperative nodes would typically interfere with one another, and in order to remove the multistream interference, successive interference cancellation (SIC) is used. Assume we have N cooperative nodes, and let $\mathbf{x} = [x_1, x_2 \ldots x_N]$ denote the transmitted vector, and $\mathbf{y} = [y_1, y_2 \ldots y_R]$ denote the received vector at the destination node with R receive antennas. The received signal vector $\mathbf{y}$, after matched filtering, can be shown to be given by

$$\mathbf{y} = \mathbf{H}\mathbf{x} + \mathbf{n}, \tag{4.2}$$

where $\mathbf{H}$ represents the channel matrix between the cooperative cluster and the destination node, and has dimension $R \times N$, and $\mathbf{n} = [n_1, n_2 \ldots n_R]^T$ represents *i.i.d.* Gaussian noise with zero mean and variance σ_n^2. For simplicity, if we assume that the correlation only resides at the transmitter side, then the channel matrix $\mathbf{H}$ can be expressed as [77]

$$\mathbf{H} = \mathbf{H}_w \mathbf{R}_T^{1/2}, \tag{4.3}$$

where $\mathbf{H}_w$ is an $R \times N$ matrix whose elements are *i.i.d.* complex Gaussian random variables with zero mean and unit variance, and $\mathbf{R}_T$ is an $N \times N$ correlation matrix among the cooperative nodes, i.e., among the transmit antennas. From (4.1), $\mathbf{R}_T$ can be expressed as follows:

$$\mathbf{R}_T = \begin{bmatrix} 1 & \beta^{\frac{d_{12}}{D}} & \cdots & \beta^{\frac{d_{1N}}{D}} \\ \beta^{\frac{d_{21}}{D}} & 1 & \cdots & \beta^{\frac{d_{2N}}{D}} \\ \vdots & \vdots & \vdots & \vdots \\ \beta^{\frac{d_{N1}}{D}} & \beta^{\frac{d_{N2}}{D}} & \cdots & 1 \end{bmatrix}, \tag{4.4}$$

where d_{ij} is the distance between node i and node j, and $d_{ij} = d_{ji}$.

4.2.2 Local Distribution and Long-Haul Transmission

We assume that, in total, the source node has a bit stream of L_0 bits to be sent to the destination. By using the proposed node selection algorithms described in Sec IV, N nodes are selected to perform cooperation. Then, during the local distribution stage, the source node forms N different substreams, and distributes the N substreams to the N selected cooperative nodes such that each cooperative node has one distinct substream. During this step, under the assumption that the system is time-slotted with slot duration T_s, and that TDMA is employed to distribute the source information, delay is introduced. We let $T^{(1)}_{tot}$ denote the total delay introduced during the local distribution. Also, the local distribution requires a minimum energy in order to guarantee the transmissions from the source node to its neighbors are reliably received. We let $E^{(1)}_{tot}$ denote the total energy consumed in this stage, and assume it contains both the transmission energy and the circuit energy consumption, as detailed in Section III. For simplicity, we assume that the source node knows the location of each neighbor and the corresponding channel gain between them.

In the second stage, i.e., the long haul transmission, all the N selected cooperative nodes collaborate together and form a virtual MIMO system with the destination node. The total transmission power for all the cooperative nodes is constrained to be less than or equal to P_T, as in [90, 91]. Further, we let $E^{(2)}_{tot}$ be the total energy used in this stage by all the cooperative nodes and the destination node, where $E^{(2)}_{tot}$ contains both the transmission energy consumption and circuit energy consumption. Lastly, the total delay associated with this stage is given by $T^{(2)}_{tot}$. All the parameters associated with these two stages will be discussed in more detail in a later section.

4.2.3 Spatial Multiplexing and ZF-SIC with QR Decomposition

We assume that the receiver has perfect CSI, and in order to exploit the capacity of a MIMO system, we consider the use of spatial multiplexing, where the source node first divides the incoming bit stream into N substreams, and then the source node distributes each of these substreams to one of the N cooperative node. Finally, each cooperative node sends an independent bit stream to the destination node simultaneously with other cooperative nodes via the virtual MIMO structure between the cooperating nodes and the destination node.

At the destination node, in order to detect the original bit-stream in MIMO-like transmissions, many receiver design strategies can be considered, such as linear receivers (zero-forcing or MMSE), V-BLAST (Ordered Successive Interference Cancellation) and Successive Interference Cancellation (SIC) [77]. In this chapter, we employ successive interference cancellation with fixed detection order in conjunction with ZF at each detection stage. For simplicity, we assume all previous decisions in the ZF-SIC are correct` as in [86]. Then, based on a matrix QR decomposition [78], the channel matrix $\mathbf{H}$ can be decomposed as $\mathbf{H} = \mathbf{QR}$, where $\mathbf{Q}$ is an $R \times N$ unitary matrix with orthonormal columns, i.e., $\mathbf{Q}^{\mathrm{H}}\mathbf{Q} = \mathbf{I}_{\mathrm{N}}$, $((\cdot)^{\mathrm{H}}$ denotes the Hermitian transpose), and $\mathbf{R}$ is an $N \times N$ upper triangular matrix. The QR decomposition is widely used in MIMO communications due to its simplicity and high computational efficiency [82, 83]. Multiplying the received signal vector, Eq (4.2), with $\mathbf{Q}^{\mathrm{H}}$, we obtain the following modified received signal vector:

$$\begin{aligned}\hat{\mathbf{y}} &= \mathbf{Q}^H\mathbf{y} = \mathbf{Rx} + \mathbf{Q}^H\mathbf{n} = \mathbf{Rx} + \mathbf{u} \\ &= \begin{bmatrix} R_{1,1} & R_{1,2} & \cdots & R_{1,N} \\ 0 & R_{2,2} & \cdots & R_{2,N} \\ \vdots & \vdots & \vdots & \vdots \\ 0 & 0 & \cdots & R_{N,N} \end{bmatrix} \times \begin{bmatrix} x_1 \\ x_2 \\ \vdots \\ x_N \end{bmatrix} + \begin{bmatrix} u_1 \\ u_2 \\ \vdots \\ u_N \end{bmatrix},\end{aligned} \tag{4.5}$$

where $\mathbf{u}$ has the same statistics as $\mathbf{n}$, since $\mathbf{Q}$ is a unitary matrix. Since $\mathbf{R}$ is an upper triangular matrix, it is clear that the i-th element of $\hat{\mathbf{y}}$ is only a function of the i-th and

higher stream symbols, and can be expressed as follows:

$$\widehat{y}_i = R_{i,i}x_i + \sum_{j=i+1}^{N} R_{i,j}x_j + u_i \ . \tag{4.6}$$

On the assumption that the detection order is from symbols with higher indexes to lower indexes, i.e., x_N to x_1, with SIC, the estimated symbol x_i can be shown to be given by

$$\hat{x}_i = D\left(\frac{\widehat{y}_i - \sum_{j=i+1}^{N} R_{i,j}\hat{x}_j}{R_{i,i}}\right) = D\left(\frac{R_{i,i}x_i + u_i + \sum_{j=i+1}^{N} R_{i,j}x_j - \sum_{j=i+1}^{N} R_{i,j}\hat{x}_j}{R_{i,i}}\right), \tag{4.7}$$

where $\hat{x}_i$ is the estimated symbol of x_i, and $D[\cdot]$ is the decision operation. As in [77], ZF-SIC with a fixed detection order naturally converts an $R \times N$ MIMO channel into a set of N parallel subchannels. Under the assumption that all the previous decisions are correct, the last two summations in (4.7) cancel each other, so the quantity $|R_{i,i}|^2$ can be viewed as the corresponding channel gain for the i-th subctream from the cooperative node i. Finally, the QR decomposition can be performed with the modified Gram-Schmidt method [78].

4.2.4 Performance Metric

As we discussed previously, we desire to jointly select the optimal subset of cooperative nodes and the per-node power level as well as per-node rate (constellation size) in order to minimize the BER at the receiver. For simplicity, we use the minimum Euclidean distance d_i as a performance metric on the i-th subchannel. Suppose an *M-ary* QAM modulation is employed, and we have N cooperative nodes and N corresponding subchannels, where the i-th subchannel has power level P_i, constellation size B_i and corresponding channel gain $|R_{i,i}|^2$. Then, the received minimum squared

Euclidean distance of the output constellation of the *i*-th subchannel is given by [27] for high SNR regime as

$$d_i^2 = \frac{6P_i \cdot \left|R_{i,i}\right|^2}{B_i - 1}. \tag{4.8}$$

Our overall objective function is the average received minimum squared Euclidean distance of the output constellations of all the N subchannels, which is given by $(1/N)\Sigma_{i=1}^{N} d_i^2$, and we want this quantity to be as large as possible. Based on the inequality that the arithmetic mean of multiple positive numbers is greater than or equal to their geometric mean, it is clear that such a metric can be lower-bounded as

$$\frac{1}{N}\sum_{i=1}^{N} d_i^2 \geq \left(\prod_{i=1}^{N} d_i^2\right)^{1/N}, \tag{4.9}$$

where equality is achieved when $d_i = d_j$ ($i \neq j$). By letting $d_i = d_j = d_0$, the average received minimum squared Euclidean distance of all the subchannels can be lower-bounded by

$$\frac{1}{N}\sum_{i=1}^{N} d_i^2 \geq \left(\prod_{i=1}^{N} d_i^2\right)^{1/N} = d_0^2. \tag{4.10}$$

Thus, the objective becomes maximizing d_0^2. This is consistent with the conclusions in other works, such as [86], where in a MIMO spatial multiplexing system, the performance is limited by the weakest link. In order to maximize the system performance, we want the output minimum Euclidean distance for each subchannel to be the same, and we then maximize that minimum Euclidean distance, subject to given system constraints.

4.2.5 Optimization Problem Formulations

In this subsection, we first present the details of the problem, given that N

cooperative nodes have been chosen for the long haul transmission stage. Then we discuss the overall optimization problem where node selection and power/bit allocation are combined together with the local distribution, and long haul transmission stages are jointly considered. Given that N nodes have been chosen for the long haul transmission, the targets are to find the power/bit allocations for each of these selected nodes under the transmit power constraint, P_T, and the total bit rate constraint, b_T.

Therefore, the optimization problem for the long haul transmission stage is given by

$$\begin{aligned} &\max_{\{P_i, B_i\}} \left\{ d_0^2 \right\} \\ &s.t. \quad 1. \sum_{i=1}^{N} P_i = P_T; \quad 2. \sum_{i=1}^{N} \log_2(B_i) = b_T; \end{aligned} . \tag{4.11}$$

Since $d_i = d_0$, from (4.8), we have B_i given by

$$B_i = \frac{6P_i \cdot \left| R_{i,i} \right|^2}{d_0^2} + 1 . \tag{4.12}$$

Plugging (4.12) into the second constraint in (4.11), we obtain the following equation:

$$\begin{aligned} &\sum_{i=1}^{N} \log_2 \left(\frac{6P_i \cdot \left| R_{i,i} \right|^2}{d_0^2} + 1 \right) = b_T \\ &\Rightarrow \log_2 \left(\prod_{i=1}^{N} \left[\frac{6P_i \cdot \left| R_{i,i} \right|^2}{d_0^2} + 1 \right] \right) = b_T \end{aligned} . \tag{4.13}$$

Hence,

$$\begin{aligned} 2^{b_T} = \prod_{i=1}^{N} \left[\frac{6P_i \cdot \left| R_{i,i} \right|^2}{d_0^2} + 1 \right] &\Leftrightarrow 2^{b_T} \geq \prod_{i=1}^{N} \left[\frac{6P_i \cdot \left| R_{i,i} \right|^2}{d_0^2} \right] \\ &\Leftrightarrow d_0^{2N} \geq 2^{-b_T} \prod_{i=1}^{N} 6P_i \cdot \left| R_{i,i} \right|^2 \end{aligned} . \tag{4.14}$$

Thus, based on (4.14), the original problem (4.11) becomes

$$\max_{\{P_i\}} \left\{ \prod_{i=1}^{N} 6P_i \cdot \left| R_{i,i} \right|^2 \right\} \quad s.t. \quad 1. \sum_{i=1}^{N} P_i = P_T; \tag{4.15}$$

It is clear that in order to maximize (4.15), we need to maximize the product of P_i, i.e., $P_1 \cdot P_2 \cdot \ldots \cdot P_N$, since the $|R_{i,i}|^2$, $i = 1,\ldots, N$, can be viewed as constants. Furthermore, due to the constraint in (4.15), where the summation of P_i, $i = 1,\ldots,N$, is equal to the total power P_T, the maximization is achieved when the total power P_T is *equally* distributed to all the cooperative nodes, which means $P_i = P_T/N$, $i = 1,\ldots,N$. Thus, a simple power allocation is achieved, and the amount of power distributed to each cooperative node varies as a function of the number of cooperative nodes we choose to use in the virtual MIMO system. Then, the resulting d_0^2 and corresponding P_i and B_i, $i = 1,\ldots,N$, can be solved for a given N by using (4.12) and (4.14).

In order to consider the local distribution and long haul transmission together, we need to include the energy consumptions and the delays of the two stages in the optimization problem. That is, given K possible candidates, the optimization should look for the optimal subset of cooperative nodes, labeled as Φ^*, with N nodes, as well as the corresponding power/bit allocations for each of them, P_i and B_i, $i = 1,\ldots, N$. We denote by E_{tot} and T_{tot} the total end-to-end energy and the total end-to-end delay, respectively, with maximum allowable values E_o and T_o, respectively. Then, the overall optimization problem is given by:

$$\max_{\{\Phi, N, P_i, B_i\}} \left\{ d_0^2 \right\}$$

$$s.t. \quad 1. \sum_{i=1}^{N} P_i = P_T; \quad 2. E_{tot} = E_{tot}^{(2)} + E_{tot}^{(1)} \le E_o; \quad 3. T_{tot} = T_{tot}^{(2)} + T_{tot}^{(1)} \le T_o; \quad 4. 0 < N \le K; \tag{4.16}$$

In order to find the optimal Φ^*, N, P_i and B_i, $i = 1,\ldots, N$, an exhaustive search is necessary, but this type of problem usually has a large search space when K is large. In what follows, we first present the details on the energy consumption and delay associated with the local distribution, and then we provide some simple heuristic

algorithms to reduce the complexity such that the optimization problem can be more easily solved.

4.3 Local Distribution Analysis

During the local distribution stage, the source node sends the data information to the selected nodes. As a result, it is clear that the more the cooperative nodes, the more delay and energy are potentially needed for this stage. The energy for the local distribution to each cooperative node consists of the transmission energy which ensures reliable communications from the source node to that particular cooperative node, and the circuit energy consumption, which is the sum of the energy consumptions of all the circuit blocks [69, 80].

Since the transmission from the source node to a given cooperative node is in the form of packets, we assume that the source node has L_i bits within a packet to be transmitted to cooperative node i, and in the local distribution stage, a fixed M_0-ary QAM is used together with coherent modulation/demodulation. Since a given $M_0 = I \times Q$ rectangular QAM signal can be treated as two independent pulse amplitude modulation (PAM) signals on phase-quadrature carriers, i.e., I-ary PAM and Q-ary PAM, the two PAM signals can ideally be perfectly separated at the demodulator, and the probability of error for the original QAM signal can be shown to be

$$SER = 1 - \left(1 - SER_I\right)\left(1 - SER_Q\right), \tag{4.17}$$

where SER_I and SER_Q are the probabilities of symbol error for the two PAM signals. Hence, at relatively high SNR, the symbol error rate SER, can be tightly approximated as [27]

$$SER \simeq 4Q\left(\sqrt{\frac{3\varsigma}{M_0 - 1}}\right), \tag{4.18}$$

where $Q(\cdot)$ is the Gaussian tail function, and ζ is the corresponding signal-to-noise-ratio for the transmission to node i, given by

$$\zeta = \frac{\alpha_i P_i^{(1)}}{N_0}, \tag{4.19}$$

in (4.19) α_i is the channel gain (path loss plus fading), $P_i^{(1)}$ is the employed transmission power per symbol, and N_0 is the noise power. From (4.18) and (4.19), for a packet of L_i bits which has $C_0 = L_i/b_0$ symbols ($b_0 = \log_2(M_0)$), when a symbol error rate threshold SER_t is required for the local transmission, the minimal transmission power $P_i^{(1)}$ for the local transmission to node i is given by

$$P_i^{(1)} = \frac{(M_0 - 1) \cdot N_0}{3\alpha_i} \times \left[Q^{-1}\left(\frac{SER_t}{4} \right) \right]^2. \tag{4.20}$$

On the other hand, the circuit power for each symbol can be assumed to be a constant P_c for all the nodes [69]. In this chapter, we assume that the source node has L_0 bits and the number of bits allocated to node i is L_i. Thus, the total energy consumed in the local distribution, $E^{(1)}_{tot}$, can be shown to be

$$E_{tot}^{(1)} = \sum_{i=1}^{N} \left(\frac{T_s L_i}{b_0} \times \left[P_c + P_i^{(1)} \right] \times I(i) \right), \tag{4.21}$$

where L_i/b_0 is the number of symbols in the packet. Since, when node i is source node itself, there is no power consumption and delay introduced for the local distribution to node i, we thus define the indicator function $I(i)$ as

$$I(i) = \begin{cases} 0, & \text{when node } i \text{ is the source node;} \\ 1, & \text{when node } i \text{ is not the source node;} \end{cases}. \tag{4.22}$$

Under the assumption that TDMA is used for the local distribution with fixed symbol duration T_s, the total delay in this stage is the sum of the delays associated with the transmission to each of the N cooperative nodes:

$$T_{tot}^{(1)} = \sum_{i=1}^{N} \frac{L_i}{b_0} \times T_s \times I(i) . \quad (4.23)$$

From (4.21) and (4.23), it is clear that the subset and the number of cooperative nodes, Φ and N, should be carefully chosen such that the constraints in (4.16) can be satisfied.

4.4 Cooperation Node Selection

In order to solve the optimization problem in Sec. II-E, one usually resorts to heuristic algorithms to select appropriate subset of cooperative nodes, in order to avoid an exhaustive search which may require huge computational complexity, since we have to try all the possible combinations of the K cooperative nodes. By using heuristic algorithms, we can search only a reduced space, and for each possible combination in the subspace, we can solve the constrained optimization problem and find out the resulting d_0^2 as well as (Φ, N, P_i and B_i, i = 1,…, N). Finally, we pick the subset Φ* which achieves the largest d_0^2 to start the cooperative transmission. This technique is similar to antenna selection techniques used in MIMO system, where enhanced system performance and reduced system complexity can be achieved [84-86]. However, it is applied in this chapter with different application scenarios and different system constraints. In what follows, we describe the heuristic algorithms in two different scenarios, i.e., perfect instantaneous CSI is available at the source node or only the channel correlation information is available at the source node. As shown below, each of these two algorithms will only need to search a subspace with K possible cooperative node combinations, which is much less than that required by an exhaustive search.

4.4.1 Perfect CSI

In this case, the source node knows the instantaneous CSI between all the K cooperative nodes and the destination node, i.e., the channel gain matrix $\mathbf{H}$ with dimension $R \times K$, and the correlation information among all the nodes. This case is reasonable for a slowly-varying channel where CSI can be obtained in a timely and accurate manner.

It is clear that, when N is given, in order to maximize the target function in (4.15), we want the product of those channel gains, $\prod_{i=1}^{N} |R_{i,i}|^2$, to be as large as possible. Due to the fact that the eigenvalues of $\mathbf{R}$ are equal to $R_{i,i}$, we have the following properties:

$$\begin{aligned} \prod_{i=1}^{N} \left|R_{i,i}\right|^2 &= \prod_{i=1}^{N} \left|\lambda_i(\mathbf{R})\right|^2 = \det\left(\mathbf{R}^H\mathbf{R}\right) \\ &= \det\left(\mathbf{R}^H\mathbf{Q}^H\mathbf{Q}\mathbf{R}\right) = \det\left(\mathbf{H}^H\mathbf{H}\right) \end{aligned}, \tag{4.24}$$

where $\lambda(\cdot)$ is the eigenvalue of the argument. Therefore, as shown in (4.24), it is clear that in order to maximize the product of the channel gains, $|R_{1,1}|^2 \cdot |R_{2,2}|^2 \cdot \cdot |R_{N,N}|^2$, we only need to maximize the determinant of the corresponding channel matrix ($\mathbf{H}^H\mathbf{H}$).

To accomplish this, consider the use of a maximal channel gain (MCG) algorithm as follows: at the (k + 1)-th step, where k nodes have already been chosen, and the corresponding channel matrix $\mathbf{H}^{(k)}$ are known, where $\mathbf{H}^{(k)}$ is the channel matrix when k nodes are chosen, we want to select one additional node s^* from the set S containing the remaining $K - k$ nodes such that

$$s^* = \arg\max_{s^* \in S} \left\{ \det\left((\mathbf{H}^{(k+1)})^H (\mathbf{H}^{(k+1)}) \right) \right\}. \tag{4.25}$$

We repeat this until all the K nodes are chosen. Therefore, at each step, we obtain a selected subset of nodes, Φ, with an increasing number of nodes in it. In total, the algorithm runs K steps, thus the search space for the previous optimization problem has K combinations. Finally, we choose the subset Φ^* which results in the largest d_0^2 for the cooperative transmission. Therefore, by doing so, with the knowledge of the

instantaneous CSI, the source node can pick a subset of cooperative nodes which achieves the maximal product of the channel gains, and hence the maximal minimum distance as in the optimization problem of (4.16).

4.4.2 No CSI

In this case, the source node only knows the correlation information among the K potential cooperative nodes. This case is suitable for scenarios where fast fading exists, and accurate instantaneous CSI may not be possible for the source node. Therefore, the MCG algorithm proposed above should be modified as follows, due to the lack of CSI. The channel matrix $\mathbf{H}$ can be expressed as $\mathbf{H} = \mathbf{H}_w\mathbf{R}_T^{1/2}$ as in (4.3). By using the QR decomposition twice [86], $\mathbf{R}_T^{1/2} = \mathbf{Q}_1\mathbf{R}_1$, $\mathbf{H}_w \cdot \mathbf{Q}_1 = \mathbf{Q}_2\mathbf{R}_2$, we can express the received signal vector as follows:

$$\begin{aligned} &\mathbf{y} = \mathbf{H}_W\mathbf{R}_T^{1/2}\mathbf{x} + \mathbf{n} = \mathbf{Q}_2\mathbf{R}_2\mathbf{R}_1\mathbf{x} + \mathbf{n} \\ &\Leftrightarrow \hat{\mathbf{y}} = \mathbf{R}_2\mathbf{R}_1\mathbf{x} + \mathbf{Q}_2^H\mathbf{n} \end{aligned} . \tag{4.26}$$

Similarly, the optimization formulation in (4.15) becomes

$$\max\left\{\prod_{i=1}^{N} 6P_i \cdot \left|\mathbf{R}_2(i,i)\mathbf{R}_1(i,i)\right|^2\right\}. \tag{4.27}$$

In (4.27), we only knows $\mathbf{R}_1$, since $\mathbf{R}_2$ is unknown due to the lack of CSI. However, since $\mathbf{H}_w \cdot \mathbf{Q}_1 = \mathbf{Q}_2\mathbf{R}_2$ and $\mathbf{H}_w \cdot \mathbf{Q}_1$ has the same statistics as $\mathbf{H}_w$, which has *i.i.d.* complex Gaussian elements, $|\mathbf{R}_2(i,i)|$ in (4.27) has a chi-distribution with $2(R + 1 - i)$ degrees of freedom[87]. For notation simplicity, let $z = |\mathbf{R}_2(i,i)|$. Then, the PDF of z with v degree of freedom is

$$f\left(z;v\right) = \frac{2^{1-\frac{v}{2}} z^{v-1} e^{\frac{-z^2}{2}}}{\Gamma\left(\frac{v}{2}\right)}. \tag{4.28}$$

where $\Gamma(\cdot)$ is the gamma function. Hence, as an approximation, we can use the mean of

$|\mathbf{R}_2(i,i)|^2$ to replace $|\mathbf{R}_2(i,i)|^2$ in (4.27), where $E\{z^2\}$ is equal to

$$E\left(z^2\right)=\int_0^{+\infty} z^2 f\left(z,v\right)=v\,. \tag{4.29}$$

Thus, $E\{|\mathbf{R}_2(i,i)|^2\}$ is equal to $2(R+1-i)$. Correspondingly, the goal of (4.27) becomes maximizing the following:

$$\prod_{i=1}^{N} 6P_i\cdot\left|\mathbf{R}_2(i,i)\mathbf{R}_1(i,i)\right|^2 \simeq \prod_{i=1}^{N} 6P_i\cdot 2(R+1-i)\cdot\left|\mathbf{R}_1(i,i)\right|^2\,. \tag{4.30}$$

Analogous to the previous discussion, we want the product of $|\mathbf{R}_1(i,i)|^2$, $i = 1,\ldots,N$, to be as large as possible in the node selection. Thus, our modified MCG algorithm is as follows: at the $(k+1)$-th step, where k nodes have been chosen, and the corresponding correlation matrix $(\mathbf{R}_\mathrm{T}^{1/2})^{(k)}$ are known, we want to select one additional node s^* from the set S which contains the remaining $K-k$ nodes such that $\det(((\mathbf{R}_\mathrm{T}^{1/2})^{(k+1)})^H((\mathbf{R}_\mathrm{T}^{1/2})^{(k+1)}))$ is maximized:

$$s^*=\arg\max_{s^*\in S}\left\{\det\left(((\mathbf{R}_\mathrm{T}^{1/2})^{(k+1)})^H((\mathbf{R}_\mathrm{T}^{1/2})^{(k+1)})\right)\right\}. \tag{4.31}$$

In essence, only the channel correlation information $\mathbf{R}_\mathrm{T}$ is exploited in order to select the cooperative nodes. Again, the search space is also reduced to a subspace with K possible combinations. Hence, when full CSI is not available, we still can significantly reduce the search space, and thus the optimization problem can be solved. However, this also results in degraded system performance compared to the case where the instantaneous CSI is available at the transmitter.

Consider now an alternative to the use of the modified MCG algorithm, namely, the least channel correlation (LCC) algorithm, which only makes use of the channel correlation information at the source node and tries to minimize the correlation among the cooperative nodes. Compared to the modified MCG algorithm, the LCC algorithm has less complexity.

As is well known, channel correlation typically has a significant impact on the performance of a spatial multiplexing MIMO system. The best performance of a spatial

multiplexing system can be reached when channels are independent. However, MIMO channels are often characterized with channel correlations. Previous studies have demonstrated that channel correlation is detrimental to spatial multiplexing MIMO systems [81, 85, 88] due to the fact that high correlation at the transmitter side increases dependence among input substreams' channel responses, and results in less effective substream separation and decoding at receiver side. Hence, it motivates us to choose cooperative nodes with minimal correlation among each other. Since in this chapter, correlation is modeled as a decreasing function of distance between two points, this is equivalent to choosing nodes with maximal distance among each other. Therefore, the algorithm can be described as follows: at the (k + 1)-th step, where k nodes have been chosen, we want to select one additional node s* from the set S which contains the remaining $K - k$ nodes such that the average distance $D^{(k)}_{ave}$ to all the previous k nodes can be maximized:

$$s^* = \arg\max_{s^* \in S} \left\{ D^{(k)}_{ave} \right\}, \tag{4.32}$$

where the average distance $D^{(k)}_{ave}$ can be computed as

$$D^{(k)}_{ave} = \frac{1}{k} \sum_{i=1}^{k} \sqrt{\left(X_i - X_{k+1} \right)^2 + \left(Y_i - Y_{k+1} \right)^2}, \tag{4.33}$$

and (X_i, Y_i) is the axis-position of the i-th node. More specifically, at the first step, the source node is chosen; at the second step, one additional node is chosen such that $D^{(1)}_{ave}$ is maximized; we then repeat the same process, where at each further step, one more node is added to the selected subset. The algorithm ends when all the K nodes are chosen. Therefore, at each step, we obtain a selected subset of nodes, Φ, with an increasing number of nodes in it, which significantly decreases the search space for the previous optimization problem.

4.5 Procedure to Realize the Cooperation

In this section, we briefly describe how the cooperation can be realized in a real system, and we assume that each node in the network has a unique user ID number [92]. The procedure works as follows:

Step1: *Neighbor maintenance* step: each node periodically broadcasts a cooperation-request (CR) message to the nodes within its transmission range; when a neighbor receives the CR message from a specific node, based on its current traffic and energy conditions, it determines whether or not to participate in the cooperation; if it is able to cooperate with the requesting node, it will reply with an agree-on-cooperation message (AoC) with its own user ID included; when the requesting node receives the AoC message from a neighbor, it will save this user ID; Thus, each node can maintain a neighbor set which includes the possible neighbors that can facilitate its transmission.

Step2: *Information exchange* step: when a source node plans to transmit to the destination node, which may be a powerful data collection node with multiple antennas and unlimited resources, the source node first sends a transmission request along with its neighbor set to the destination; if channel information is needed at the transmitter side, the destination node will perform channel estimation which may involve multiple packet exchanges. This process requires higher system complexity [90], but with CSI at the transmitter side, better system performance can be achieved. If the channel information is not available to the transmitter side, no such channel estimation process is needed, and only the channel correlation information is used, which is much simpler to obtain due to the slowly-varying characteristic of the correlation. After the information is obtained, the destination sends back this information to the source node.

Step3: *Local distribution* step: when the source node receives the necessary information, it runs one of the proposed algorithms described previously to perform node selection and data/power allocation. After that, it forms a TDMA schedule with those information included and broadcasts this schedule to all the selected cooperating nodes; finally, it distributes the data stream to each selected cooperating node, and then the long-haul virtual MIMO transmission starts.

By using the above procedure, the cooperation can be realized. It is worth noting that this procedure is only for single-hop transmission between the source and destination. However, if multi-hop is involved, i.e., multiple virtual MIMO transmissions are needed to complete the transmission between the source and the destination, similar procedures can also be designed, but with increased complexity and out of the scope of this chapter.

4.6 Numerical Results and Discussion

In this section, we provide selected numerical results to show the performance of the proposed node selection algorithms under the system constraints, such as the delay and energy consumption constraints. We choose $K = R = 6$, which means 6 potential cooperative nodes including the source node, and the destination node has 6 receive antennas. The distance between the source node and the destination node, D_1, is 100 m, and the radius of the cooperative cluster, D_0, is 10 m. Throughout this chapter, the path loss exponent is set to be 4, the system bandwidth is set to be 10 KHz, and the circuit power is set to be 250 mw [69]. The fixed data rate is chosen to be $b_T = 14$ bps/Hz. During the local distribution, the fixed modulation size is assumed to be $b_0 = 4$. The maximum QAM constellation size used for each node is 256-QAM. Finally, the correlation caused by shadowing uses parameters $\beta = 0.3$ and $D = 10$ m [76] unless

otherwise stated.

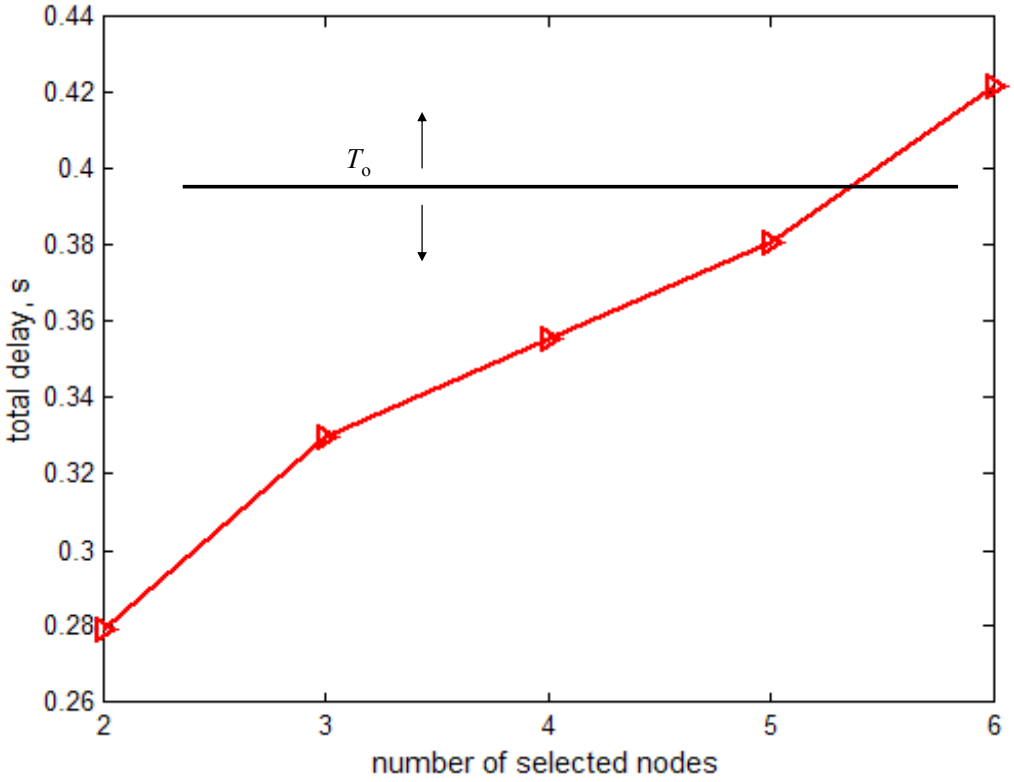

Fig. 4. 2. MCG algorithm with perfect CSI; no constraints; average SNR = 21 dB.

First of all, we demonstrate the necessity for judicious selection of cooperative nodes in a constrained environment. In Figs. 4. 2 and 4. 3, we let the system constraints E_o and T_o be infinite, i.e., no constraints, and the MCG algorithm with perfect CSI is employed. As we can see from Fig. 4. 2 and Fig. 4. 3, when the number of nodes participating in the cooperation increases, the required total delay and total energy consumption also increases, since more data may be distributed by the source node during the local distribution, and thus more energy and delay may be needed. Furthermore, if we have delay and energy constraints present, it is clear that the more stringent the constraints are, the fewer cooperative nodes we can choose. As a result, it turns out that the two system constraints, i.e., E_o and T_o, play important roles for the

selection of cooperative nodes. On the other hand, it is also clear that the overall system performance is somehow dependent on the system constraints, i.e., E_o and T_o, which determine the number of cooperative nodes that can participate the cooperation. For example, if E_o and T_o are small, it may not be able to choose the optimal number of nodes, and will result in degraded overall system performance.

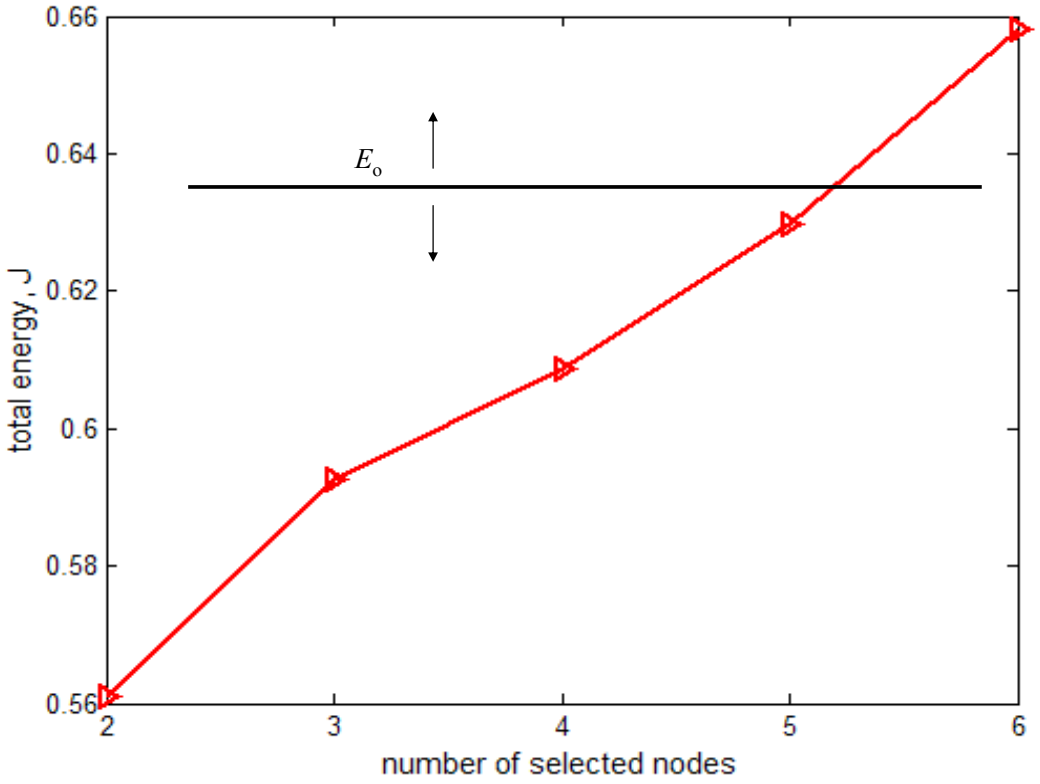

Fig. 4. 3. MCG algorithm with perfect CSI; no constraints; average SNR = 21 dB.

In Fig. 4. 4, we show the performance of the MCG algorithm with perfect CSI as a function of the average SNR with distinct delay constraints. As can be seen, when no delay constraint is present, i.e., T_o is infinite, the best system performance can be achieved. However, when the delay constraint becomes stringent, the system performance degrades substantially, as shown in the figure. This is because when a delay constraint is present, we cannot always choose the optimal set of nodes that can

achieve the best performance, and as the constraint becomes more stringent, fewer nodes can be chosen, thus worse performance is expected. This figure further demonstrates that in a cooperative MIMO system for an ad hoc network, the local distribution and long haul transmission stages should be jointly considered, and the overall system constraints limit the system performance that can be achieved.

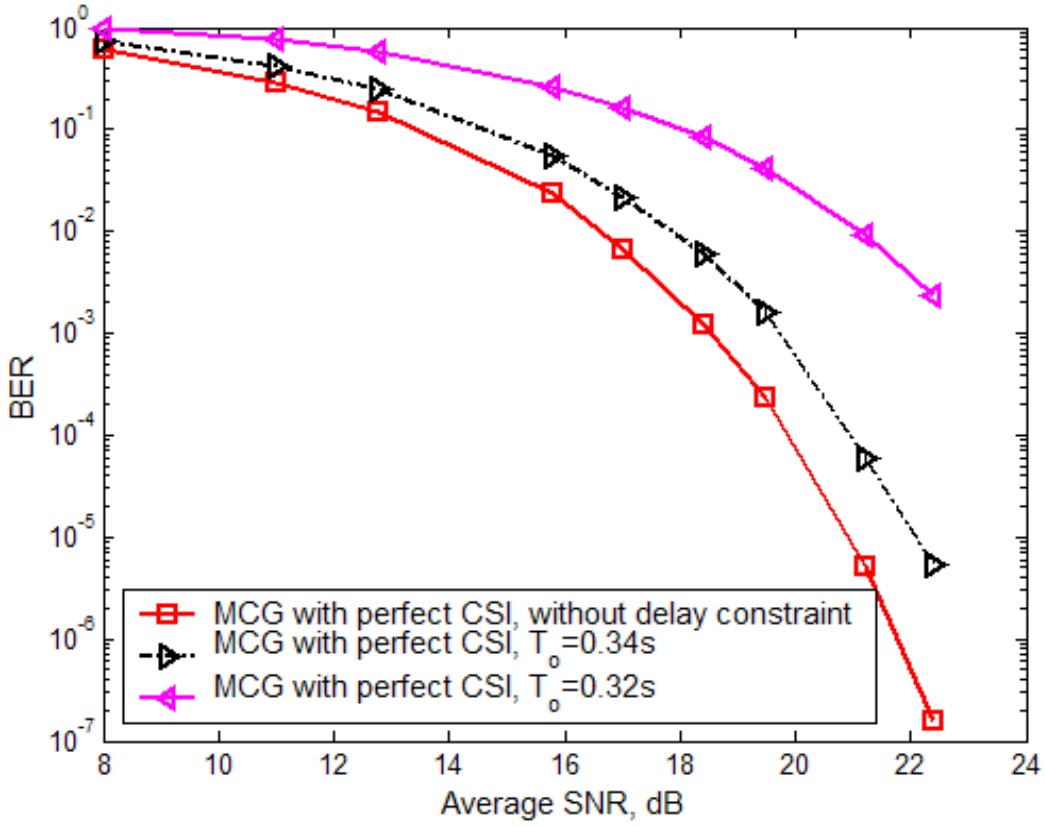

Fig. 4. 4. MCG algorithm with perfect CSI; with different delay constraints; E_o = 0.8 J.

In Fig. 4. 5, we show the performance comparison among the proposed algorithms under different channel correlation levels. As we can see, for the same channel correlation level, the MCG algorithm with perfect CSI can achieve the best performance since it exploits the perfect instantaneous CSI to achieve the cooperative node selection. On the other hand, when no CSI is available, we still can implement the

proposed node selection algorithm by making use of only the channel correlation information, and this can be achieved by the proposed modified MCG algorithm with no CSI and the LCC algorithm. As shown in Fig. 4. 5, the MCG algorithm with no CSI and LCC algorithm would result in degraded system performance compared to that of MCG with perfect instantaneous CSI. Therefore, when instantaneous CSI is not available in a practical scenario, we can resort to the algorithms that only exploit the channel correlation which varies relatively slow compared to the channel state information. Lastly, we also observe that when the channel correlation increases, system performance is degraded for all the algorithms. On the other hand, it is worth noting that when the correlation level increases, the performance gap between MCG with perfect instantaneous CSI and either the MCG without CSI or the LCC decreases. That means, the proposed MCG without CSI and the LCC algorithms can result in more performance gain in scenarios with high channel correlation.

Finally, in Fig. 4. 6, we show the system performance of the MCG algorithm with channel estimation error. The channel estimation error is modeled as a complex Gaussian random variable with zero mean and variance σ_e^2 [60]. The estimation error can be caused by various factors, such as feedback delay and node mobility. The estimated CSI is assumed to be the sum of the true CSI plus the random variable with zero mean and variance σ_e^2. In Fig. 4. 6, the MCG algorithm with perfect CSI achieves the best performance, and as estimation error increases, system performance degrades. It is worth noting that the dotted curve is achieved with the MCG algorithm with no CSI, but with channel correlation information which is not affected by the channel estimation error. It is clear that when the channel estimation error gets large, it is desirable to use the channel correlation information instead of the erroneous CSI.

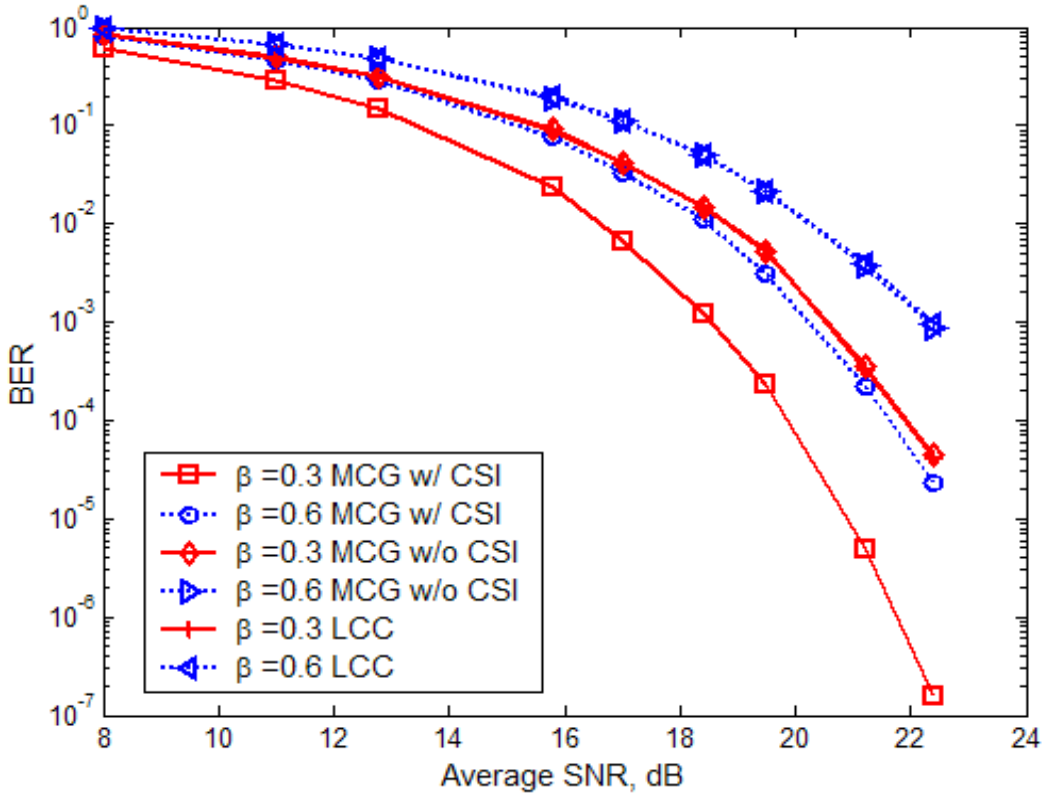

Fig. 4. 5. Performance comparison between MCG with perfect CSI, MCG w/o CSI, and LCC; T_o = 0.41 s and E_o = 0.8 J.

4.7 Summary and Conclusions

In this chapter, we investigated the cooperative and constrained virtual MIMO communications in ad hoc or sensor networks. More specifically, we have taken into account a complete view of the node cooperation procedure, under the specified system constraints, such as the energy and delay constraints. Then, we quantified the energy consumption and delay incurred during the local distribution stage, and jointly combined the local distribution stage and the long haul transmission stage. Finally, the subset of cooperative nodes participating in the virtual MIMO communication is chosen by considering the overall system constraints, and the power level and data rate

for each selected cooperative node are adaptively assigned in order to optimize the system performance.

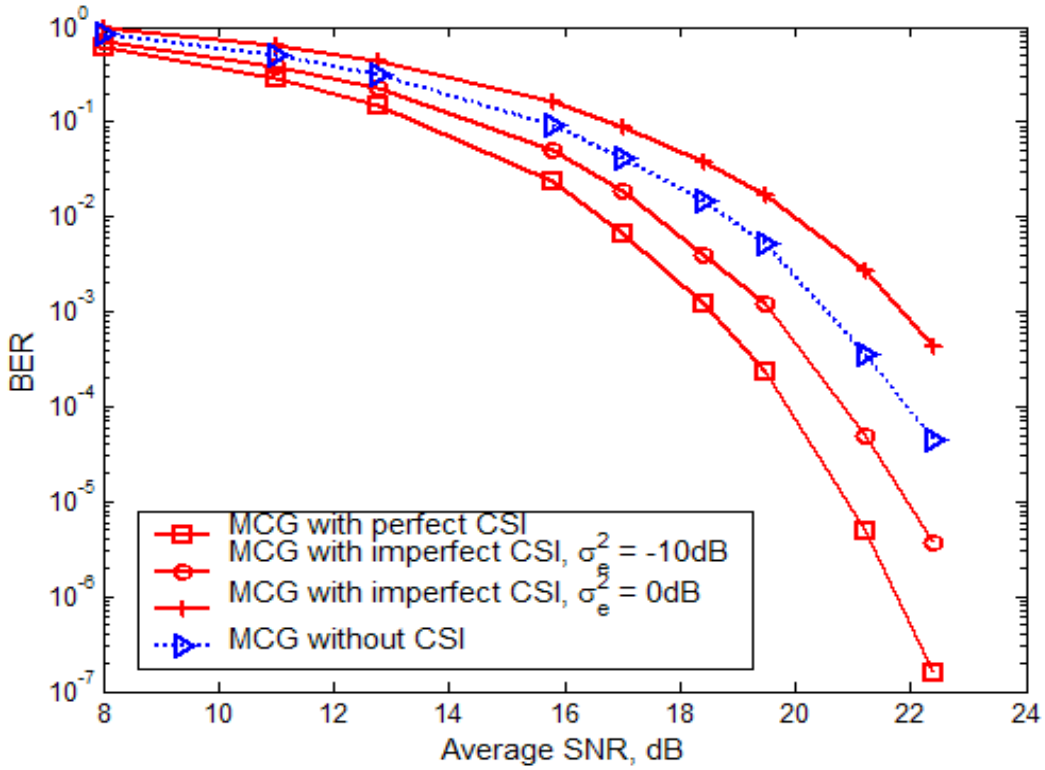

Fig. 4. 6. Performance comparison of MCG with distinct channel estimation error; T_o = 0.41 s and E_o = 0.8 J.

Acknowledgement

This chapter, in full, is a reprint of the material as it appears in Qi Qu, Laurence B. Milstein and Dhadesugoor R. Vaman, "Cooperative and Constrained MIMO Communications in Wireless Ad Hoc/Sensor Networks", which is being prepared for publication. The dissertation author was the primary investigator and author of this publication.

5

Conclusions

In this dissertation, we investigated system design approaches and algorithms to achieve power efficient and spectrum efficient communications in wireless ad hoc networks. The system design has covered multiple layers, including physical layer, MAC layer and application layer. The system optimization requires cooperation between different layers, which is usually referred as cross-layer optimization.

In Chapter 2, we proposed a cross-layer distributed joint power control and scheduling approach for delay-sensitive applications, such as multimedia, over CDMA-based wireless ad hoc networks. The cross-layer framework consisted of distributed power control at physical layer, and distributed scheduling algorithm at MAC layer. Herein, we have taken into account a delay constraint as well as an SINR constraint for system performance optimization, and proposed a novel delay control mechanism where power control is used to combat delay. The constrained optimization problem under both the delay and SINR constraints was solved via three simple but effective steps: delay control, validity scheduling and power control. Based on these three consecutive steps, the complexity of the optimization problem was greatly reduced and the power control at the physical layer was substantially simplified. Finally, we investigated the impact of Doppler spread and channel estimation errors upon the system performance, and provided a robust system which employed the combination of power control, coding and interleaving to combat the effects of Doppler spread by exploiting the time diversity when the Doppler spread got large.

Simulation results have demonstrated the effectiveness of the proposed approach.

In Chapter 3, we proposed a cognitive radio based multi-user resource allocation framework for mobile ad hoc networks using multi-carrier DS CDMA modulation over a frequency-selective fading channel. More specifically, given the existing spectral conditions and existing primary users, we first proposed a detection and estimation mechanism to detect the availability of each subcarrier, as well as to estimate the channel state information and the noise power; based on that, a distributed resource allocation approach was provided to jointly allocate spectral bands, power and data rate among multiple cognitive radio users. Finally, we investigated the performance of the system under different scenarios and examined the impact of multiple key parameters.

In Chapter 4, we investigated the cooperative and constrained virtual MIMO communications in ad hoc or sensor networks. More specifically, we have taken into account a complete view of the node cooperation procedure, under the specified system constraints, such as the energy and delay constraints. Then, we quantified the energy consumption and delay incurred during the local distribution stage, and jointly combined the local distribution stage and the long haul transmission stage. Finally, the subset of cooperative nodes participating in the virtual MIMO communication is chosen by considering the overall system constraints, and the power level and data rate for each selected cooperative node are adaptively assigned in order to optimize the system performance.

In conclusion, one possible direction for the future work could be to extend the power efficient and spectrum efficient design approaches to specific applications, such as video transmissions, and combine the characteristics of video content together with the design issues in the lower layers. For example, one may consider how to perform video streaming or video transmission in a cognitive radio network, where primary

users and secondary users co-exist. In the design of such a secondary user system, in addition to the physical layer spectrum dynamics and channel state information dynamics, the video contend dynamics at the application layer could also be jointly considered, such as the rate-distortion characteristic of video content. By doing that, we have one more degree of freedom in the system design and more specific algorithm can be proposed for specific applications. This is also our on-going work.

Bibliography

[1] M. Krunz, A. Muqattash, and S.-J. Lee, "Transmission power control in wireless ad hoc networks: challenges, solutions, and open issues", *IEEE Network*, pp.8-14, Sept./Oct. 2004.

[2] S. Narayanaswamy, V. Kawadia, R. S. Sreenivas and P. R. Kumar, "Power control in ad-hoc networks: theory, architecture, algorithm and implementation of the COMPOW protocol", in *Proc. European Wireless 2002 Next Generation Wireless Networks: Technologies, Protocols, Services and Applications*, pp. 156-162, Feb. 2002.

[3] C. Oestges and B. Clerckx, "MIMO wireless communications: from real-world propagation to space-time coding design", Academic Press, 2007.

[4] B. Chen, and M. J. Gans, "MIMO Communications in Ad Hoc Networks", *IEEE Trans. on Signal Processing*, vol. 54, no. 7, pp.2773-2783, July 2006.

[5] A. Muquttash and M. Krunz, "CDMA-based MAC Protocol for Wireless Ad Hoc Nerworks", in *Proc. of MobiHoc'03*, June 2003.

[6] T. Elbatt and A. Ephremides, "Joint Scheduling and Power Control for Wireless Ad Hoc Networks", *IEEE Trans. on Wireless Communications*, vol. 3, pp. 74-85, Jan. 2004.

[7] B. Radunovic and J-Y. L. Boudec, "Optimal Power Control, Scheduling, and Routing in UWB Networks", in *IEEE JSAC*, vol. 22, pp. 1252-1270, Sept. 2004.

[8] K. Wang, C. F. Chiasserini, R. R. Rao and J. G. Proakis, "A Distributed Joint Scheduling and Power Control Algorithm for Multicasting in Wireless Ad Hoc Networks", in *Proc. of ICC'03*, pp. 725-731, May 2003.

[9] G. J. Foschini and Z. Miljanic, "A Simple Distributed Autonomous Power Control Algorithm and its Convergence", *IEEE Trans. on Vehicular Technology*, vol. 4, pp. 641-646, Nov. 1993.

[10] J. Zander, “Distributed Cochannel Interference Control in Cellular Radio Systems”, *IEEE Trans. on Vehicular Technology*, vol. 41, pp. 305-311, Aug. 1992.

[11] S. Ramanathan and E. Lloyd, “Scheduling Algorithms for Multihop Radio Networks”, *IEEE/ACM Trans. on Networking*, vol.1, pp.166-177, 1993.

[12] R. L. Cruz and A. V. Santhanam, “Hierarchical Link Scheduling and Power Control in Multihop Wireless Networks”, *in Proc. of Allerton Conference*, Oct. 2002.

[13] H-L. Chao and W. Liao, “Fair Scheduling with QoS Support in Wireless Ad Hoc Networks”, *IEEE Trans. on Wireless Communications*, vol. 3, pp. 2119-2128, Nov. 2004.

[14] L. Pond and V. Li, “A Distributed Time-Slot Assignment Protocol for Mobile Multi-hop Broadcast Packet Radio Networks”, in *Proc. of IEEE Milcom,* 1989.

[15] A. J. Goldsmith and S. B. Wicker, “Design Challenges for Energy-Constrained Ad Hoc Wireless Networks”, *IEEE Wireless Communications Magazine*, Vol. 9, No. 4, pp. 8-27, Aug. 2002.

[16] H. Sui, E. Masry, B. D. Rao, "Chip-Level DS-CDMA Downlink Interference Suppression with Optimized Finger Placement," *IEEE Transaction on Signal Processing*, vol.54, No.10, pp. 3908-3921, Oct. 2006.

[17] E. Sousa and J. A. Silvester, “Spreading Code Protocols for Distributed Spread-Spectrum Packet Radio Networks”, *IEEE Trans. On Communications*, pp. 272-281, Mar. 1998.

[18] J. Schiller, “Mobile Communications”, Pearson Education, 2000.

[19] H. Stark and J. W. Woods, “Probability and Random Processes with Applications to Signal Processing”, 3rd Edition.

[20] L. Hu, “Distributed Code Assignments for CDMA Packet Radio Networks”, in *IEEE/ACM Trans. on Networking*, vol. 1, pp. 668-677, Dec. 1993.

[21] L. Williams, "Technology Advances from Small Unit Operations Situation Awareness System Development", *IEEE Personal Communication Mag.,* pp. 30-33, Feb. 2001.

[22] M. Mauve, J. Widmer and H. Hartenstein, "A Survey on Position-based Routing in Mobile Ad Hoc Networks", *IEEE Networks*, pp. 30-39, Nov./Dec. 2001.

[23] D. Gross and C. M. Harris, "Fundamentals of Queueing Theory", Second Edition.

[24] R. C. Larson and A. R. Odoni, "Urban Operations Research", Prentice-Hall, NJ 1981.

[25] V. Kanodia, et. al., "Ordered Packet Scheduling in Wireless Ad Hoc Networks: Mechanisms and Performance Analysis", in *Proc. of ACM Mobihoc'02*.

[26] B. Liang, "Performance of Multihop Latency Aware Scheduling in Delay Constrained Ad Hoc Networks", in *Proc. of ICC'05*, pp. 3499-3504, May 2005.

[27] John G. Proakis, "Digital Communications", 4th Edition, McGraw-Hill, 2000.

[28] W. C. Jakes, "Microwave Mobile Communications", IEEE Press, NJ 1994.

[29] F. Simpson and J. M. Holtzman, "Direct Sequence CDMA Power Control, Interleaving, and Coding", *IEEE JSAC*, vol. 11, pp. 1085-1095, Sept. 1993.

[30] C. Fleming, "A Tutorial of Convolutional Coding with Viterbi Decoding", Spectrum Applications, Jan. 2003.

[31] V. Rodoplu and T. Meng, "Position based CDMA with multiuser detection (P-CDMA/MUD) for wireless ad hoc networks", in *Proc. of IEEE Sixth International Symposium on Spread Spectrum Techniques and Applications*, pp. 336-340, 2000.

[32] C. R. Lin and M. Gerla, "Adaptive Clustering for Mobile Wireless Networks", *IEEE JASC*, vol. 15, pp. 1265-1275, Sept. 1997.

[33] B. Karp and H. T. Kung, "GPSR: Greedy Perimeters Stateless Routing for Wireless Networks", in *Proc. of ACM MobiCom*, 2000.

[34] X. Wu, G. Ding, B. Bhargava, and S. Lci, “Improving Throughput By Link Distance Control In a Multi-Rate Ad Hoc Networks”, *Technical Report*, Dept. of Computer Science, Purdue Univ., Aug. 2004.

[35] R. C. Manso, “Performance Analysis of M-QAM with Viterbi Soft-Decision Decoding”, Naval Postgraduate School, 2003.

[36] Y. Shen, P. C. Cosman, and L. B. Milstein, "Error Resilient Video Communications over CDMA Networks with a Bandwidth Constraint", *IEEE Trans. on Image Processing*, vol.15, no.11, pp.3241-3252, Nov. 2006.

[37] J. Jang and K. B. Lee, “Transmit power adaptation for multiuser OFDM systems”, *IEEE JSAC*, vol. 21, pp. 171-178, Feb. 2003.

[38] C. Y. Wong, R. S. Cheng, K. B. Letaief and R. D. Murch, “Multiuser OFDM with adaptive subcarrier, bit, and power allocation”, *IEEE JSAC*, vol. 17, pp.1747-1758, Oct. 1999.

[39] Y. H. Kim, I. Song, S. Yoon and S. R. Park, “A multicarrier CDMA system with adaptive subchannel allocation for forward links”, *IEEE Trans. on Vehicular Tech*., vol. 48, pp. 1428-1437, Sept. 1999.

[40] M. A. Enright, and C.-C. J. Kuo, “Fast linearized energy allocation for multimedia loading on multicarrier systems”, *IEEE JSAC,* vol. 24, pp. 470-481, Mar. 2006.

[41] S. Haykin, “Cognitive radio: brain-empowered wireless communications”, *IEEE JSAC*, vol.23, pp.201-220, Feb.2005.

[42] Q. Zhao, L. Tong, A. Swami, and Y. Chen, “Decentralized cognitive MAC for opportunistic spectrum access in ad hoc networks: A POMDP framework”, in *IEEE JSAC*, vol. 25, no. 3, pp. 589-600, Apr. 2007.

[43] R. Etkin, A. Parekh, and D. Tse, “Spectrum sharing for unlicensed bands”, in *IEEE JSAC*, vol. 25, no. 3, pp. 517-528, Apr. 2007.

[44] G. Ganesan, and Y. Li, “Cooperative spectrum sensing in cognitive radio, part I: two users networks”, in *IEEE trans. on Wireless Communications*, vol.6, no. 6, pp. 2204-2213, June 2007.

[45] Y.-C. Liang, Y. Zeng, E. Peh, and A. T. Hoang, “Sensing-throughput tradeoff for cognitive radio networks”, in *Proc. of IEEE ICC’07*, June 2007.

[46] S. Kondo, and L. B. Milstein, “Performance of multicarrier DS CDMA systems”, *IEEE Trans. on Communications*, vol.44, pp. 238-246, Feb. 1996.

[47] J. Mitola and G. Q. Maguire, “Cognitive radio: making software radios more personal”, *IEEE Personal Communications*, vol.6, pp.13-18, Aug. 1999.

[48] D. Guo, S. Verdu, and L.K. Rasmussen, ``Asymptotic normality of linear multiuser receiver outputs," in *IEEE Trans. on Information Theory*, vol.48, No.12, pp.3080 - 3095, 2002.

[49] J. Zhang, E. Chong, and D. Tse, ``Output MAI distributions of linear MMSE multiuser receivers in DS-CDMA systems", in *IEEE Trans. Information Theory*, vol.47, No. 3, pp.1028 - 1144, 2001.

[50] J. S. D. Eaddy and T. Kadota, “On the approximation of the optimum detector by the energy detector in detection of colored Gaussian signals in noise”, *IEEE Trans. on Acoust., Speech, Signal Processing*, vol.32, pp.661-664, Jun.1984.

[51] M. E. Mann and J. Park, “Oscillatory spatialtemporal signal detection in climate studies: A multiple-taper spectral domain approach”, in *Advance in Geophyisics*, New York, Academic, vol. 41, 1999.

[52] D. J. Thomson, “Spectrum estimation and harmonic analysis”, *Proc. of IEEE*, vol. 20, pp. 1055-1096, Sep. 1982.

[53] W. J. Fitzgerald, et al, “Nonlinear and nonstationary signal processing”, Cambridge Univ. Press, 2000.

[54] A. Sendonaris, E. Erkip and B. Aazhang, "User cooperation diversity: part I-system description", *IEEE Trans. on Communications*, vol.51, Nov. 2003.

[55] S. M. Mishra, A. Sahai, and R. W. Broderson, "Cooperative sensing among cognitive radios", in *Proc. of ICC* 2006.

[56] L. Cohen, "Time-frequency analysis", Prentice Hall, 1995.

[57] T. C. Hou and V. O. K. Li, "Transmission range control in multihop packet radio networks", *IEEE Trans. on Communications*, vol. 34, pp. 38-44, Jan. 1986.

[58] P. Stoica and T. Sundin, "On nonparametric spectral estimation", *Circuits, Syst., Signal Process*, vol. 16, pp. 169-181, 1999.

[59] M.-A. R. Baissas and A. M. Sayeed, "Pilot-based estimation of time-varying multipath channels for coherent CDMA receivers", *IEEE Trans. on Signal Processing*, vol.50, pp. 2037-2049, Aug. 2002.

[60] D. Piazza and L. B. Milstein, "Impact of feedback errors in multiuser diversity systems", in *Prof. of IEEE VTC-2005 (Fall)*, pp. 257-261, Sept. 2005.

[61] V. Srinivasan, P. Nuggehalli, C. F. Chiasserini, and Ramesh R. Rao, "Cooperation in wireless ad hoc networks", in *Proc. of IEEE INFOCOM'03*, 2003.

[62] A. Stranne, O. Edfors, and B.-A. Molin, "Energy-based interference analysis of heterogeneous packet radio networks", in *IEEE Trans. on Communications*, vol.54, pp.1299-1309, July 2006.

[63] N. Bambos, S. C. Chen, and G. J. Pottie, "Channel access algorithm with active link protection for wireless communication networks with power control", in *IEEE/ACM Trans. on Networking*, vol.8, pp.583-597, Oct. 2000.

[64] E. Peh and Y.-C. Liang, “Optimization for cooperative sensing in cognitive radio networks”, in *Proc. of IEEE WCNC’07*, 2007.

[65] S. S. Jeong, W. S. Jeon, and D. G. Jeong, “Dynamic channel sensing management for ofdma-based cognitive radio systems”, in *Proc of IEEE 65th VTC*(*Spring*), 2007.

[66] C. Sun, W. Zhang, and K. B. Letaief, “Cluster-based cooperative spectrum sensing in cognitive radio systems”, in *Proc. of IEEE ICC’07*, 2007.

[67] H. Sui, J. R. Zeidler, "A Robust Coded MIMO FH-CDMA Transceiver for Mobile Ad Hoc Networks," *IEEE J. on Selected Areas in Communications,* special issue on Optimization of MIMO Transceivers for Realistic Communication Networks, to appear Sept. 2007.

[68] H. Sui, J. R. Zeidler, "Information Efficiency and Transmission Range Optimization for Coded MIMO FH-CDMA Ad Hoc Networks in Time-Varying Environment,” submitted to *IEEE Trans. on Communications*, Feb. 2007.

[69] S. Cui, A. J. Goldsmith and A. Bahai, “Energy-efficiency of MIMO and cooperative MIMO techniques in sensor networks”, in *IEEE JSAC*, vol. 22, no. 6, pp. 1089-1098, Aug. 2003.

[70] M. Dohler, E. Lefranc, and H. Aghvami, “Space-time block codes for virtual antenna arrays”, in *Proc. of IEEE PIMRC*, Sept. 2002.

[71] S. K. Jayaweera, “Virtual MIMO-based cooperative communication for energy-constrained wireless sensor networks”, in *IEEE Trans. on Wireless Communications*, vol. 5, no. 5, pp. 984-989, May 2006.

[72] J. N. Laneman, and G. W. Wornell, “Distributed space-time-coded protocols for exploiting cooperative diversity in wireless networks”, *IEEE Trans. on Information Theory*, vol. 49, no. 10, pp. 2415-2425, Oct. 2003.

[73] Q. Zhou, H. Zhang, and H. Dai, "Adaptive spatial multiplexing techniques for distributed MIMO systems", in *Proc. of CISS'04*, Mar. 2004.

[74] M. O. Hasna, and M.-S. Alouini, "Optimal power allocation for relayed transmission over Rayleigh fading channels", *IEEE Trans. on Wireless Communications*, vol. 3, Nov. 2004.

[75] J. Luo, R. S. Blum, L. Cimini, L. Greenstein, and A. Haimovich, "Power allocation in a transmit diversity system with mean channel gain information", *IEEE Communication letters*, vol. 9, no. 7, pp. 616-618, July 2005.

[76] M. Gudmundson, "Correlation model for shadow fading in mobile radio systems", *Electronics Letters*, vol. 27, no. 23, pp. 2145-2146, Nov. 1991.

[77] A. Paulraj, R. Nabar, and D. Gore, "Introduction to space-time wireless communications", Cambridge University Press, 2003.

[78] G. H. Colub, and C. F. Van Loan, "Matrix Computations", 3rd edition, Johns Hopkins University Press, 1996.

[79] V. Srinivasan, P. Nuggehalli, C. F. Chiasserini, and R. R. Rao,"Energy Efficiency of Ad Hoc Wireless Networks with Selfish Users," *European Wireless Conference 2002* (*EW2002*), Florence, Italy, February 2002.

[80] C. Schurgers, O. Aberthorne, and M. B. Srivastava, "Modulation scaling for energy aware communication systems", in *Proc. of Int. Symp. Low Power Electronics Design*, pp. 96-99, Aug. 2002.

[81] H. Bolcskei, and A. J. Paulraj, "Performance analysis of space-time codes in correlated Rayleigh fading environments", *Asilomar Conference*, Nov. 2000.

[82] M. O. Damen, K. Abed-Meriam, and S. Burykh, "Iterative QR detection for an uncoded space-time communication architecture," in *Proc. Allerton Conf. Communications, Control, and Computing*, Monticello, IL, Oct. 2000.

[83] J.-K. Zhang, A. Kavcic, and K. M. Wong, "Equal-diagonal QR decomposition and its application to precoder design for successive-cancellation detection", *IEEE Trans. on Information Theory*, vol. 51, no. 1, pp. 154-172, Jan. 2005.

[84] D. Gore, R. Heath, and A. Paulraj, "Statistical antenna selection for spatial multiplexing system", in *Proc. of ICC'02*, pp. 450-454, May 2002.

[85] R. Narasimhan, "Spatial multiplexing with transmit antenna and constellation selection for correlated MIMO channels", *IEEE Trans. on Signal Processing,* vol. 51, no. 11, pp. 2829-2838, Nov. 2003.

[86] Q. Zhou, and H. Dai, "Joint antenna selection and link adaptation for MIMO systems", *IEEE Trans. on Vehicular Technology*, vol. 55, no. 1, pp. 243-255, Jan. 2006.

[87] R. J. Muirhead, "Aspects of Multivariate Statistical Theory", New York, Wiley, 1982.

[88] H. Bolcskei, M. Borgmann, and A. J. Paulraj, "Performance of space-frequency coded broadband OFDM under real-world propagation conditions", in *Proc. of Eur. Conf. Signal Process.*, Sept. 2002.

[89] N. Jindal, U. Mitra, A. Goldsmith, "Capacity of ad-hoc networks with node cooperation", in *Proc. of IEEE ISIT'04*, 2004.

[90] S.-J. Kim, R. E. Cagley, and R. A. Iltis, "Spectrally efficient communication for wireless sensor networks using a cooperative MIMO technique", *Wireless Networks*, pp. 397-407, May 2006.

[91] J. Liang and Q. Liang, "SVD-QR-T FCM approach for virtual MIMO channel selection in wireless sensor networks", in *Proc. of IEEE WASA'07*, pp.63-70, 2007.

[92] W. R. Heinzelman, A. Chandrakasan, and H. Balarislman, “An application-specific protocol architecture for wireless microsensor networks“, in *IEEE Trans. on Wireless Communications*, vol.1, pp.660-670, Oct 2002.